Mathematisches Forschungsinstitut Oberwolfach

Report No. 03/2013

DOI: 10.4171/OWR/2013/03

Computational Electromagnetism and Acoustics

Organised by
Ralf Hiptmair, Zürich
Ronald H. W. Hoppe, Augsburg/Houston
Patrick Joly, Le Chesnay
Ulrich Langer, Linz

20 January – 26 January 2013

Abstract. Computational electromagnetics and acoustics revolve around a few key challenges, among which are the non-local nature of the underlying phenomena and resonance effects. The bulk of the contributions to the workshop addressed mathematical and numerical approaches meant to grapple with these two difficulties.

Frequency domain integral equation methods continue to receive much attention, with a particular focus on (i) frequency robust matrix compression algorithms through so-called directional schemes or "butterfly algorithms", and (ii) domain decomposition approaches. Time domain integral equation methods still enjoy rapid development and much progress was made in their numerical analysis. Of course, efficient and accurate absorbing boundary conditions remain a persistent topic and were covered in a few contributions.

Resonance induced phenomena in a broad sense affect the analytical and numerical model for meta-materials, periodic structures, and micro-structured media. There is a lot left to be explored in this field in terms of analysis and algorithm development and a few presentations were devoted to such issues.

Mathematics Subject Classification (2010): 65Mxx, 65Nxx, 65Rxx, 78-04.

Introduction by the Organisers

"There is life in the old dog yet" (in German, "Totgesagte leben länger") and so the series of Oberwolfach Workshops on Computational Electromagnetism and Acoustics, which was announced to come to its end in the 2010 report, saw another event taking place in 2013. It was attended by 52 researchers in the field, and, after a bumpy start due to large scale disruptions in European air traffic, it provided a splendid demonstration that this field of mathematical and computational

research is well and thriving. Maybe surprisingly so, because Computational Electromagnetism and Acoustics have matured and, with essentially linear problems in their focus, may not be counted among the new and fashionable areas in applied mathematics.

A total of 26 presentations were given at the workshop, their topics providing a glimpse of major current directions of investigation in the field of Computational Electromagnetism and Acoustics. To some extent at least, because, firstly, only a fraction of eligible researchers could finally be invited to join this event, and, secondly, abiding by a request made by the institute's director, only half of the 52 participants were "lucky" and had the opportunity to present. Thus, many an important development might not be covered in this report and the range of topics can be regarded as partly random.

The general flavor of the presentations was distinctly theoretical this time. We guess that quite a few participants welcomed the opportunity to discuss fundamental mathematical ideas or specific research problem, which may not be that appropriate for other settings. Moreover, we encouraged the speakers to do exactly this and even asked them to make use of the blackboards. The schedule was also kept flexible. As a result, the participants could enjoy excellent talks that dwelt on ideas and made a big effort to convey them.

Now, let us survey the subjects chosen by the speakers. Throughout the years **integral equations methods** in frequency domain were always covered prominently, this time in the presentations, but with new twists: *A Mortar Element Method for the Electric Field Integral Equation* proposed a domain decomposition approach, which was also the objective in *A Discontinuous Galerkin Surface Integral Equation Method for Time-harmonic Maxwell's Equations*, whereas *Recent Advances in Well-conditioned EM Integral Equations* proposes a cure for the notorious low-frequency instability of EM integral equations. Integral equation methods for periodic settings were treated in *New tools for the high-order solution of frequency-domain wave scattering problems at high frequencies and in periodic geometries* and *Efficient solutions of three dimensional periodic scattering problems.* Related coding issued were addressed in *Solution of electromagnetic problems using BEM++.* Integral equations for scattering at complicated screens were considered in *Scattering by Arbitrary Planar Screens.* Another contribution of a theoretical nature was *On the inf-sup constant of the divergence alias LBB constant*, which examined the norm of the inverse divergence operator.

Very interesting new results concerned the compression and inversion of discrete boundary integral operator at medium frequencies via **"directional multipole"/"butterfly"** techniques, see *Wideband Nested Cross Approximation for Helmholtz problems*, *Aide-mémoire: fast multipole and butterfly algorithms*, *Interpolation based Directional Fast Multipole Method*, and *On MLMDA/Butterfly Compressibility of Inverse Integral Operators.* Recent progress in understanding of discrete **time-domain boundary integral equations** was covered in *A mathematical toolkit for TDBIE.*

Of course, **volume mesh based methods** for the discretization of wave propagation problems are still an active area of research. A profound analysis of polynomial Galerkin methods was given in *hp-FEM and hp-DGFEM for Helmholtz problems*, whereas *DPG Method, an Overview. Global Properties of DPG Test Spaces* introduced a new class of schemes, same as *A sign-definite formulation of the Helmholtz impedance problem. Stabilized Galerkin for Magnetic Advection* was dedicated to transport dominated problems for electromagnetic fields. This time **Fast iterative solvers** for volume discretization were addressed by only one speaker in *A parallel space-time multigrid method*.

Issues connected with novel **absorbing boundary conditions** for wave propagation problems in the frequency domain were discussed in *Hardy space method for exterior Maxwell problems*, stability issues were the focus of *Stability Analysis of Time-Domain PML*, whereas an analysis for periodic structures case was presented in *On the far field of the solutions of Helmholtz equations in periodic waveguide*. This latter topic also touched upon models for **complex media**, some of which are advertised as meta-materials with exotic properties, and a mathematical analysis of related interface problems was the subject of *Negative materials and corners in electromagnetism*. Numerical methods that deal with wave propagation in complex materials were discussed in *Finite Element Heterogeneous Multiscale Method for the Wave Equation: Long Time Effects*.

Of course, **inverse problems** and wave propagation are intimately connected, though topics from inverse problems have never been strongly represented in this series of workshops. Also this time only a few presentations belonged to this category, namely *Acoustic Reverse Time Migration for Extended Obstacles*, *Inverse Problems with Poisson Data*, and, in a loose sense, *Selective Focusing for Time Dependent Waves*.

Workshop: Computational Electromagnetism and Acoustics

Table of Contents

Abstracts

Recent Advances in Well-conditioned EM Integral Equations

Francesco P. Andriulli
(joint work with Ignace Bogaert, Kristof Cools, and Eric Michielssen)

Integral equation solvers are widely used for simulating electromagnetic scattering and radiation from arbitrarily shaped, Perfect Electrically Conducting (PEC) objects. Long popular in academic circles, these solvers recently have been incorporated into several commercial electromagnetic analysis and design tools, after the advent of fast multipole and related algorithms [15, 18, 19].

Among the many available alternatives, the surface Electric Field Integral Equation (EFIE) plays a dominant role. Although the EFIE initially was developed for simulating scattering and radiation from PEC surfaces, its underlying Electric Field Integral Operator (EFIO) also is used in integral equations applicable to resistive, surface impedance, and penetrable surfaces. This explains the large effort of the scientific community, currently underway, to stably discretize and invert the EFIO, a process that is plagued by numerous problems. When the EFIO is discretized with boundary elements with average diameter h, the resulting matrix has a condition number that grows as $(kh)^{-2}$, where k is the wavenumber. As a result, when k approaches zero, the EFIE becomes increasingly difficult and sometimes impossible to solve. This so-called low frequency breakdown phenomenon traditionally has been remedied by using Loop-Star/Tree (quasi-Helmholtz, or Hodge) decompositions [23, 22, 26, 17, 12]. When using these decompositions with the EFIO and after appropriate matrix scaling with suitably chosen powers of (kh), the low frequency breakdown is solved; that is, in the limit of k going to zero, the matrix condition number is constant. That said, these methods do not cure the undesirable scaling of the matrix condition number with h. Following their application, the matrix condition number scales as h^{-1}, h^{-2}, or h^{-3} (depending on the formulation). This h-breakdown phenomenon is due to the combined effect of the spectral properties of the EFIO and the instability of the Loop-Star/Tree bases [2].

To protect an EFIE against both low frequency and h-dependent breakdown, a simple rescaling of the EFIO does not suffice. Instead, a more invasive procedure aimed at modifying its spectrum is called for. This can be achieved by using hierarchical quasi-Helmholtz decompositions [4, 16] and/or Calderón techniques [10, 11, 1, 5, 21, 24], or the Epstein-Greengard method based on generalized Debye sources [14].

In addition to suffering from an h-breakdown, Loop-Star/Tree decompositions also require the detection of global loops when the surface is a non-simply connected geometry. Existing general-purpose algorithms for finding global loops exhibit quadratic complexity. Their cost therefore scales worse than that of fast integral equation solvers, which exhibit quasi-linear complexity.

Finally, several of the above schemes are susceptible to very low frequency cancelations in the solution vector. In fact, even if the equations are made well-conditioned, for plane wave scattering problems the non-solenoidal and solenoidal components of the current scale as k and are frequency independent, respectively. If these two components are not separated during the solution process, numerical cancelations that deteriorate the accuracy of the far field computation ensue. This phenomenon has been first pointed out in [25], and further studied in [9, 20] and [7] and [6] as well as in [13].

This talk, after surveying the issues of the EFIO and some of their above mentioned solutions, has presented a new integral equation [3] for simulating scattering and radiation from arbitrarily shaped, perfect electrically conducting objects that: (i) gives rise to well-conditioned systems when the frequency is low (ii) and/or when the discretization density is high, (iii) it does not require a search for topological loops, (iv) it is immune from numerical cancelations in the solution when the frequency is very low. The new formulation is obtained starting from a Helmholtz decomposition of two discretizations of the electric field integral operator obtained by using Raviart-Thomas and dual bases [8] respectively. The new decomposition does not leverage Loop and Star/Tree basis functions, but projectors that derive from them. Following the decomposition, the two discretizations are combined in a Calderon-like fashion resulting in a new overall equation that is shown to exhibit self-regularizing properties without suffering from the limitations of existing formulations.

References

[1] R. J. Adams, *Physical and analytical properties of a stabilized electric field integral equation*, IEEE Transactions on Antennas and Propagation, 52 (2004), pp. 362–372.

[2] F. Andriulli, *Loop-star and loop-tree decompositions: analysis and efficient algorithms*, IEEE Transactions on Antennas and Propagation, 60 (2012), pp. 2347 –2356.

[3] F. Andriulli, K. Cools, I. Bogaert, and E. Michielssen, *On a well-conditioned electric field integral operator for multiply connected geometries*, IEEE Transactions on Antennas and Propagation, Online Early Access, (2012).

[4] F. Andriulli, A. Tabacco, and G. Vecchi, *Solving the EFIE at low frequencies with a conditioning that grows only logarithmically with the number of unknowns*, IEEE Transactions on Antennas and Propagation, 58 (2010), pp. 1614 –1624.

[5] F. P. Andriulli, K. Cools, H. Bagci, F. Olyslager, A. Buffa, S. Christiansen, and E. Michielssen, *A multiplicative calderon preconditioner for the electric field integral equation*, IEEE Transactions on Antennas and Propagation, 56 (2008), pp. 2398–2412.

[6] I. Bogaert, K. Cools, F. Andriulli, and D. De Zutter, *Low frequency scaling of the mixed MFIE for scatterers with a non-simply connected surface*, in International Conference on Electromagnetics in Advanced Applications (ICEAA), 2011, Sept. 2011, pp. 951 –954.

[7] I. Bogaert, K. Cools, F. Andriulli, J. Peeters, and D. De Zutter, *Low frequency stability of the mixed discretization of the MFIE*, in Proceedings of the 5th European Conference on Antennas and Propagation (EUCAP), Apr. 2011, pp. 2463 –2465.

[8] A. Buffa and S. H. Christiansen, *A dual finite element complex on the barycentric refinement*, Math. Comp., 76 (2007), pp. 1743–1769.

[9] W. C. Chew, M. S. Tong, and B. Hu, *Integral equation methods for electromagnetic and elastic waves*, Synthesis Lectures on Computational Electromagnetics, 3 (2008), pp. 1–241.

[10] S. H. Christiansen and J.-C. Nedélec, *A preconditioner for the electric field integral equation based on Calderon formulas*, SIAM J. Num. Anal., 40 (2002), pp. 1100–1135.
[11] H. Contopanagos, B. Dembart, M. Epton, J. Ottusch, V. Rokhlin, J. Visher, and S. M. Wandzura, *Well-conditioned boundary integral equations for three-dimensional electromagnetic scattering*, IEEE Transactions on Antennas and Propagation, 50 (2002), pp. 1824–1930.
[12] T. F. Eibert, *Iterative-solver convergence for loop-star and loop-tree decompositions in method-of-moments solutions of the electric field integral equation*, IEEE Antennas and Propagation Magazine, 46 (2004), pp. 80–85.
[13] C. L. Epstein, Z. Gimbutas, L. Greengard, A. Klöckner, and M. O'Neil, *A consistency condition for the vector potential in multiply-connected domains*, arXiv:1203.3993, (2012).
[14] C. L. Epstein and L. Greengard, *Debye sources and the numerical solution of the time harmonic Maxwell equations*, Communications on Pure and Applied Mathematics, 63 (2010), pp. 413–463.
[15] L. Greengard and V. Rokhlin, *A fast algorithm for particle simulations*, Journal of Computational Physics, 73 (1987), pp. 325 – 348.
[16] R. Hiptmair and S.-P. Mao, *Stable multilevel splittings of boundary edge element spaces*, BIT, 52 (2012), pp. 661–685.
[17] J.-F. Lee, R. Lee, and R. J. Burkholder, *Loop star basis functions and a robust preconditioner for EFIE scattering problems*, IEEE Transactions on Antennas and Propagation, 51 (2003), pp. 1855–1863.
[18] C.-C. Lu and W. Chew, *A multilevel algorithm for solving a boundary integral equation of wave scattering*, Microwave Opt. Technol. Lett., 7 (1994), pp. 466–470.
[19] E. Michielssen and A. Boag, *A multilevel matrix decomposition algorithm for analyzing scattering from large structures*, IEEE Transactions on Antennas and Propagation, 44 (1996), pp. 1086–1093.
[20] Z.-G. Qian and W. C. Chew, *Enhanced A-EFIE with perturbation method*, IEEE Transactions on Antennas and Propagation, 58 (2010), pp. 3256 –3264.
[21] M. Stephanson and J.-F. Lee, *Preconditioned electric field integral equation using Calderon identities and dual loop/star basis functions*, IEEE Transactions on Antennas and Propagation, 57 (2009), pp. 1274–1279.
[22] G. Vecchi, *Loop-star decomposition of basis functions in the discretization of the EFIE*, IEEE Transactions on Antennas and Propagation, 47 (1999), pp. 339–346.
[23] D. R. Wilton and A. W. Glisson, *On improving the stability of the electric field integral equation at low frequencies*, USNC/URSI Spring Meeting Digest, (1981), p. 24.
[24] S. Yan, J.-M. Jin, and Z. Nie, *EFIE analysis of low-frequency problems with loop-star decomposition and Calderon multiplicative preconditioner*, IEEE Transactions on Antennas and Propagation, 58 (2010), pp. 857 –867.
[25] Y. Zhang, T. J. Cui, W. C. Chew, and J.-S. Zhao, *Magnetic field integral equation at very low frequencies*, IEEE Transactions on Antennas and Propagation, 51 (2003), pp. 1864 – 1871.
[26] J. S. Zhao and W. C. Chew, *Integral equation solution of Maxwell's equations from zero frequency to microwave frequencies*, IEEE Transactions on Antennas and Propagation, 48 (2000), pp. 1635–1645.

New tools for the high-order solution of frequency-domain wave scattering problems at high frequencies and in periodic geometries

Alexander Barnett

(joint work with Leslie Greengard, Zydrunas Gimbutas, Andreas Klöckner, Mike O'Neil, and Adrianna Gillman)

Abstract. *Boundary integral equation methods are efficient for frequency-domain wave scattering problems in piecewise-homogeneous media. A correct choice of representation leads to a 2nd-kind equation which can be solved by the Nyström method in a well-conditioned manner. We present a simple new scheme, called "quadrature by expansion" (QBX), for high-order Nyström quadratures of weakly-singular kernels on curves in 2D and surfaces in 3D. This exploits local expansions at centers near the surface, and avoids singularities altogether. We demonstrate its performance for sound-soft scattering from a torus* 30 *wavelengths in size. We also sketch new schemes for periodizing the integral equations that rely on free-space Green's functions alone, without the need for lattice sums, which are high-order accurate and robust at Wood's anomalies.*

Introduction. The aim of this report is to summarize the key ideas in some recent progress in numerical algorithms. For simplicity we consider the sound-soft (Dirichlet boundary condition) case. Let Ω be the complement of a bounded obstacle in $\mathbb{R}^2$ or $\mathbb{R}^3$, and $\partial\Omega$ be its smooth boundary. An incident plane wave $u^{\mathrm{i}}(x) = e^{i\omega x\cdot d}$, where $\|d\| = 1$ is a direction vector, impinges on the obstacle. We care about the case of frequency ω large. The total field $u^{\mathrm{t}} = u^{\mathrm{i}} + u$ satisfies the physical zero boundary condition on $\partial\Omega$, where u is the scattered field which solves the boundary value problem,

$$\begin{aligned} (\Delta + \omega^2)u &= 0 \qquad \text{in } \Omega \\ u &= -u^{\mathrm{i}} \qquad \text{on } \partial\Omega \\ u &\quad \text{radiative as } \|x\| \to \infty \ . \end{aligned}$$

The standard indirect "combined field" integral equation (IE) approach [6] sets $u = (\mathcal{D} - i\omega\mathcal{S})\tau$ in Ω, with unknown density $\tau \in C(\partial\Omega)$, where $\mathcal{S}$ and $\mathcal{D}$ are the single- and double-layer representations based on the free-space Green's function, e.g. $\Phi(x,y) = \frac{i}{4}H_0^{(1)}(\omega\|x-y\|)$ in 2D [6]. Evaluating u^+ (the exterior limit of u on $\partial\Omega$) using the jump relations gives the 2nd-kind IE,

$$(\tfrac{1}{2} + D - i\omega S)\tau = -u^{\mathrm{i}}|_{\partial\Omega}$$

which is approximated in the Nyström method [14] by the linear system

$$A\boldsymbol{\tau} = \mathbf{b}$$

by the use of an N-node quadrature scheme (nodes x_j, weights w_j) on $\partial\Omega$, for instance a composite Legendre (panel-based) rule in 2D, or high-order patches in 3D. For large N the system can only be solved iteratively, for instance via GMRES, applying A via the fast multipole method (FMM) [5]. The rule for matrix elements of A is trivial for "distant" (non-touching) panels (this can be applied via FMM),

but is difficult for neighboring panels or the self-interaction of a panel, due to the singular kernel (this part must be applied as a local *correction* to the FMM). For global quadratures on curves in 2D, a variety of methods exist [13, 11, 1], reviewed in [9]; for panels the generalized Gaussian approach due to Rokhlin or analytic method of Helsing [10] are excellent. However, these schemes do not generalize well to 3D.

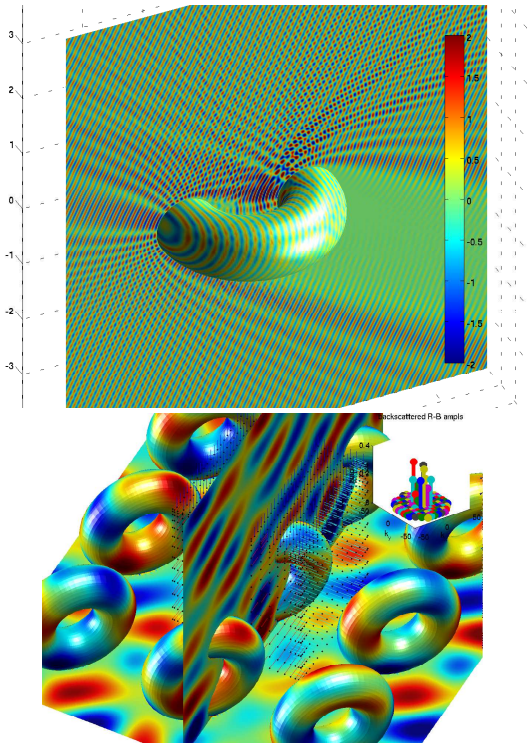

FIGURE 1. Left: Scattering from a torus 30 wavelengths across, computed using QBX quadratures, FMM and GMRES (full field shown on slice). Right: Scattering from a doubly-periodic infinite array of tori (full field shown on slices; diffracted fluxes inset).

f

Quadrature by expansion. Our recent scheme, QBX [2, 12], was invented with 3D in mind. Notice the following: *applying the matrix A to a vector $\boldsymbol{\tau}$ is equivalent to evaluating u^+ at the nodes for the potential generated by the interpolating function of τ.* Thus we have a *close evaluation* problem at a target point x which approaches $\partial\Omega$; this is hard because the integrand becomes nonsmooth. Howeve, for τ and $\partial\Omega$ analytic, u continues as a Helmholtz solution some distance *beyond* $\partial\Omega$ (i.e. inside the obstacle). Let $x_0 \in \Omega$ be a "center" point sufficiently near $\partial\Omega$ (typically around $3h$ distance, where h is the local node spacing), then

the local expansion (expressing x in local polar coordinates $(r,\theta) = x - x_0$)

$$u(x) = \sum_{n\in\mathbb{Z}} c_n J_n(\omega r) e^{in\theta} \qquad \text{local expansion (LE)}$$

converges uniformly in a ball which includes some target nodes on $\partial\Omega$. Fixing an order p (e.g. 10), the recipe for evaluating u^+ is then:

(i) Compute c_n for $|n| < p$ via Graf's addition theorem [15, (10.3.7)], e.g. for the single-layer case,

$$c_n = \frac{i}{4}\int_{\partial\Omega} H_n^{(1)}(\omega\|x_0 - y\|) e^{-in\theta_{x_0-y}} \tau(y) ds_y \tag{1}$$

where θ_x denotes the angle of vector x. This integral is evaluated on a set of "fine" nodes that are a factor β finer (typically $2 \le \beta \le 6$) in each dimension than the N original quadrature nodes, and τ is interpolated to high order onto these fine nodes.

(ii) Evaluate the LE to give u^+ on the sufficiently nearby target nodes on $\partial\Omega$.

This scheme ("global QBX") is proven to be exponentially convergent in p and β in the 2D Laplace case [2], and high-order convergent in Helmholtz in 2D and 3D [7]. In practice we often do not use the whole of $\partial\Omega$ in (1), only the 3 (in 2D) or 9 (in 3D) self and neighboring panels for each target panel; the remaining distant elements of A are applied via the FMM. The latter is called "local QBX", and introduces errors (as in any local quadrature-correction scheme) which can be made arbitrarily small by increasing p. The above two steps can be expressed as formulae for all near-diagonal elements of A involving small matrix-matrix products.

We implement QBX in 3D for the first time, using product $q \times q$ Legendre patches covering a parametrized surface, and the local (spherical harmonic) expansion

$$u(r,\theta,\phi) = \sum_{|n|\le p} \sum_{m=-n}^{n} c_{nm} j_n(\omega r) Y_n^m(\theta,\phi)$$

for which there is an addition formula. We precompute near-diagonal elements of A via QBX, then use these and the FMM to apply A in each GMRES iteration. Fig. 1 (left side) shows a result for a high-frequency scattering problem to 5 digit accuracy, achieved via $N = 145000$, $q = 8$, $p = 10$, $\beta = 4.5$, 1 hour for QBX, and 1 hour for 57 GMRES iterations (on a quad-core i7 laptop CPU).

Periodic scattering problems. The periodic scattering problem is also efficiently solved with IEs [16, 4], but the usual method involves handling the quasi-periodic Green's function Φ_{QP}. Our recent scheme [3] uses only free-space Green's kernels combined with a small extra "periodizing" basis set, i.e. the representation

$$u = \sum_{-1\le j\le 1} \alpha^j (\mathcal{D}_j - i\omega\mathcal{S}_j)\tau + \sum_{m=1}^{M} c_m \varphi_m \ ,$$

where $\mathcal{S}_j, \mathcal{D}_j$ denote layer representations living on the jth copy of $\partial\Omega$ in the grating, and $\alpha \in S^1$ is the Bloch phase. The basis functions φ_m must solve the Helmholtz equation in the unit cell (e.g. a local expansion). Enforcing the

boundary condition, and quasi-periodicity on the unit cell walls, gives a linear system with block structure,

$$\begin{bmatrix} A & B \\ C & Q \end{bmatrix} \begin{bmatrix} \tau \\ \mathbf{c} \end{bmatrix} = \begin{bmatrix} -u^{\mathrm{i}}|_{\partial\Omega} \\ 0 \end{bmatrix} . \tag{2}$$

See [3] for interpretations of the blocks. At so-called *Wood's anomalies* Φ_{QP} does not exist, and Q is singular, but one may solve (2) directly to get a robust scheme. On the other hand, if Φ_{QP} exists, we propose as an IE the Schur complement,

$$(A - BQ^{\dagger}C)\tau = -u^{\mathrm{i}}|_{\partial\Omega} . \tag{3}$$

The matrix $Q^{\dagger}C$ is in practice backwards-stably computed via MATLAB's backslash. Either approach is compatible with FMM, and needs only free-space kernels. (3) is a low-rank update to the free-space scattering problem, which we exploit in a direct solver 600× faster than the state-of-the-art FMM and GMRES iterative solution [8].

Finally, we may drop the Fourier Sommerfeld scheme of [3, 8], in favor of simply matching on the four walls of a finite "box" to construct the above operator blocks. This cleanly handles the case of half-space periodic Green's functions, which exist even at Wood's anomalies. Combining these techniques in the case of scattering from a bi-periodic array of tori in 3D (with QBX quadrature), we get preliminary results shown in Fig. 1 (right side): 5 digit accuracy with $N = 4032$, $M = 1339$, in 31 GMRES iterations, in 1 minute (20 s to construct QBX quadratures).

References

[1] B. K. Alpert, *Hybrid Gauss-trapezoidal quadrature rules*, SIAM J. Sci. Comput., 20 (1999), pp. 1551–1584.

[2] A. H. Barnett, *Evaluation of layer potentials close to the boundary for laplace and helmholtz problems on analytic planar domains*, 2012. submitted, *SIAM J. Sci. Comput.*

[3] A. H. Barnett and L. Greengard, *A new integral representation for quasi-periodic scattering problems in two dimensions*, BIT Numer. Math., 51 (2011), pp. 67–90.

[4] O. P. Bruno and M. C. Haslam, *Efficient high-order evaluation of scattering by periodic surfaces: deep gratings, high frequencies, and glancing incidences*, J. Opt. Soc. Am. A, 26 (2009), pp. 658–668.

[5] H. Cheng, W. Y. Crutchfield, Z. Gimbutas, G. L., F. Ethridge, J. Huang, V. Rokhlin, N. Yarvin, and J. Zhao, *A wideband fast multipole method for the Helmholtz equation in three dimensions*, J. Comput. Phys., 216 (2006), pp. 300–325.

[6] D. Colton and R. Kress, *Inverse acoustic and electromagnetic scattering theory*, vol. 93 of Applied Mathematical Sciences, Springer-Verlag, Berlin, second ed., 1998.

[7] C. L. Epstein, L. Greengard, and A. Klöckner, *On the convergence of local expansions of layer potentials*, 2012. `arXiv:1212.3868`.

[8] A. Gillman and A. H. Barnett, *A fast direct solver for quasi-periodic scattering problems*, 2012. submitted, *J. Comput. Phys.*

[9] S. Hao, A. H. Barnett, P. G. Martinsson, and P. Young, *High-order accurate Nyström discretization of integral equations with weakly singular kernels on smooth curves in the plane*, 2012. accepted, Adv. Comput. Math., `arxiv:1112.6262v2`.

[10] J. Helsing, *Solving integral equations on piecewise smooth boundaries using the RCIP method: a tutorial*, 2012. preprint, 34 pages, `arXiv:1207.6737v3`.

[11] S. Kapur and V. Rokhlin, *High-order corrected trapezoidal quadrature rules for singular functions*, SIAM J. Numer. Anal., 34 (1997), pp. 1331–1356.

[12] A. Klöckner, A. H. Barnett, L. Greengard, and M. O'Neil, *Quadrature by expansion: a new method for the evaluation of layer potentials*, 2012. to appear, J. Comput. Phys., arxiv:1207.4461.
[13] R. Kress, *Boundary integral equations in time-harmonic acoustic scattering*, Mathl. Comput. Modelling, 15 (1991), pp. 229–243.
[14] R. Kress, *Linear Integral Equations*, vol. 82 of Applied Mathematical Sciences, Springer, second ed., 1999.
[15] F. W. J. Olver, D. W. Lozier, R. F. Boisvert, and C. W. Clark, eds., *NIST Handbook of Mathematical Functions*, Cambridge University Press, 2010. http://dlmf.nist.gov.
[16] B. Zhang and S. N. Chandler-Wilde, *Integral equation methods for scattering by infinite rough surfaces*, Math. Meth. Appl. Sci., 26 (2003), pp. 463–488.

Wideband Nested Cross Approximation for Helmholtz problems

Mario Bebendorf
(joint work with Christian Kuske, Raoul Venn)

In this talk, the efficient numerical solution of Helmholtz problems

$$-\Delta u - \kappa^2 u = 0 \quad \text{in } \Omega^c, \tag{1a}$$

$$u + \alpha \partial_\nu u = u_0 \quad \text{on } \Gamma := \partial\Omega \tag{1b}$$

used to model acoustics and electromagnetic scattering will be considered. Herein, κ denotes the *wave number* and $\Omega^c := \mathbb{R}^3 \setminus \overline{\Omega}$ the exterior domain of the obstacle $\Omega \subset \mathbb{R}^3$. The paramter α and the right-hand side u_0 appearing in the impedance condition (1b) are given. A convenient way to solve exterior problems is the reformulation as an integral equation [7, 10, 9] over the boundary Γ of the scatterer Ω. The Galerkin discretization leads to large-scale fully populated matrices $A \in \mathbb{C}^{M\times N}$,

$$a_{ij} = \int_\Gamma \int_\Gamma K(x,y)\varphi_i(x)\psi_j(y)\,\mathrm{d}s_y\,\mathrm{d}s_x, \quad i \in I := \{1,\dots,M\},\ j \in J := \{1,\dots,N\}, \tag{2}$$

with test and ansatz functions φ_i, ψ_j, having supports $X_i := \operatorname{supp}\varphi_i$ and $Y_j := \operatorname{supp}\psi_j$, respectively. We consider kernel functions K of the form

$$K(x,y) := f(x,y)\exp(\mathrm{i}\kappa|x-y|) \tag{3}$$

with an arbitrary *asymptotically smooth* (with respect to x and y) function f, i.e., there are constants $c_{\mathrm{as},1}, c_{\mathrm{as},2} > 0$ such that for $\boldsymbol{\alpha}, \boldsymbol{\beta} \in \mathbb{N}^3$

$$|\partial_x^{\boldsymbol{\alpha}}\partial_y^{\boldsymbol{\beta}} f(x,y)| \le c_{\mathrm{as},1} c_{\mathrm{as},2}^p\, \boldsymbol{\alpha}!\boldsymbol{\beta}!\, \frac{|f(x,y)|}{|x-y|^p}, \quad p := |\boldsymbol{\alpha}+\boldsymbol{\beta}|.$$

An example is $K(x,y) = S(x-y)$ used in the single layer ansatz, where $S(x) = \exp(\mathrm{i}\kappa|x|)/(4\pi|x|)$ denotes the fundamental solution. Notice that the double layer potential $K(x,y) = \partial_{\nu_y} S(x-y)$ is of the form (3) only if Γ, i.e. the unit outer normal ν, is sufficiently smooth.

Depending on the application, low or high-frequency problems are to be solved. For low-frequency problems, i.e. for $\kappa \operatorname{diam}\Omega \le 1$, the *treecode algorithm* [4] and *fast multipole methods* (FMM) [26, 19, 18, 20] were introduced to treat A with

log-linear complexity. The *panel clustering method* [23] is directed towards more general kernel functions. All previous methods rely on *degenerate approximations*

$$K(x,y) \approx \sum_{i=1}^{k} u_i(x) v_i(y), \quad x \in X,\, y \in Y, \tag{4}$$

using a short sum of products of functions u_i and v_i depending on only one of the two variables x and y chosen from a pair of domains $X \times Y$ which satisfies the *far-field condition*

$$\eta_{\text{low}} \operatorname{dist}(X,Y) \geq \max\{\operatorname{diam} X, \operatorname{diam} Y\} \tag{5}$$

with a given parameter $\eta_{\text{low}} > 0$. Since replacing the kernel function K in the integrals (2) with degenerate approximations (4) leads to matrices of low rank, a more direct approach to the efficient treatment of matrices (2) are algebraic methods such as *mosaic-skeletons* [29] and *hierarchical matrices* [21, 22]. These methods also allow to define approximate replacements for the usual matrix operations such as addition, multiplication, inversion, and LU factorization; cf. [17]. An efficient and comfortable way to construct low-rank approximations is the *adaptive cross approximation* (ACA) method [5]. The advantage of this approach compared with explicit kernel approximation is that significantly better approximations can be expected due the quasi-optimal approximation properties; cf. [6]. Furthermore, ACA has the practical advantage that only few of the original entries of A are used for its approximation. A second class are *wavelet compression techniques* [1], which lead to sparse and asymptotically well-conditioned approximations of the coefficient matrix.

It is known that the fundamental solution S (and its derivatives) of any elliptic operator allows for a degenerate approximation (4) on a pair of domains (X,Y) satisfying (5); see [6]. This applies to the *Yukawa operator* $-\Delta + \kappa^2$ for any κ, because the decay of S benefits from the positive shift κ^2. However, the negative shift $-\kappa^2$ in the Helmholtz operator introduces oscillations in S. Hence, for high-frequency Helmholtz problems, i.e. for $\kappa \operatorname{diam} \Omega > 1$, the wave number κ enters the degree of degeneracy k in (4) in a way that k grows linearly with κ. In addition to this difficulty, the mesh width h of the discretization has to be chosen such that $\kappa h \sim 1$ for a sufficient accuracy of the solution. We assume that

$$h_\kappa := \kappa h < \frac{1}{4}, \quad h := \max\{\operatorname{diam} X_i, \operatorname{diam} Y_j,\, i \in I,\, j \in J\} \;\sim\; 1/\sqrt{N},$$

which implies that $\kappa \sim \sqrt{N} \sim \sqrt{M}$. Notice that the recent formulation [12] allows to avoid the previous condition and hence leads to significantly smaller N. For high-frequency Helmholtz problems, one- and two-level versions [27, 28] were presented with complexity $O(N^{3/2})$ and $O(N^{4/3})$, respectively. Multi-level algorithms [14, 2] are able to achieve logarithmic-linear complexity. The previous methods are based on an extensive analytic apparatus that is tailored to the kernel function K. To overcome the instability of some of the employed expansions at low frequencies, a wideband version of FMM was presented in [13]. The $\mathcal{H}^2$-matrix

approach presented in [3] is based on the explicit kernel expansions used in [2, 27] for two-dimensional problems.

A well-known idea from physical optics is to approximate $K(\cdot, y)$ in a given direction $e \in \mathbb{S}^2$ by a plane wave; cf. Figure 1. The desired boundedness of k with respect to κ when approximating

$$\hat{K}(x, y) := K(x, y) \exp(-\mathrm{i}\kappa(x - y, e))$$

can be achieved if (5) is replaced by a condition which depends on κ and which is directionally dependent. This is exploited by the fast multipole methods presented

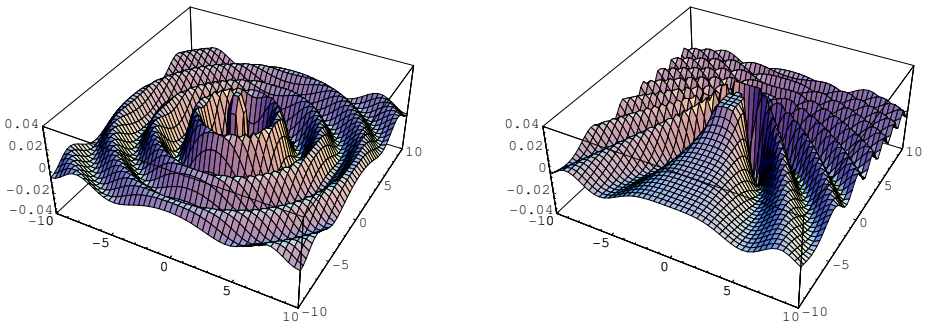

FIGURE 1. Re $K(x_1, x_2, 0)$ and Re $\hat{K}(x_1, x_2, 0)$ with $e = (0, 1, 0)^T$.

in [8, 15, 16, 24] and the so-called butterfly algorithm [25, 11]. The aim of this paper is to combine this approach with the ease of use of ACA, i.e., our aim is to construct approximations to A with complexity $kN \log N$ using only few of the original entries of A. In this sense, this paper generalizes ACA (which achieves log-linear complexity only for low-frequencies) to high-frequency Helmholtz problems. An interesting and important property of the new method is that it will allow a continuous and numerically stable transition from low to high wave numbers κ by a generalized far-field condition that fades to the usual condition (5) if the wave number becomes small. Since we approximate the operator rather than just its application to a vector, this paper is expected to lay ground to future work related to the definition of approximate arithmetic operations and hence to efficient preconditioners for high-frequency problems.

REFERENCES

[1] B. K. ALPERT, G. BEYLKIN, R. COIFMAN, AND V. ROKHLIN, *Wavelet-like bases for the fast solution of second-kind integral equations*, SIAM J. Sci. Comput., 14 (1993), pp. 159–184.

[2] S. AMINI AND A. PROFIT, *Multi-level fast multipole solution of the scattering problem*, Engineering Analysis with Boundary Elements, 27 (2003), pp. 547–654.

[3] L. BANJAI AND W. HACKBUSCH, *Hierarchical matrix techniques for low- and high-frequency Helmholtz problems*, IMA J. Numer. Anal., 28 (2008), pp. 46–79.

[4] J. BARNES AND P. HUT, *A hierarchical $\mathcal{O}(N \log N)$ force calculation algorithm*, Nature, 324 (1986), pp. 446–449.

[5] M. Bebendorf, *Approximation of boundary element matrices*, Numer. Math., 86 (2000), pp. 565–589.
[6] ———, *Hierarchical Matrices: A Means to Efficiently Solve Elliptic Boundary Value Problems*, vol. 63 of Lecture Notes in Computational Science and Engineering (LNCSE), Springer, 2008. ISBN 978-3-540-77146-3.
[7] H. Brakhage and P. Werner, *Über das Dirichletsche Außenraumproblem für die Helmholtzsche Schwingungsgleichung*, Arch. Math., 16 (1965), pp. 325–329.
[8] A. Brandt, *Multilevel computations of integral transforms and particle interactions with oscillatory kernels*, Comput. Phys. Comm., 65 (1991), pp. 24–38.
[9] A. Buffa and R. Hiptmair, *A coercive combined field integral equation for electromagnetic scattering*, SIAM J. Numer. Anal., 42 (2003), pp. 621–640.
[10] A. J. Burton and G. F. Miller, *The application of integral equation methods to the numerical solution of boundary value problems*, Proc. Roy. Soc., London, A232 (1971), pp. 201–210.
[11] E. Candès, L. Demanet, and L. Ying, *A fast butterfly algorithm for the computation of Fourier integral operators*, Multiscale Model. Simul., 7 (2009), pp. 1727–1750.
[12] S. N. Chandler-Wilde, I. G. Graham, S. Langdon, and E. A. Spence, *Numerical-asymptotic boundary integral methods in high-frequency acoustic scattering*, Acta Numerica, 21 (2012), pp. 89–305.
[13] H. Cheng, W. Y. Crutchfield, Z. Gimbutas, L. F. Greengard, J. F. Ethridge, J. Huang, V. Rokhlin, N. Yarvin, and J. Zhao, *A wideband fast multipole method for the Helmholtz equation in three dimensions*, J. Comput. Phys., 216 (2006), pp. 300–325.
[14] E. Darve, *The fast multipole method: numerical implementation*, J. Comput. Phys., 160 (2000), pp. 195–240.
[15] B. Engquist and L. Ying, *Fast directional multilevel algorithms for oscillatory kernels*, SIAM J. Sci. Comput., 29 (2007), pp. 1710–1737 (electronic).
[16] ———, *A fast directional algorithm for high frequency acoustic scattering in two dimensions*, Commun. Math. Sci., 7 (2009), pp. 327–345.
[17] L. Grasedyck and W. Hackbusch, *Construction and arithmetics of $\mathcal{H}$-matrices*, Computing, 70 (2003), pp. 295–334.
[18] L. Greengard, *The rapid evaluation of potential fields in particle systems*, MIT Press, Cambridge, MA, 1988.
[19] L. F. Greengard and V. Rokhlin, *A fast algorithm for particle simulations*, J. Comput. Phys., 73 (1987), pp. 325–348.
[20] L. F. Greengard and V. Rokhlin, *A new version of the fast multipole method for the Laplace equation in three dimensions*, in Acta numerica, 1997, vol. 6 of Acta Numer., Cambridge Univ. Press, Cambridge, 1997, pp. 229–269.
[21] W. Hackbusch, *A sparse matrix arithmetic based on $\mathcal{H}$-matrices. Part I: Introduction to $\mathcal{H}$-matrices*, Computing, 62 (1999), pp. 89–108.
[22] W. Hackbusch and B. N. Khoromskij, *A sparse $\mathcal{H}$-matrix arithmetic: general complexity estimates*, J. Comput. Appl. Math., 125 (2000), pp. 479–501. Numerical analysis 2000, Vol. VI, Ordinary differential equations and integral equations.
[23] W. Hackbusch and Z. P. Nowak, *On the fast matrix multiplication in the boundary element method by panel clustering*, Numer. Math., 54 (1989), pp. 463–491.
[24] M. Messner, M. Schanz, and E. Darve, *Fast directional multilevel summation for oscillatory kernels based on Chebyshev interpolation*, J. Comput. Phys., 231 (2012), pp. 1175–1196.
[25] E. Michielssen and A. Boag, *A multilevel matrix decomposition for analyzing scattering from large structures*, IEEE Trans. Antennas Propag., 44 (1996), pp. 1086–1093.
[26] V. Rokhlin, *Rapid solution of integral equations of classical potential theory*, J. Comput. Phys., 60 (1985), pp. 187–207.
[27] ———, *Rapid solution of integral equations of scattering theory in two dimensions*, J. Comput. Phys., 86 (1990), pp. 414–439.

[28] ———, *Diagonal forms of translation operators for the Helmholtz equation in three dimensions*, Appl. Comput. Harmon. Anal., 1 (1993), pp. 82–93.
[29] E. E. Tyrtyshnikov, *Mosaic-skeleton approximations*, Calcolo, 33 (1996), pp. 47–57 (1998). Toeplitz matrices: structures, algorithms and applications (Cortona, 1996).

Solution of electromagnetic problems using BEM++

Timo Betcke
(joint work with Simon Arridge, Joel Phillips, Martin Schweiger and Wojciech Śmigaj)

BEM++ (`www.bempp.org`) is a novel open source boundary element library for complex boundary element simulations of problems in three space dimensions. The first official version of BEM++, 1.0, was released in October 2012. The library lets the user construct Galerkin discretisations of all standard boundary integral operators (single-layer potential, double-layer potential, adjoint double-layer potential, hypersingular operator) for Laplace, Helmholtz and modified Helmholtz problems in three dimensions. These operators can be represented either as dense matrices or, if the library is linked against the AHMED library by M. Bebendord [2], as $\mathcal{H}$-matrices [1]. In the latter case, the adaptive cross approximation (ACA) algorithm is used to accelerate the assembly. On shared-memory multicore machines, matrix assembly can be done in parallel.

The library makes it easy to combine the standard integral operators into arbitrary integral equations or systems of integral equations. It also provides wrappers to a wide range of iterative solvers from the Trilinos library. On systems with AHMED, preconditioners based on approximate H-LU decompositions of operators stored in the $\mathcal{H}$-matrix format can be constructed to accelerate solver convergence.

A distinctive feature of BEM++ is its dual, C++/Python interface. The library is implemented principally in C++, and all its features can be used from this language. To facilitate rapid development, however, BEM++ provides also Python bindings for most of its high-level features. The possibility of interactive work in a Python shell is very convenient in practice. More details about BEM++ are given in [4].

The highlight of the upcoming 2.0 release of BEM++ is support for the solution of Maxwell equations in three dimensions. In this contribution we will briefly discuss the implementation of the features necessary for this purpose and present the results of some test calculations.

The treatment of Maxwell equations in BEM++ closely follows that of [3]. Thus, it is based on two integral operators only: the single-layer potential operator $\boldsymbol{\Psi}_{\mathrm{SL}}$ and the double-layer potential operator $\boldsymbol{\Psi}_{\mathrm{DL}}$. The action of the single-layer potential operator is defined as

$$(1) \qquad (\boldsymbol{\Psi}_{\mathrm{SL}}\boldsymbol{v})(\boldsymbol{x}) \equiv \mathrm{i}k \int_{\Gamma} G(\boldsymbol{x},\boldsymbol{y})\boldsymbol{v}(\boldsymbol{y})\Gamma(\boldsymbol{y}) - \frac{1}{\mathrm{i}k}\boldsymbol{\nabla}_{\boldsymbol{x}} \int_{\Gamma} G(\boldsymbol{x},\boldsymbol{y})(\boldsymbol{\nabla}_{\Gamma}\cdot\boldsymbol{v})(\boldsymbol{y})\Gamma(\boldsymbol{y}),$$

where

$$G(\boldsymbol{x},\boldsymbol{y}) \equiv \frac{\exp(\mathrm{i}k|\boldsymbol{x}-\boldsymbol{y}|)}{4\pi|\boldsymbol{x}-\boldsymbol{y}|} \tag{2}$$

is the Green's function of the Helmholtz equation with wave number k and $\boldsymbol{v}(\boldsymbol{x})$ is a vector-valued function defined on a surface Γ. This definition is almost identical to eq. (27) in [3]; compared to that equation, we include an additional factor i to make the operator real-valued for purely imaginary values of k. The action of the *double-layer potential operator*, in turn, is defined by

$$(\Psi_{\mathrm{DL}}\boldsymbol{v})(\boldsymbol{x}) \equiv \boldsymbol{\nabla}_{\boldsymbol{x}} \times \int_{\Gamma} G(\boldsymbol{x},\boldsymbol{y})\boldsymbol{v}(\boldsymbol{y})\Gamma(\boldsymbol{y}), \tag{3}$$

identically as in eq. (28) from [3]. In the Python interface of BEM++, the operators defined above can be constructed using functions

`createMaxwell3dSingleLayerPotentialOperator()`

and

`createMaxwell3dDoubleLayerPotential-Operator()`.

Taking the interior and exterior Dirichlet and Neumann traces of the Stratton-Chu representation formula [3, theorem 6] for the solutions of Maxwell equations with wave number k in a bounded domain Ω with boundary Γ, one arrives at the following boundary integral equations:

$$(-\tfrac{1}{2}\boldsymbol{I} + \boldsymbol{C})\gamma_{\mathrm{D,int}}\boldsymbol{u} + \boldsymbol{S}\gamma_{\mathrm{N,int}}\boldsymbol{u} = 0 \tag{4}$$

$$-\boldsymbol{S}\gamma_{\mathrm{D,int}}\boldsymbol{u} + (-\tfrac{1}{2}\boldsymbol{I} + \boldsymbol{C})\gamma_{\mathrm{N,int}}\boldsymbol{u} = 0. \tag{5}$$

Here, $\boldsymbol{u}$ can denote either the electric or the magnetic field. The *interior Dirichlet trace* $\gamma_{\mathrm{D,int}}\boldsymbol{u}$ at a point $\boldsymbol{x} \in \Gamma$ is defined as

$$(\gamma_{\mathrm{D,int}}\boldsymbol{u})(\boldsymbol{x}) \equiv \boldsymbol{u}|_{\Gamma,\mathrm{int}}(\boldsymbol{x}) \times \boldsymbol{n}(\boldsymbol{x}), \tag{6}$$

where $\boldsymbol{n}$ is the outward unit vector normal to Γ at $\boldsymbol{x}$ and $\boldsymbol{u}|_{\Gamma,\mathrm{int}}(\boldsymbol{x})$ is the limit of $\boldsymbol{u}(\boldsymbol{y})$ as $\boldsymbol{y}$ approaches $\boldsymbol{x}$ from within Ω. The *interior Neumann trace* $\gamma_{\mathrm{N,int}}\boldsymbol{u}$ at $\boldsymbol{x} \in \Gamma$ is defined as

$$(\gamma_{\mathrm{N,int}}\boldsymbol{u})(\boldsymbol{x}) \equiv (\mathrm{i}k)^{-1}(\boldsymbol{\nabla} \times \boldsymbol{u})|_{\Gamma,\mathrm{int}}(\boldsymbol{x}) \times \boldsymbol{n}(\boldsymbol{x}). \tag{7}$$

Compared to Buffa and Hiptmair, we include an additional i factor in the denominator of the Neumann trace. The *exteror* Dirichlet and Neumann traces are defined analogously, with the relevant quantities assumed to approach the point $\boldsymbol{x}$ from within the complement of Ω. The *interior single-layer boundary operator* $\boldsymbol{S}$ and *double-layer boundary operator* $\boldsymbol{C}$ denote the averages of the interior and exterior traces of the corresponding potential operators with wavenumber k, and $\boldsymbol{I}$ stands for the identity operator.

Galerkin discretisations of the above equations involve the weak forms of operators $\boldsymbol{S}$ and $\boldsymbol{C}$. Following [3], the weak forms are defined with respect to the antisymmetric pseudo-inner product

$$\langle \boldsymbol{u},\boldsymbol{v}\rangle_{\boldsymbol{\tau},\Gamma} \equiv \int_{\Gamma} \boldsymbol{u}^* \cdot (\boldsymbol{v} \times \boldsymbol{n})\mathrm{d}\Gamma, \tag{8}$$

where $*$ denotes complex conjugation. Explicit expressions for the weak forms of $\boldsymbol{S}$ and $\boldsymbol{C}$ are given in eqs. (32) and (33) from [3] (the former needs to be multiplied by i to adapt it to the convention used in BEM++). Boundary operators with those weak forms are most easily constructed in BEM++ using the `createMaxwell3dSingleLayerBoundaryOperator()` and `createMaxwell3dDoubleLayerBoundaryOperator()` functions. In addition, the function `createMaxwell3dIdentityOperator()` yields an identity operator with weak form defined under the above pseudo-inner product.

Maxwell equations in an exterior domain $\mathbb{R}^3 \setminus \Omega$, with the Silver-Muller boundary conditions imposed at infinity, can be reduced to the following boundary integral equations:

$$(\tfrac{1}{2}\boldsymbol{I} + \boldsymbol{C})\gamma_{\mathrm{D,ext}}\boldsymbol{u} + \boldsymbol{S}\gamma_{\mathrm{N,ext}}\boldsymbol{u} = 0 \tag{9}$$

$$-\boldsymbol{S}\gamma_{\mathrm{D,ext}}\boldsymbol{u} + (\tfrac{1}{2}\boldsymbol{I} + \boldsymbol{C})\gamma_{\mathrm{N,ext}}\boldsymbol{u} = 0. \tag{10}$$

The exterior traces of $\boldsymbol{u}$ are defined in the obvious way.

Both the Dirichlet and Neumann traces of the electric and magnetic field, as defined in eqs. (6) and (6), belong to the Sobolev space $\boldsymbol{H}_{\times}^{-1/2}(\mathrm{div}_{\Gamma}, \Gamma)$ defined in [3]. Currently BEM++ provides a single discrete approximation of $\boldsymbol{H}_{\times}^{-1/2}(\mathrm{div}_{\Gamma}, \Gamma)$, the space of lowest-order Raviart-Thomas functions. It is represented with the class `RaviartThomas0VectorSpace`.

A common application of BEM in electromagnetics is the solution of scattering problems. These can involve both perfectly conducting and permeable objects. As a particular example, we consider the scattering of a plane wave from a dielectric hexagonal column with relative permittivity $\epsilon = 3.2$, approximately corresponding to that of ice at microwave frequencies. The ratio of column height to base diameter is set to 1.25. The problem is solved using the so-called CTF formulation, which has been found [5] to yield good accuracy at the price of sometimes poor conditioning. The equations take the form

$$\begin{bmatrix} \boldsymbol{S}_{\mathrm{ext}} + \boldsymbol{S}_{\mathrm{int}} & -(\frac{1}{2}(1-\rho^{-1})\boldsymbol{I} + \boldsymbol{C}_{\mathrm{ext}} + \rho^{-1}\boldsymbol{C}_{\mathrm{int}}) \\ \frac{1}{2}(1-\rho)\boldsymbol{I} + \boldsymbol{C}_{\mathrm{ext}} + \rho\boldsymbol{C}_{\mathrm{int}} & \boldsymbol{S}_{\mathrm{ext}} + \boldsymbol{S}_{\mathrm{int}} \end{bmatrix} \begin{bmatrix} \gamma_{\mathrm{D,ext}}\boldsymbol{E} \\ \gamma_{\mathrm{N,ext}}\boldsymbol{E} \end{bmatrix} = \begin{bmatrix} -\gamma_{\mathrm{N,ext}}\boldsymbol{E}_{\mathrm{inc}} \\ \gamma_{\mathrm{D,ext}}\boldsymbol{E}_{\mathrm{inc}} \end{bmatrix}, \tag{11}$$

where the operators with subscripts $_{\mathrm{int}}$ and $_{\mathrm{ext}}$ corresspond to wave numbers $k_0\sqrt{\epsilon_{\mathrm{int}}}$ and $k_0\sqrt{\epsilon_{\mathrm{ext}}}$, with ϵ_{int} and ϵ_{ext} denoting the relative permittivities of the scatterer and the medium in which it is embedded and k_0 standing for the wave number in vacuum. The symbol $\boldsymbol{E}_{\mathrm{inc}}$ is the electric field of the incident wave.

An approximate $\mathcal{H}$-LU decomposition of the weak form of the block-diagonal part of the operator above was used as a preconditioner. The accuracy of the LU decomposition was chosen as 1E−2, and the ACA tolerance ϵ as 1E−5. The remaining parameters were identical to those from the first example. Table 1 lists the time and memory consumption for increasing problem sizes. A somewhat unwelcome feature is the increasing fraction of time spent in the construction of the

TABLE 1. Benchmarks for the calculation of field scattered by a hexagonal ice column. The memory use of the operator $\boldsymbol{S}_{\text{int}}$ is given in megabytes and in percent of the memory use of an equivalent dense operator. The memory and time requirements of $\boldsymbol{C}_{\text{int}}$ are very similar and those of $\boldsymbol{S}_{\text{ext}}$ and $\boldsymbol{C}_{\text{ext}}$, lower.

		$\boldsymbol{S}_{\text{int}}$		Preconditioner		Solver	
H/λ	#Elem.	Mem. (MB / %)	t (s)	Mem. (MB)	t (s)	#It.	t (s)
1	638	9.9 (100 %)	0.5	4.66	0.75	44	0.4
2	2718	123.6 (57 %)	7.5	49.1	8.6	116	12.0
4	10740	986.7 (25 %)	45.7	471.9	91.6	192	93.1
8	46016	7541 (11 %)	325.6	4605.6	1293.2	472	1463.0

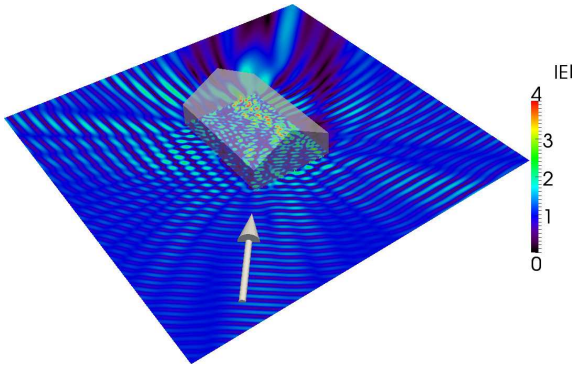

FIGURE 1. Magnitude of the electric field generated by a plane wave impinging on a hexagonal column with permittivity 3.2 surrounded by vacuum. The free-space wavelength λ of the wave is 8 times smaller than the height of the column. The arrow indicates the direction of the incident wave.

preconditioner. This is partly due to the serial nature of the current implementation of the $\mathcal{H}$-LU decomposition routine, as opposed to matrix assembly and matrix-vector multiplication, which are done in parallel.

Figure 1 shows a cross-section of the field generated in the highest-k case. The ACA algorithm was used in the evaluation of off-surface potentials, reducing the time used to evaluate the field at the chosen 400×400-point grid by a factor of four with respect to standard brute-force quadrature.

REFERENCES

[1] M. BEBENDORF, *Hierarchical Matrices: A Means to Efficiently Solve Elliptic Boundary Value Problems*, Lecture Notes in Computational Science and Engineering, 63, Springer, Berlin Heidelberg, 2008.

[2] M. BEBENDORF, *Another software library on hierarchical matrices for elliptic differential equations (AHMED)*, 2012. `http://bebendorf.ins.uni-bonn.de/AHMED.html`.

[3] A. Buffa and R. Hiptmair, *Topics in Computational Wave Propagation. Direct and inverse Problems*, Springer, 2003, ch. Galerkin boundary element methods for electromagnetic scattering, pp. 83–124.
[4] W. Śmigaj, S. R. Arridge, T. Betcke, J. Phillips, and M. Schweiger, *Solving boundary integral equations with BEM++*, tech. rep., University College London, 2012.
[5] P. Ylä-Oijala, M. Taskinen, and S. Järvenpää, *Surface integral equation formulations for solving electromagnetic scattering problems with iterative methods*, Radio Sci., 40 (2005), p. RS6002.

Selective Focusing for Time Dependent Waves

Maxence Cassier
(joint work with Christophe Hazard and Patrick Joly)

Abstract

We are concerned with focusing effects for time-dependent waves using an array of pointlike transducers. We consider a two-dimensional problem which models acoustic wave propagation in a medium which contains several unknown pointlike scatterers. Spatial focusing properties have been studied in the frequency domain in the context of the DORT method ("Decomposition of the Time Reversal Operator"). This method consists in doing a Singular Value Decomposition of the scattering operator, that is, the operator which maps the input signals sent to the transducers to the measure of the scattered wave. We show how to construct a wave that focuses in space and time near one of these scatterers, in the form of a superposition of time-harmonic waves related to the singular vectors of the scattering operator. Numerical results will be shown.

Introduction

We consider a reference medium, possibly inhomogeneous, filling the whole plane $\mathbb{R}^2$. We denote by G the time-dependent Green function of the acoustic wave equation, that is the causal solution to

$$\frac{1}{c^2(x)}\frac{\partial^2 G(x,y;t)}{\partial t^2} - \Delta_x G(x,y;t) = \delta(x-y)\otimes\delta(t)$$

where c is the wave speed function of the medium (e.g., $G(x,y;t) = -H(t-|x-y|)/(2\pi(t^2-|x-y|^2))^{\frac{1}{2}}$ for $c\equiv 1$, where H is the Heaviside function). We assume that the reference medium is perturbed by the presence of a family of P pointlike scatterers whose positions $s_1,\dots,s_P$ are unknown. Using an array of N point-like transducers located at x_n for $n=1,\dots,N$ (with $N\geq P$), our aim is to generate a wave that focuses in space and time on one of the scatterers. Such a wave is defined by

$$w(x,t) = \sum_{n=1}^{N}\left(G(x,x_n;\cdot)\overset{t}{\star} q_n\right)(t) \tag{1}$$

where $\mathbf{q}_{inp}(t) := (q_1(t), \ldots, q_N(t))^\top$ represents the input signals applied to the transducers and $\overset{t}{\star}$ denotes the time convolution. The question is to find signals $q_{\rm inp}(t)$ for which most part of the energy of the wave will be concentrated near one obstacle at a given time. In the present paper, we show how to deduce such signals from the only knowledge of the *scattering operator* $\mathbb{S} : \mathbf{q}_{\rm inp} \mapsto \mathbf{q}_{\rm mes}$ where $q_{\rm mes}$ represents the measures at points $x_1, \ldots, x_N$ of the scattered wave associated with the incident wave (1), that is, the perturbation of this incident wave due to the presence of the unknown scatterers. The idea is to take advantage of the so-called DORT method (see, e.g., [2, 4]) whose spatial focusing properties in the frequency domain are well known.

1. Space focusing in the frequency domain

Let $\widehat{G}$ denote the time-harmonic Green function of the reference medium which is related to the time-dependent Green function G by the Fourier transform:

$$G(x, y; t) = \frac{1}{\pi}\mathrm{Re}\left(\int_0^{+\infty} \widehat{G}(x, y; \omega)\, e^{-i\omega t}\, d\omega\right).$$

At a fixed frequency ω, the array of transducers emits a time-harmonic incident wave defined by

$$\hat{w}(x) = \sum_{n=1}^{N} \hat{q}_n\, \widehat{G}(x, x_n; \omega),$$

for a given $\hat{\mathbf{q}}_{\rm inp} := (\hat{q}_1, \ldots, \hat{q}_N)^\top \in \mathbb{C}^N$ (complex amplitudes of the input signals at the N transducers). Then, the array measures the scattered wave $\hat{q}_{mes}$. This yields the time-harmonic scattering operator $\widehat{\mathbb{S}}_\omega : \hat{\mathbf{q}}_{\rm inp} \mapsto \hat{\mathbf{q}}_{\rm mes}$ which can be written here as a product of three matrices:

$$\widehat{\mathbb{S}}_\omega \quad = \quad \underbrace{\widehat{\mathbb{G}}_\omega^\top}_{\text{back propagation}} \quad \underbrace{\widehat{\Sigma}_\omega}_{\text{reflection}} \quad \underbrace{\widehat{\mathbb{G}}_\omega}_{\text{direct propagation}} \quad ,$$

where $\widehat{\mathbb{G}}_\omega$ is a $P \times N$ matrix defined by $(\widehat{\mathbb{G}}_\omega)_{pn} := \widehat{G}(x_n, s_p; \omega)$ and $\widehat{\Sigma}_\omega$ is a $P \times P$ symmetric matrix ($\widehat{\Sigma}_\omega^\top = \widehat{\Sigma}_\omega$) which represents the reflections on the scatterers. The latter matrix depends on the choice of an asymptotic model for the scatterers. In the simplest case (no interaction between the scatterers), this is a diagonal matrix composed of the reflection coefficients of the scatterers. The more elaborate Foldy–Lax model [1] takes into account isotropic interactions.

The DORT method consists in a Singular Value Decomposition (SVD) of $\widehat{\mathbb{S}}_\omega$:

$$\widehat{\mathbb{S}}_\omega = \widehat{\mathbb{P}}_\omega\, \widehat{\mathbb{D}}_\omega\, \overline{\widehat{\mathbb{Q}}}_\omega^\top, \tag{2}$$

where $\widehat{\mathbb{D}}_\omega$, $\widehat{\mathbb{P}}_\omega$, $\widehat{\mathbb{Q}}_\omega$ are respectively the diagonal matrix of singular values, the matrices of the left and right singular vectors. It is now well understood ([2, 4]) that in a homogeneous medium, for distant enough scatterers, the number of nonzero singular values of $\widehat{\mathbb{S}}_\omega$ coincide with the number of scatterers. Moreover if such a singular value $\lambda_p(\omega)$ is simple, the associated right singular vector $\widehat{\mathbf{q}}_p(\omega)$

(pth column of $\widehat{\mathbb{Q}}_\omega$) generates a wave which focuses selectively on one scatterer, say s_p.

2. Space-time focusing

Suppose that in a given frequency band $[\omega_1, \omega_2]$ (imposed by the physical properties of our array), we know a right singular vector $\widehat{\mathbf{q}}_p(\omega) \in \mathbb{C}^N$ associated with the pth obstacle and a simple singular value $\lambda_p(\omega)$. How can one choose a function $A(\omega)$ defined on the frequency band such that the superposition of the time-harmonic input signals:

$$\mathbf{q_p}(t) = \mathrm{Re} \int_{\omega_1}^{\omega_2} A(\omega)\, \widehat{\mathbf{q}}_p(\omega)\, e^{-\mathrm{i}\omega t}\, \mathrm{d}! \tag{3}$$

generates an incident wave which focuses not only in space near s_p, but also in time?

We look for a function A as a product $A(\omega) = \chi(\omega)e^{i\phi(\omega)}$ with χ a given real cutoff function and ϕ an unknown phase. This is a problem of frequency phase synchronization. The phase choice that we propose is based on a particular SVD of the scattering operator related to its symmetry. $\widehat{\mathbb{S}}_\omega$ is a symmetric operator, therefore up to a change of sign, there exists a unique $\phi_{sym} \in [-\pi, \pi[$ such that

$$\widehat{\mathbb{S}}_\omega\, e^{\mathrm{i}\phi_{sym}(\omega)} \widehat{\mathbf{q}}_p(\omega) = \lambda_p(\omega)\, \overline{e^{\mathrm{i}\phi_{sym}(\omega)} \widehat{\mathbf{q}}_p(\omega)}, \tag{4}$$

$e^{i\phi_{sym}(\omega)}\widehat{\mathbf{q}}_p(\omega)$ is then a right singular vector of a symmetric SVD of $\widehat{\mathbb{S}}_\omega$: $\overline{\mathbb{U}}_\omega \mathbb{D}_{\gtrless} \overline{\mathbb{U}}_\omega^\top$ (see [3] for more details). Does this signal yield an *optimal* focusing? We did not succeed in finding a mathematical functional representing the focusing quality which would be maximal for this particular choice. But several arguments are pointing in that direction.

The first one is heuristic. As the time reversal operation $\mathbb{J} : f(t) \mapsto f(-t)$ becomes a complex conjugation in the frequency domain, we see with (4) that at each frequency, the measure of the scattered field is (up to a positive real factor $\lambda_p(\omega)$) the time reversed emitted signal. This temporal symmetry synchronizes the spectral components of the emitted wave at the focusing time $t = 0$. The mathematical counterpart of this property lies in the following proposition. We denote for a function $\phi \in L^\infty([\omega_1, \omega_2])$,

$$\mathbf{q}_p[\phi] := \mathrm{Re} \left(\int_{\omega_1}^{\omega_2} \chi(\omega)\, e^{i\phi(\omega)}\, \hat{\mathbf{q}}_p(\omega)\, e^{-\mathrm{i}\omega\cdot}\, \mathrm{d}\omega \right).$$

Proposition 1. *ϕ_{sym} satisfies the following optimization problem:*

$$\inf_{\nu \in \mathbb{R}^{+*}, \phi \in L^\infty([\omega_1,\omega_2]} \| (\mathbb{S} - \nu \mathbb{J})\, \mathbf{q}_p[\phi] \|_{L^2(\mathbb{R}, \mathbb{C}^N)}$$

As $\mathbb{J}$ is an isometry, roughly speaking this proposition says that the input signal $\mathbf{q}_p[\phi_{sym}]$ is close (for the L^2 norm) to an eigenfunction of the operator $\mathbb{J}\mathbb{S}$ associated to a positive eigenvalue.

The second one is related to the well-known time-reversal experiment: a time-reversed wave back-propagates towards the source. In this sense, the time-reversed

Green function G emmited at s_p is some kind of optimal space-time focusing wave. We have checked that for high ω, the phases ϕ_{sym} given by (4) become close to those of the frequency components of the measures of the time-reversed Green function.

The last arguments are numerical experiments which confirm these focusing properties. In particular, we measured the focusing quality of (3) by means of an energy criterion. We compute the ratio of the local acoustic energy contained in a box which surrounds the obstacle s_p by the total energy sent by the transducers during the emission. In Figure 1 we compare this ratio for input signals $\mathbf{q}_p$ constructed with the time reversed Green function emitted at s_p (these signals require also the position of the pth obstacle) with those constructed with ϕ_{sym}.

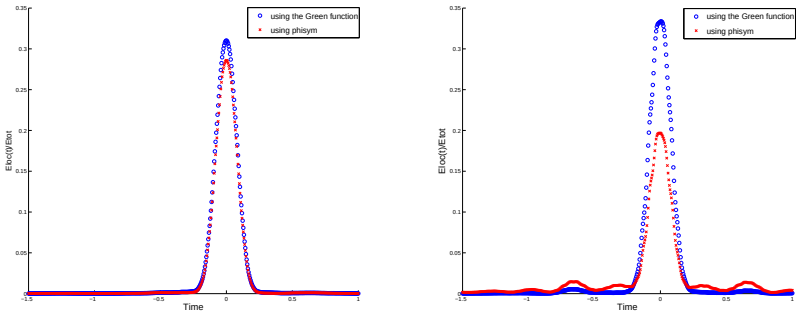

(a) Distant scatterers (b) Close scatterers

FIGURE 1. Two scatterers in a diffusive medium

REFERENCES

[1] M.Cassier and C. Hazard, *Multiple scattering of acoustic waves by small sound-soft obstacles in two dimensions: Mathematical justification of the Foldy-Lax model*, Wave Motion , **50** (2013), pp. 18–28.

[2] C. Hazard and K. Ramdani, *Selective acoustic focusing using time-harmonic reversal mirrors*, SIAM J. Appl. Math, **64** (2004), pp. 1057–1076.

[3] R. Horn and C. A. Johnson, *Matrix Analysis*, Cambridge University Press, 1985.

[4] C. Prada and M. Fink, *Eigenmodes of time reversal operator: A solution to selective focusing in multiple target media*, Wave Motion , **20** (1994), pp. 151–163.

Scattering by Arbitrary Planar Screens

Simon N. Chandler-Wilde
(joint work with Dave Hewett)

This talk is concerned with the classical problem of time harmonic acoustic scattering by an infinitely thin, finite planar screen. We work in d dimensions, with $d = 2$ or 3, and, without loss of generality, suppose that the screen Γ is some bounded subset of $\Gamma_\infty := \{x = (x_1, ..., x_d) \in \mathbb{R}^d : x_d = 0\}$ (which we identify with $\mathbb{R}^{d-1}$). We restrict attention throughout to the case that Γ is either a closed or an open subset of Γ_∞, and set $D := \mathbb{R}^d \setminus \overline{\Gamma}$. We suppose that an incident wave u^i that is a linear combination of plane waves, i.e.,

$$u^i(x) = \sum_{m=1}^{N} a_m \exp(\mathrm{i}kx \cdot d_m), \tag{1}$$

where $a_m \in \mathbb{C}$ and the d_m are unit vectors, is incident on the screen Γ. This incident wave is a solution of the Helmholtz equation

$$\Delta u + k^2 u = 0 \tag{2}$$

for wavenumber $k > 0$. The two scattering problems, **SPD** and **SPN**, that we consider, corresponding to a sound soft and a sound hard screen, respectively, are the following:

Given u^i having the form (1)*, find $u \in C^2(D) \cap W^{1,2}_{\mathrm{loc}}(D)$ such that* (2) *holds in D, $u^s := u - u^i$ satisfies the standard Sommerfeld radiation condition, and $u = 0$ on Γ (scattering problem* **SPD***) or $\partial u/\partial n = 0$ on Γ (scattering problem* **SPN***).*

Our focus in this talk is on integral equation formulations of these two screen problems. This is hardly a new topic. Indeed, already Stephan [9] derives well-posed boundary integral equation formulations, for both planar and non-planar screen problems, under the assumption that Γ is a C^∞ relatively open subset of the boundary of some smooth domain. More recently this smoothness requirement has been relaxed, but, to the best of our knowledge, all previous studies of boundary integral equation methods for screen problems assume that the screen is a Lipschitz domain or, at least, satisfies a uniform cone condition.

This is to some extent surprising, in particular in the electromagnetics (EM) context given the large interest there in the design of *fractal antennae*, requiring the computation of radiation from objects that, to a good approximation, are planar screens occupying a fractal subset of the plane (e.g., a Cantor-type set [8]). On the other hand, it is only relatively recently that the correct formulations and trace spaces for EM screen problems of regular (i.e., Lipschitz) shape have been elucidated [2].

The focus in this talk is to develop a theory of integral equations for the problems **SPD** and **SPN** in the case that Γ occupies an *arbitrary* (e.g., fractal) subset of Γ_∞. Our Sobolev space notations are those of [7], and we identify $H^s(\Gamma_\infty)$ with $H^s(\mathbb{R}^{d-1})$ in the obvious way. In particular, for a closed set $C \subset \Gamma_\infty$, H^s_C is the set of those $\phi \in H^s(\Gamma_\infty)$ with support in C and, for an open set $O \subset \Gamma_\infty$,

$\tilde{H}^s(O) \subset H^s(\Gamma_\infty)$ is the closure of $C_0^\infty(O)$ in the $H^s(\Gamma_\infty)$ norm. Both H^s_C and $\tilde{H}^s(O)$ are closed subspaces of $H^s(\Gamma_\infty)$; further $H^s_{\overline{O}} = \tilde{H}^s(O)$ if O is C^0 [7].

As a first step let us recall the case when the screen $\Gamma = \overline{\Omega}$, where Ω is some C^∞ open subset of Γ_∞. Then it is well-known [9] that u satisfies **SPD** iff

$$u(x) = u^i(x) - \int_\Gamma \Phi(x,y) \left[\frac{\partial u}{\partial n}\right](y)\mathrm{d}s(y), \quad x \in D, \tag{3}$$

and $S[\partial u/\partial n] = u^i|_\Omega$. Here $[\partial u/\partial n] \in H^{-1/2}_\Gamma = \tilde{H}^{-1/2}(\Omega)$ is the jump in the normal derivative across Γ_∞ and S is the standard acoustic single-layer potential operator on Γ, which is an isomorphism from $H^{-1/2}_\Gamma = \tilde{H}^{-1/2}(\Omega)$ to $H^{1/2}(\Omega)$. We note that the behaviour of $[\partial u/\partial n]$ near $\partial\Omega$ is well understood when Ω is C^∞ [9], and in particular $[\partial u/\partial n] \in L^1(\Omega)$ so that (3) is well-defined. Similarly [9], u satisfies **SPN** iff

$$u(x) = u^i(x) + \int_\Gamma \frac{\partial \Phi(x,y)}{\partial n(y)}[u](y)\mathrm{d}s(y), \quad x \in D, \tag{4}$$

and $T[u] = -(\partial u^i/\partial n)|_\Omega$. Here $[u] \in H^{1/2}_\Gamma = \tilde{H}^{1/2}(\Omega)$ is the jump in the trace of u across Γ_∞ and T is the standard acoustic hypersingular integral operator on Γ, an isomorphism from $H^{1/2}_\Gamma = \tilde{H}^{1/2}(\Omega)$ to $H^{-1/2}(\Omega)$.

S and T are both isomorphisms. It is less well appreciated, though the more difficult hypersingular case is shown already in [5], that S and T have the stronger property that they are both coercive. In particular, in the case that $\Omega = \Omega_R := \{x = (\tilde{x}, 0) : |\tilde{x}| < R\}$ and $\Gamma = \Gamma_R := \overline{\Omega_R}$, it holds that

$$|\langle S\phi, \phi\rangle| \;\geq\; C_R\|\phi\|^2_{H^{-1/2}(\Gamma_\infty)} \;\text{ and }\; |\langle T\psi, \psi\rangle| \;\geq\; c_R\|\psi\|^2_{H^{1/2}(\Gamma_\infty)}, \tag{5}$$

for $\phi \in H^{-1/2}_{\Gamma_R}$, $\psi \in H^{1/2}_{\Gamma_R}$, where $\langle\cdot,\cdot\rangle$ is the usual extension of the inner product on $L^2(\Gamma_\infty)$ to a sesquilinear form on $H^s(\Gamma_\infty) \times H^{-s}(\Gamma_\infty)$ and C_R, c_R are positive constants depending only on k and R. This implies, of course, by the Lax-Milgram lemma, that the variational forms of these integral equations have exactly one solution. These variational forms are to find $[\partial u/\partial n] \in H^{-1/2}_{\Gamma_R}$ and $[u] \in H^{1/2}_{\Gamma_R}$, respectively, such that

$$\langle S[\partial u/\partial n], \phi\rangle = \langle u^i, \phi\rangle,\ \forall \phi \in H^{-1/2}_{\Gamma_R} \text{ and } \langle T[u], \psi\rangle = -\langle \partial u^i/\partial n, \psi\rangle,\ \forall \psi \in H^{1/2}_{\Gamma_R}. \tag{6}$$

These observations immediately give us well-posedness of variational formulations of integral equations on *arbitrary* bounded open or closed subsets of Γ_∞. For any such subset Γ is contained in Γ_R for some $R > 0$. These variational formulations are (6) with $H^s_{\Gamma_R}$ replaced by $H^s_\Gamma \subset H^s_{\Gamma_R}$ in the case that $\Gamma \subset \Gamma_R$ is closed, and (6) with $H^s_{\Gamma_R}$ replaced by $\tilde{H}^s(\Gamma) \subset H^s_{\Gamma_R}$ in the case that $\Gamma \subset \Gamma_R$ is open. It is immediate from (5) and the Lax-Milgram lemma that these variational formulations are well-posed. This gives the proof of most of the following theorem. In this theorem $\gamma_+ u$ and $\gamma_- u$ denote traces of u on Γ_∞, the traces taken from the upper and lower half-spaces respectively, and similarly $\partial_n^\pm u$ are normal derivatives of u on Γ_∞ taken from above and below.

Theorem 1. *In the case that $\Gamma \subset \Gamma_R$ is closed, the variational formulations* (6)*, with $H_{\Gamma_R}^{\pm 1/2}$ replaced by $H_{\Gamma}^{\pm 1/2}$, have exactly one solution, and u given by* (3) *satisfies* **SPD***, with the boundary condition understood in the sense that $\gamma_{\pm} u \in \tilde{H}^{1/2}(\Gamma_\infty \setminus \Gamma)$, while u given by* (4) *satisfies* **SPN***, with the boundary condition understood in the sense that $\partial_n^{\pm} u \in \tilde{H}^{-1/2}(\Gamma_\infty \setminus \Gamma)$. In the case that $\Gamma \subset \Gamma_R$ is open, the variational formulations* (6)*, with $H_{\Gamma_R}^{\pm 1/2}$ replaced by $\tilde{H}^{\pm 1/2}(\Gamma)$, have exactly one solution, and u given by* (3) *satisfies* **SPD***, with the boundary condition understood in the sense that $\gamma_{\pm} u = 0$ on Γ, while u given by* (4) *satisfies* **SPN***, with the boundary condition understood in the sense that $\partial_n^{\pm} u = 0$ on Γ.*

We note that, in general, the integral in the representation (3) has to be interpreted as a duality pairing. The proof that (3) and (4) satisfy the boundary conditions in the sense indicated depends on the following characterizations of dual spaces, that, if Γ is open, then

$$(\tilde{H}^s(\Gamma))^* = H^{-s}(\Gamma), \quad (H^s(\Gamma))^* = \tilde{H}^{-s}(\Gamma),$$

in the sense that the natural embeddings are unitary isomorphisms. Similarly,

$$(H_\Gamma^s)^* = \tilde{H}^{-s}(\Gamma_\infty \setminus \Gamma)^\perp, \quad \left(\tilde{H}^s(\Gamma_\infty \setminus \Gamma)^\perp\right)^* = H_\Gamma^{-s},$$

where here the superscript $\perp$ denotes the orthogonal complement. In the case that Γ is C^0 the first of these identifications is known, e.g., [7], but otherwise these results may be new.

To illustrate the application of the theorem to a fractal scatterer, choose $\alpha > 2$, and let $\ell_k = \alpha^{-k}$, for $k = 0, 1, ...$ Set $E_0 := [0, \ell_0]$. Let E_1 be the set obtained by removing an open interval from the middle of E_0 to leave two closed intervals of length ℓ_1, E_2 the set obtained by removing an open interval from the middle of the two intervals comprising E_1 to leave 4 closed intervals of length ℓ_2, and similarly define E_3, E_4, ..., so that E_k is a union of 2^k disjoint closed intervals of length ℓ_k. Finally, let $E := \cap_{k=0}^{\infty} E_k$, so that E is the classic "middle third" Cantor set in the case $\alpha = 3$. Clearly E_k has Lebesgue measure $m(E_k) = (2/\alpha)^k$, so that $m(E) = 0$. A more refined measure of the size of E is given by computing its Hausdorff dimension which is [4] $\dim_H(E) = \log 2 / \log \alpha$.

We will consider first scattering in 3D ($d = 3$) by the closed screen Γ that is the "Cantor dust", $\Gamma = \{(x_1, x_2, 0) : x_j \in E, j = 1, 2\}$, which has Hausdorff dimension [4] $\dim_H(\Gamma) = 2 \log 2 / \log \alpha$. The relevance of the Hausdorff dimension is the following result [1, 6].

Lemma 1. *Suppose C is a closed subset of $\mathbb{R}^m$, for some $m \in \mathbb{N}$. If $0 < s \leq m/2$ and $H_C^{-s} = \{0\}$, then $\dim_H(C) \leq m - 2s$. Conversely, if $0 < s < m/2$ and $\dim_H(C) < m - 2s$, then $H_C^{-s} = \{0\}$. If $s \geq 0$ and $m(C) = 0$ then $H_C^s = \{0\}$.*

It might be thought that the screen Γ, which has zero surface Lebesgue measure, is invisible to the incident field, i.e., that $u^s = 0$. For our variational formulation, in which we look for a solution $[u] \in H_\Gamma^{1/2}$, this is the case for **SPN** as, by the above lemma, $H_\Gamma^{1/2} = \{0\}$. For **SPD** the situation is more subtle. The above lemma,

plus other arguments specific to the Cantor set [1], show that $H_{\Gamma}^{-1/2} = \{0\}$ iff $\dim_H(\Gamma) \leq 1$. This is the proof of most of the following result.

Corollary 1. *In the case that Γ is the Cantor dust screen, which has $m(\Gamma) = 0$ and $\dim_H(\Gamma) = 2\log 2/\log\alpha$, the solution to our variational formulation of* **SPN** *is $u = u^i$; if $\alpha \geq 4$ this is also the solution to our variational formulation of* **SPD**. *If $2 < \alpha < 4$ there are incident fields u^i for which $u^s \neq 0$ so that $u \neq u^i$.*

We note that, in particular, in the case **SPD** with $0 < \alpha < 2$, $u^s \neq 0$ whenever u^i given by (1) is such that γu^i has a component in $\tilde{H}^{1/2}(\Gamma_\infty \setminus \Gamma)^\perp$. Since $\tilde{H}^{1/2}(\Gamma_\infty \setminus \Gamma)^\perp \subset H_{\Gamma_R}^{1/2}$ and the traces of the incident fields of the form (1) are dense in $H_{\Gamma_R}^{1/2}$, there are many such incident fields.

As a final example let us consider the variational formulation of **SPN** for the cases: $\Gamma = \Gamma_1 := [0,1]^2$; $\Gamma = \Gamma_2 := (0,1)^2$; $\Gamma = \Gamma_3 := (0,1)^2 \setminus E^2$. Clearly Γ_1 is closed and Γ_2 and Γ_3 are open, with $\overline{\Gamma_2} = \overline{\Gamma_3} = \Gamma_1$. Let u_j denote the solution to our integral equation variational formulation of **SPN** when $\Gamma = \Gamma_j$. Then, since $H_{\Gamma_1}^{1/2} = \tilde{H}^{1/2}(\Gamma_2)$ (since Γ_2 is C^0) it follows that $u_1 = u_2$. The question as to whether $u_2 = u_3$ is answered by the following result.

Theorem 2. *Suppose $\Gamma_a \subset \Gamma_b$ are bounded open subsets of Γ_∞, let $C = \overline{\Gamma_b} \setminus \Gamma_a$, and let u_a and u_b denote the solutions to our variational formulation of* **SPN** *for $\Gamma = \Gamma_a$ and Γ_b, respectively. Then the following are equivalent: (i) $\tilde{H}^{1/2}(\Gamma_a) = \tilde{H}^{1/2}(\Gamma_b)$; (ii) $H_C^{-1/2} = \{0\}$; (iii) for every incident field (1) it holds that $u_a = u_b$.*

This theorem and the observations in and immediately above Corollary 1 imply that $u_2 = u_3$ for every incident field (1) iff $\alpha \geq 4$. Thus, if $2 < \alpha < 4$, there are incident fields for which $u_3 \neq u_1$ although $\overline{\Gamma_3} = \Gamma_1$ and $m(\Gamma_1 \setminus \Gamma_3) = 0$.

We refer the reader to [3] for further details.

References

[1] D. R. Adams and L. I. Hedberg, *Function Spaces and Potential Theory*, Springer, 1999, corrected 2nd printing.

[2] A. Buffa, S. H. Christiansen, *The electric field integral equation on Lipschitz screens: definition and numerical approximation*, Numerische Mathematik **94** (2003), 229–267.

[3] S. N. Chandler-Wilde, D. P. Hewett, *Scattering by fractal planar screens and apertures*, in preparation.

[4] K. J. Falconer, *Fractal Geometry - Mathematical Foundations and Applications*, John Wiley, 2nd Edition, 2003.

[5] T. Ha-Duong, *On the boundary integral equations for the crack opening displacement of flat cracks*, Integral Equations and Operator Theory **15** (1992), 427–453.

[6] V. Maz'ya, *Sobolev Spaces with Applications to Elliptic Partial Differential Equations*, Springer, 2nd Edition, 2011.

[7] W. McLean, *Strongly Elliptic Systems and Boundary Integral Equations*, CUP, 2000.

[8] G. Srivatsun, S. S. Rani, G. S. Krishnan, *A Self-Similar Fractal Cantor Antenna for MICS Band Wireless Applications*, Wireless Engineering and Technology **2** (2011), 107–111.

[9] E. P. Stephan, *Boundary integral equations for screen problems in $\mathbb{R}^3$*, Integral Equations and Operator Theory **10** (1987), 236–257.

Acoustic Reverse Time Migration for Extended Obstacles

Zhiming Chen
(joint work with Junqing Chen, and Guanghui Huang)

We propose and study an imaging algorithm to find the support of an unknown obstacle embedded in a known background medium from a knowledge of scattered acoustic waves measured on a given acquisition surface which is assumed to be far away from the obstacle.

Let the obstacle occupy a bounded Lipschitz domain $D \subset \mathbb{R}^2$ with ν the unit outer normal to its boundary Γ_D. We assume the incident wave is emitted by a point source located at x_s on a closed surface Γ_s away from the obstacle. For penetrable obstacles D, the measured wave u is the solution of the following acoustic scattering problem:

$$\Delta u + k^2 n(x) u = -\delta_{x_s}(x) \quad \text{in } \mathbb{R}^2, \tag{1}$$

$$\sqrt{r}\left(\frac{\partial u}{\partial r} - \mathrm{i}ku\right) \to 0 \quad \text{as } r \to \infty, \quad r = |x|, \tag{2}$$

where $k > 0$ is the wave number, $n(x) \in L^\infty(D)$ is a positive scalar function supported in D, δ_{x_s} is the Dirac source located at x_s. The condition (2) is the well-known Sommerfeld radiation condition. For non-penetrable obstacles D, the measured wave u is the solution of the following scattering problem:

$$\Delta u + k^2 u = -\delta_{x_s}(x) \quad \text{in } \mathbb{R}^2, \tag{3}$$

$$u = 0 \ \text{ or } \ \frac{\partial u}{\partial \nu} + \mathrm{i}k\lambda(x)u = 0 \quad \text{on } \Gamma_D, \tag{4}$$

$$\sqrt{r}\left(\frac{\partial u}{\partial r} - \mathrm{i}ku\right) \to 0 \quad \text{as } r \to \infty, \quad r = |x|, \tag{5}$$

where $\lambda(x) \geq 0$ is a bounded function on Γ_D. The Dirichlet boundary condition $u = 0$ on Γ_D corresponds to the sound soft obstacle. The second condition on Γ_D in (4) is the impedance condition and it reduces to the sound hard obstacle when $\lambda(x) = 0$. The existence and uniqueness of the problem (1)-(2) such that $u^s = u - u^i$ in $H^1_{\mathrm{loc}}(\mathbb{R}^2)$ and the problem (3)-(5) such that $u^s = u - u^i$ in $H^1_{\mathrm{loc}}(\mathbb{R}^2 \backslash \bar{D})$ is well-known [11, 18, 6], where $u^i(x) = \frac{\mathrm{i}}{4} H_0^{(1)}(k|x - x_s|)$ is the fundamental solution of the Helmholtz equation, $H_0^{(1)}(z)$ is the Hankle function of the first type and order zero.

The direct methods for solving inverse scattering problems have drawn considerable interests in the literature in recent years. We refer to the MUltiple SIgnal Classification (MUSIC) method in [21, 13, 5, 1], the linear sampling method [10], the factorization method [16], and the point source method [19]. The reverse time migration (RTM) or the closely related depth migration methods are nowadays are widely used in exploration geophysics [2, 9]. The analysis of the migration method is usually based on the high frequency assumption [3] or small inclusion assumption [14].

We provide a new mathematical understanding of the RTM method for extended obstacles without the assumption of geometric optics approximation. We study the resolution of the RTM method for both penetrable and non-penetrable obstacles. As the outcome of our resolution analysis we propose to use the imaginary part of the cross-correlation RTM functional. We show that this new imaging functional enjoys the nice feature that it is always positive and thus may have better stability properties.

Now we introduce the RTM method for inverse scattering problems. We assume that there are N_s transducers uniformly distributed on $\Gamma_s = \partial B_s$ and N_r transducers uniformly distributed on $\Gamma_r = \partial B_r$. B_s and B_r are the circles of radius R_s and R_r, respectively. We denote by Ω the sampling domain in which the obstacle is sought. We assume the obstacle $D \subset \Omega$ and Ω is inside in Ω_s, Ω_r.

Let $G(x, y)$ be the fundamental solution of the Helmholtz equation

$$\Delta G(x, y) + k^2 G(x, y) = -\delta_y(x) \quad \text{in } \mathbb{R}^2.$$

Let $u^i(x, x_s) = G(x, x_s)$ be the incident wave and $u^s(x_r, x_s) = u(x_r, x_s) - u^i(x_r, x_s)$ be the scattered field measured at x_r, where $u(x, x_s)$ is the solution of the problem either (1)-(2) or (3)-(5).

Algorithm 1. (Reverse time migration algorithm)
Given the data $u^s(x_r, x_s)$ which is the measurement of the scattered field at x_r when the source is emitted at x_s, $s = 1, \ldots, N_s$ and $r = 1, \ldots, N_r$.
1° *Back-propagation: For $s = 1, \ldots, N_s$, compute the solution v_b of the following problem:*

$$\Delta v_b(x, x_s) + k^2 v_b(x, x_s) = \frac{|\Gamma_r|}{N_r} \sum_{r=1}^{N_r} \overline{u^s(x_r, x_s)} \delta_{x_r}(x) \quad \text{in } \mathbb{R}^2, \tag{6}$$

$$\sqrt{r}\left(\frac{\partial v_b}{\partial r} - \mathrm{i}k v_b\right) \to 0 \quad \text{as } r \to \infty. \tag{7}$$

2° *Cross-correlation: For $z \in \Omega$, compute*

$$I(z) = k^2 \cdot \operatorname{Im}\left\{\frac{|\Gamma_s|}{N_s} \sum_{s=1}^{N_s} u^i(z, x_s) v_b(z, x_s)\right\}. \tag{8}$$

The imaging functional $I(z)$ is a good trapezoid quadrature approximation of the following continuous functional:

$$\hat{I}(z) = -k^2 \operatorname{Im} \int_{\Gamma_r} \int_{\Gamma_s} G(z, x_s) G(z, x_r) \overline{u^s(x_r, x_s)} ds(x_s) ds(x_r) \quad \forall z \in \Omega. \tag{9}$$

Theorem 3. *For any $z \in \Omega$, let $\psi(x, z)$ be the radiation solution of the Helmholtz equation with penetrable scatterer D:*

$$\Delta \psi + k^2 n(x) \psi = -k^2 (n(x) - 1) \operatorname{Im} G(x, z) \quad \text{in } \mathbb{R}^2. \tag{10}$$

Then if the measured field $u^s = u - u^i$ with u satisfying the problem (1)-(2), we have

$$\hat{I}(z) = k \int_{S^1} |\psi_\infty(\hat{x}, z)|^2 d\hat{x} + w_{\hat{I}}(z) \quad \forall z \in \Omega,$$

where $\psi_\infty(\hat{x}, z)$ is the far field pattern of the solution $\psi(x, z)$ and $\|w_{\hat{I}}\|_{L^\infty(\Omega)} \leq C(R_s^{-1} + R_r^{-1})$.

Theorem 4. *For any $z \in \Omega$, let $\psi(x, z)$ be the radiation solution of the Helmholtz equation*

$$\begin{aligned} &\Delta\psi(x, z) + k^2\psi(x, z) = 0 \quad \text{in } \mathbb{R}^2 \backslash \bar{D}, \\ &\psi(x, z) = -\operatorname{Im} G(x, z) \quad \text{on } \Gamma_D. \end{aligned}$$

Then if the measured field $u^s = u - u^i$ with u satisfying the problem (3)-(5) with the Dirichlet condition in (4), we have

$$\hat{I}(z) = k \int_{S^1} |\psi_\infty(\hat{x}, z)|^2 d\hat{x} + w_{\hat{I}}(z) \quad \forall z \in \Omega,$$

where $\psi_\infty(\hat{x}, z)$ is the far field pattern of the solution $\psi(x, z)$ and $\|w_{\hat{I}}\|_{L^\infty(\Omega)} \leq C(R_s^{-1} + R_r^{-1})$.

We refer to [7] for the proof of the theorems and extensive numerical experiments and [8] for the extension of the algorithm to electromagnetic waves.

References

[1] Ammari H. and Kang H., Reconstruction of Small Inhomogeneities from Boundary Measurements, Lecture Notes in Mathematics, Vol. 1846, Springer Verlag, Berlin, 2004.

[2] Berkhout A.J., Seismic Migration: Imaging of Acoustic Energy by Wave Field Extrapolation, Elsevier, New York, 1984.

[3] Bleistein N., Cohen J.K., and Stockwell, Jr. J.W., Mathematics of Multidimensional Seismic Imaging, Migration, and Inversion, Springer, New York, 2001.

[4] Bojarski N.N., Inverse Scattering, Naval Air Systems Command Report N00019-73-C-0312, Washington, D.C., October 1973.

[5] Bruhl M., Hanke M., and Vogelius M., A direct impedance tomography algorithm for locating small inhomogeneities, Numer. Math. (2003), 635-654.

[6] Cakoni F., Colton D., and Monk P., The direct and inverse scattering problems for partially coated obstacles, Inverse Problems 17 (2001), 1997-2015.

[7] Chen J., Chen Z., and Huang G., Reverse Time Migration for Extended Obstacles: Acoustic Waves, 2012, submitted.

[8] Chen J., Chen Z., and Huang G., Reverse Time Migration for Extended Obstacles: Electromagnetic Waves, 2012, submitted.

[9] Claerbout J.F., Imaging The Earth's Interior, Blackwell Scientific Publication, Oxford, 1985.

[10] Colton D. and Kirsch A., A simple method for solving inverse scattering problems in the resonance region, Inverse Problems, 12 (1996), 383-393.

[11] Colton D. and Kress R., Inverse Acoustic and Electromagnetic Scattering Problems, Springer , Heidelberg, 1998.

[12] Colton D. and Kress R., Using fundamental solutions in inverse scattering, Inverse Problems 22 (2006), R49-R66.

[13] Devaney A.J., Super-resolution processing of multi-static data using time-reversal and MUSIC, J. Acoust. Soc. Am., in press.

[14] Garnier J., Sensor array imaging in a noisy environment, in NIMS Lecture Note Series TP1003, National Institute for Mathematical Sciences, South Korea, 2010.
[15] Hou S., Solna K., and Zhao H., A direct imaging algorithm for extended targets, Inverse Problems 22 (2006), 1151-1178
[16] Kirsch A., Characterization of the shape of a scattering obstacle using the spectral data of the far field operator, Inverse Problems 14 (1998), 1489-1512
[17] Kirsch A. and Grinberg N., The Factorization Method for Inverse Problems, Oxford University Press, Oxford, 2008.
[18] McLean W., Strongly Elliptic Systems and Boundary Integral Equations, Cambridge University Press, Cambridge, 2000.
[19] Potthast R., A fast new method to solve inverse scattering problems, Inverse Problems, 12 (1996), 731-742.
[20] Potthast R., Point Sources and Multipoles in Inverse Scattering Theory, Chapman & Hall/CRC, Boca Raton, 2001.
[21] Schmidt R., Multiple emitter location and signal parameter estimation, IEEE Trans. Antennas. Propag. 34 (1986), 276-280.

Negative materials and corners in electromagnetism

Lucas Chesnel
(joint work with Anne-Sophie Bonnet-Ben Dhia, Camille Carvalho, Patrick Ciarlet, Xavier Claeys and Sergei Nazarov)

In electromagnetism, recent years have seen a growing interest in the use of negative materials in technologies. Negative materials are materials that can be modeled for certain ranges of frequencies, neglecting the dissipation, by real negative physical parameters (permittivity ε and/or permeability μ). To summarize, there are two major families of negative materials. The *negative metamaterials* are complex structures made of small resonators, chosen so that the macroscopic medium behave as if its physical parameters were negative. For a mathematical justification of the homogenization process, we refer the reader for example to [6]. Among these materials, we distinguish the double negative metamaterials, also called the left-handed materials for which we have both $\varepsilon < 0$ and $\mu < 0$. *Metals* in visible range constitute the second family of negative materials. They are used especially in plasmonic technologies [1, 7, 14, 10] which would allow important advances in miniaturization. In this context, a key issue is to be able to manipulate light and in particular, to focus energy in specific areas of space. To do this, physicists use metallic devices with corners and edges [13, 2, 12]. This process raises challenging questions in the theoretical and numerical study of time harmonic Maxwell's equations. In this note, we investigate the behaviour of the electromagnetic field for a slightly rounded corner. We work on a rather simple setting but it foreshadows the general case. We highlight an unusual instability phenomenon for this problem in some configurations: when the interface between the two materials presents a rounded corner, it can happen that the solution depends critically on the value of the rounding parameter.

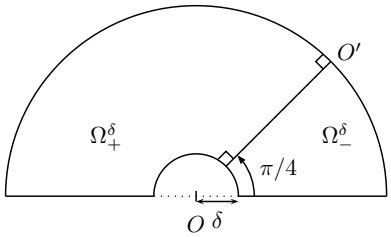

FIGURE 1. Domain Ω^δ.

1. Numerical observations

Let us denote (r, θ) the polar coordinates centered at the origin O. Consider $\delta \in (0; 1)$ and define (see Figure 1) the domains:

$$\begin{aligned}\Omega_+^\delta :=& \{(r\cos\theta, r\sin\theta) \,|\, \delta < r < 1,\ \pi/4 < \theta < \pi\};\\ \Omega_-^\delta :=& \{(r\cos\theta, r\sin\theta) \,|\, \delta < r < 1,\ \ 0 < \theta < \pi/4\};\\ \Omega^\delta :=& \{(r\cos\theta, r\sin\theta) \,|\, \delta < r < 1,\ \ 0 < \theta < \pi\}.\end{aligned}$$

We define the function $\sigma^\delta : \Omega^\delta \to \mathbb{R}$ by $\sigma^\delta = \sigma_\pm$ in $\Omega_\pm^\delta$, where $\sigma_+ > 0$ and $\sigma_- < 0$ are constants. We shall focus on the problem:

$$\left|\begin{array}{l}\text{Find } u^\delta \in \mathrm{H}_0^1(\Omega^\delta) \quad \text{such that}\\ -\div(\sigma^\delta \nabla u^\delta) = f,\end{array}\right. \tag{1}$$

where $\mathrm{H}_0^1(\Omega^\delta) := \{v \in \mathrm{H}^1(\Omega^\delta) \text{ s.t. } v|_{\partial\Omega^\delta} = 0\}$. Notice that problem (1) is not standard because the sign of σ^δ changes on Ω^δ. We choose a source term $f \in \mathrm{L}^2(\Omega^\delta)$ whose support does not meet O and we try to approximate the solution of problem (1), assuming it is uniquely defined, by a classical finite element method. Concerning the discretization of problem (1), we refer the reader to [5, 11, 8]. We call u_h^δ the numerical solution and we make δ tends to zero. The results are displayed on Figure 2. For a contrast $\kappa_\sigma := \sigma_-/\sigma_+ = -1.0001$, the sequence $(\|u_h^\delta\|_{\mathrm{H}_0^1(\Omega^\delta)})_\delta$ is relatively stable with respect to δ, for δ small enough. For $\kappa_\sigma := \sigma_-/\sigma_+ = -0.9999$, it looks that there exists of sequence of values of δ, which accumulates in zero, such that problem (1) is not well-posed. In other words, it seems that the solution of problem (1) is not stable with respect to δ when δ tends to zero. The goal of the present note is to understand these two observations.

2. Properties of the problem for $\delta = 0$

We associate with problem (1) the continuous linear operator $\mathcal{A}^\delta : \mathrm{H}_0^1(\Omega^\delta) \to \mathrm{H}^{-1}(\Omega^\delta)$ defined by $\langle \mathcal{A}^\delta u, v\rangle_{\Omega^\delta} = (\sigma^\delta \nabla u, \nabla v)_{\Omega^\delta}$, $\forall u, v \in \mathrm{H}_0^1(\Omega^\delta)$. As it is known from [3], $\mathcal{A}^\delta$ is a Fredholm operator of index 0 if and only if $\kappa_\sigma := \sigma_-/\sigma_+ \neq -1$, as the interface $\Sigma^\delta := \overline{\Omega}_+^\delta \cap \overline{\Omega}_-^\delta$ is smooth and meets $\partial\Omega^\delta$ orthogonally.

For $\delta = 0$ though, the interface no longer meets $\partial\Omega^\delta$ perpendicularly. In the sequel, we write $\mathcal{A}$, Ω and σ instead of $\mathcal{A}^0$, Ω^0 and σ^0. As shown in [3], there

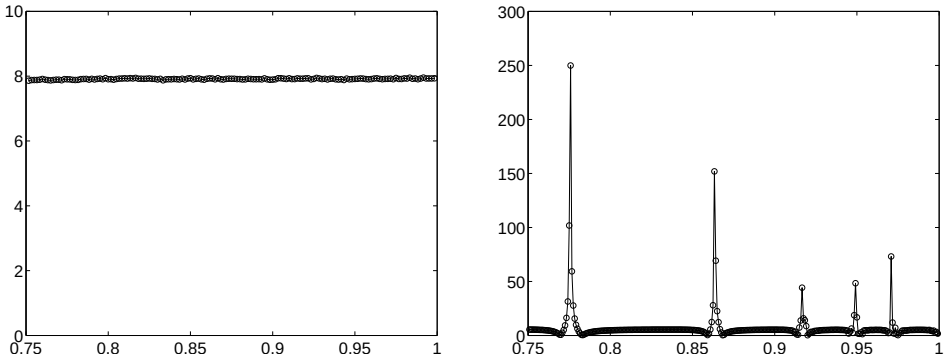

FIGURE 2. Evolution of $\|u_h^\delta\|_{\mathrm{H}_0^1(\Omega^\delta)}$ w.r.t. $1-\delta$. On the left, we take $\sigma_+ = 1$ and $\sigma_- = -1.0001$. On the right, we take $\sigma_+ = 1$ and $\sigma_- = -0.9999$.

exist values of the contrasts $\kappa_\sigma = \sigma_-/\sigma_+$ for which the operator $\mathcal{A}$ fails to be of Fredholm type. More precisely, for the chosen configuration, $\mathcal{A}$ is a Fredholm operator (and actually, an isomorphism) if and only if, $\kappa_\sigma < 0$ does not belong to the *critical interval* $[-1;-1/3]$.

$\star$ When $\kappa_\sigma = -1.0001 \notin [-1;-1/3]$, $\mathcal{A}$ is an isomorphism (c.f. [3]). In this case, we can prove that $\mathcal{A}^\delta$ is an isomorphism for δ small enough. Moreover, defining $u^\delta = (\mathcal{A}^\delta)^{-1} f$ and $u = \mathcal{A}^{-1} f$, we can show that the sequence (u^δ) converges to u for the H^1 norm. This explains the left curve of Figure 2.

$\star$ When $\kappa_\sigma = -0.9999 \in [-1;-1/3]$, $\mathcal{A}$ is not of Fredholm type (c.f. [3]). In this configuration, there is a qualitative difference between problem (1) for $\delta > 0$, and problem (1) for $\delta = 0$. In [4], we define a new functional framework to restore Fredholmness for the limit problem. More precisely, we prove that, for $\kappa_\sigma \in (-1;-1/3)$ the operator $\mathcal{A}^+ : \mathrm{V}_\beta^+ \to \mathrm{V}_\beta^1(\Omega)^*$ defined by $\langle \mathcal{A}^+ u, v\rangle_\Omega = (\sigma\nabla u, \nabla v)_\Omega$, $\forall u \in \mathrm{V}_\beta^+$, $v \in \mathscr{C}_0^\infty(\Omega)$, is an isomorphism for all $\beta \in (0;2)$. In this notation, $\mathrm{V}_\beta^+ := \mathrm{span}\{s^+\} \oplus \mathrm{V}_{-\beta}^1(\Omega)$, where $s^+ \in \mathrm{L}^2(\Omega) \setminus \mathrm{H}^1(\Omega)$ is a singular function at O and $\mathrm{V}_{-\beta}^1(\Omega)$ is the completion of $\mathscr{C}_0^\infty(\Omega)$ for the weighted norm $\|\cdot\|_{\mathrm{V}_{-\beta}^1(\Omega)} = (\|r^{-\beta}\nabla\cdot\|^2_{\mathrm{L}^2(\Omega)} + \|r^{-\beta-1}\cdot\|^2_{\mathrm{L}^2(\Omega)})^{1/2}$.

3. Asymptotic expansion of the solution inside the critical interval

For a contrast inside the critical interval, the exotic functional framework introduced for the limit problem leads to two surprising phenomena in the asymptotic expansion of the solution of problem (1). First, when we proceed to a usual matched asymptotic expansion method, we observe that we can define an asymptotic expansion of the solution u^δ only for

$$\delta \in \mathscr{S}_{\mathrm{adm}} := (0;1) \setminus \mathscr{S}_{\mathrm{forb}} \quad \text{with } \mathscr{S}_{\mathrm{forb}} := \bigcup_{k\in\mathbb{N}} \delta_\star^k \delta_0,$$

$\delta_\star, \delta_0$ being two numbers of $(0;1)$. Notice that 0 is an accumulation point for $\mathscr{S}_{\rm forb}$. For $\alpha \in (0;1/2)$, we define $I(\alpha) := \bigcup_{k\in\mathbb{N}}[\delta_\star^{k+1-\alpha}\delta_0; \delta_\star^{k+\alpha}\delta_0] \subset \mathscr{S}_{\rm adm}$. In [9], we prove the following result:

Proposition 1. *Let $\beta \in (0;2)$ and $f \in \mathrm{V}^1_\beta(\Omega)^*$. There exists δ_0 such that problem (1) is uniquely solvable for all $\delta \in (0;\delta_0) \cap \mathrm{I}(\alpha)$, with $\alpha \in (0;1/2)$. Moreover, we can build an approximation $\hat{u}^\delta \in \mathrm{H}^1_0(\Omega^\delta)$ of u^δ such that, for all ε in $(0;\beta)$, $\forall \delta \in (0;\delta_0) \cap \mathrm{I}(\alpha)$, there holds*

$$\|u^\delta - \hat{u}^\delta\|_{\mathrm{H}^1_0(\Omega^\delta)} \leq\ c\, \delta^{\beta-\varepsilon} \|f\|_{\mathrm{V}^1_\beta(\Omega)^*},$$

where $c > 0$ is a constant independent of δ and f.

The second original phenomenon in this asymptotic expansion concerns the approximation $\hat{u}^\delta$ introduced in Proposition 1. The function $\hat{u}^\delta$ depends on δ and its far field does not converge to the far field of $(\mathcal{A}^+)^{-1}f$ when $\delta \to 0$, even for the L^2 norm . This proves that the solution of problem (1), when it is well-defined, is unstable with respect to δ.

4. Discussion

In this note, we have considered a special geometry for Ω^δ because it simplifies the numerical calculations of the first paragraph. However, we observe exactly the same curiosities for a rounded corner: when the contrast lies inside the critical interval, the solution of problem (1), which is defined except for a sequence of values of δ which tends to 0, depends critically on the rounding parameter. From a physical point of view, one may wonder what happens in a neighbourhood of the corner...

References

[1] W. Barnes, A. Dereux, and T. Ebbesen, *Surface plasmon subwavelength optics*, Nature, 424 (2003), pp. 824–830.

[2] A. Boltasseva, V. Volkov, R. Nielsen, E. Moreno, S. Rodrigo, and S. Bozhevolnyi, *Triangular metal wedges for subwavelength plasmon-polariton guiding at telecom wavelengths*, Opt. Express, 16 (2008), pp. 5252–5260.

[3] A. Bonnet-Ben Dhia, L. Chesnel, and P. Ciarlet Jr., *T-coercivity for scalar interface problems between dielectrics and metamaterials*, Math. Mod. Num. Anal., 46 (2012), pp. 1363–1387.

[4] A.-S. Bonnet-Ben Dhia, L. Chesnel, and X. Claeys, *Radiation condition for a non-smooth interface between a dielectric and a metamaterial*, Accepted in Math. Models Meth. App. Sci., (2012).

[5] A.-S. Bonnet-Ben Dhia, P. Ciarlet Jr., and C. Zwölf, *Time harmonic wave diffraction problems in materials with sign-shifting coefficients*, J. Comput. Appl. Math, 234 (2010), pp. 1912–1919. Corrigendum *J. Comput. Appl. Math.*, 234:2616, 2010.

[6] G. Bouchitté, C. Bourel, and D. Felbacq, *Homogenization of the 3D Maxwell system near resonances and artificial magnetism*, C. R. Acad. Sci. Paris, Ser. I, 347 (2009), pp. 571–576.

[7] R. Charbonneau, N. Lahoud, G. Mattiussi, and P. Berini, *Demonstration of integrated optics elements based on long-ranging surface plasmon polaritons*, Opt. Express, 13 (2005), pp. 977–984.
[8] L. Chesnel and P. Ciarlet Jr., *T-coercivity and continuous Galerkin methods: application to transmission problems with sign changing coefficients*, To appear in Numer. Math., (2012).
[9] L. Chesnel, X. Claeys, and S. Nazarov, *Asymptotics expansion for a non-smooth interface between a dielectric and a negative material*, In preparation, (2013).
[10] D. Gramotnev and S. Bozhevolnyi, *Plasmonics beyond the diffraction limit*, Nature Photonics, 4 (2010), pp. 83–91.
[11] S. Nicaise and J. Venel, *A posteriori error estimates for a finite element approximation of transmission problems with sign changing coefficients*, Journal of Computational and Applied Mathematics, 235 (2011), pp. 4272–4282.
[12] D. O'Connor, M. McCurry, B. Lafferty, and A. Zayats, *Plasmonic waveguide as an efficient transducer for high-density date storage*, Appl. Phys. Lett., 95 (2009).
[13] M. Stockman, *Nanofocusing of optical energy in tapered plasmonic waveguides*, Physical review letters, 93 (2004), p. 137404.
[14] A. Zayats, I. Smolyaninov, and A. Maradudin, *Nano-optics of surface plasmon polaritons*, Physics reports, 408 (2005), pp. 131–314.

A Mortar Element Method for the Electric Field Integral Equation

Kristof Cools
(joint work with Francesco P. Andriulli, Eric Michielssen)

Boundary element methods are a very versatile and powerful modeling tool for the scattering of time-harmonic electromagnetic waves by perfect electrical conductors [8]. Their increase in popularity is due to the availability of fast algorithms such as the fast multipole algorithm [7], the multilevel matrix decomposition or butterfly algorithm [10], and the adaptive integral method [3], which reduce the solution process to a series of matrix vector multiplication requiring almost linear order computations on one hand, and preconditioning methods such as multi-resolution techniques (e.g. [2]), and Calderon preconditioning (see e.g. [5, 4, 1]), which minimize the number of matrix vector multiplication required to reach a solution on the other hand.

To optimally refine simulations based on a posteriori error analysis (see e.g. [11]) and to parallelize the computations in the most flexible way [6], it would be advantageous to be able to construct the mesh separately on all subcomponents of the scatterer. The thus constructed global mesh would be non conforming. Recently, non-overlapping domain decomposition methods for boundary integral equations have been introduced. In [12], a method for scattering from non-penetrable closed conductors was put forward. For scattering problems in acoustics, mortar element based algorithms have been shown to exhibit near (quasi-)optimal convergence properties [9]. In this contribution, a boundary mortar element method for the electric field integral equation (EFIE) is introduced that allows to find the solution of the scattering problem on a non-conforming mesh. The algorithm is fit to deal with junctions, i.e. curves where three or more PEC sheets meet. Until now,

junctions have been dealt with in an ad hoc fashion. For the most general case that can be handled, see e.g. [13].

Consider a perfectly electrically conducting object with surface Γ that can be partitioned in a set of B surfaces or sheets Γ_i. The boundary of each blade Γ_i comprises J_i curves or junctions γ_{ij}. Two sheets are either disjunct, or they meet at the union of a number of junctions γ_{ij}. The junctions can be enumerated after a suitable labeling resulting in the so called skeleton of the decomposition $(\gamma_i)_{i=1}^{J}$ in which each junction occurs only once. The structure is embedded in a background medium characterized by a permittivity ε, a permeability μ, and the corresponding wave number $k = \omega\sqrt{\varepsilon\mu}$ and impedance $\eta = \sqrt{\frac{\mu}{\varepsilon}}$.

Solving the electric field integral equation, which models scattering of $\boldsymbol{e}^i$ by Γ, amounts to finding the current $\boldsymbol{j}$ defined on Γ that radiates a scattered field $\boldsymbol{e}^s$ such that the total field $\boldsymbol{e} = \boldsymbol{e}^i + \boldsymbol{e}^s$ has vanishing tangential components on Γ. The solution $\boldsymbol{j}$ is searched for in the space X of currents $\boldsymbol{k}$ that are divergence conforming on each sheet, that have vanishing normal components at $\partial\Gamma$, and that have continuous normal components at each of the junctions, i.e.

$$\sum_{i=1}^{B} \hat{\boldsymbol{m}}_i \cdot \boldsymbol{k} = \boldsymbol{0}, \tag{1}$$

where $\boldsymbol{m}_i$ is the unit vector field defined on $\partial\Gamma_i$, tangential to Γ_i and normal to $\partial\Gamma_i$, pointing outwards with respect to Γ_i.

The scattered field on Γ should cancel the incident field $\boldsymbol{e}^i$:

$$\frac{1}{ik}\operatorname{grad} S \operatorname{div} \boldsymbol{j} - ikS\boldsymbol{j} = -\frac{1}{\eta}\boldsymbol{e}^i(\boldsymbol{r}), \forall \boldsymbol{r} \in \Gamma \tag{2}$$

with

$$S(\boldsymbol{j})\boldsymbol{r} = \int_\Gamma \frac{e^{-ik|\boldsymbol{r}-\boldsymbol{r}'|}}{4\pi|\boldsymbol{r}-\boldsymbol{r}'|}\boldsymbol{j}(\boldsymbol{r}')\, d\boldsymbol{r}' \tag{3}$$

Equation (2) is tested with all $\boldsymbol{k}$ in X. Because of (1), partial integration does not generate junction terms and the following variational formulation for the EFIE results: find $\boldsymbol{j}$ in X, such that for any $\boldsymbol{k}$ in X:

$$t(\boldsymbol{k}, \boldsymbol{j}) = -\frac{1}{ik}\left\langle \operatorname{div} \boldsymbol{k}, S \operatorname{div} \boldsymbol{j}\right\rangle_\Gamma - ik\left\langle \boldsymbol{k}, S\boldsymbol{j}\right\rangle_\Gamma = -\frac{1}{\eta}\left\langle \boldsymbol{k}, \boldsymbol{e}^i\right\rangle_\Gamma, \tag{4}$$

In the setting of mortar element methods, the continuity constraints on $\boldsymbol{j}$ and $\boldsymbol{k}$ are relaxed. Partial integration now does lead to junction terms:

$$t(\boldsymbol{k}, \boldsymbol{j}) + b(\phi, \boldsymbol{k}) = -\frac{1}{\eta}\left\langle \boldsymbol{k}, \boldsymbol{e}^i\right\rangle_\Gamma, \tag{5}$$

with

$$b(\phi, \boldsymbol{k}) = \left\langle \phi, \sum_{i=1}^{B} \hat{\boldsymbol{m}}_i \cdot \boldsymbol{k}_i \right\rangle_\gamma, \tag{6}$$

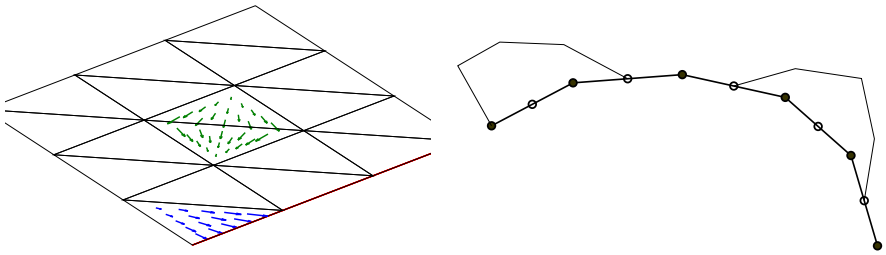

(a) (b)

FIGURE 1. (a) Basis for the Raviart-Thomas space defined on Γ_i. DoFs are associated to internal and junction edges, not to boundary edges. (b) Basis for the mortar finite element space. The functions are continuous, piecewise linear and defined subordinate to the dual mesh. Their value on the outer segments of the barycentric refinement of the mesh is chosen such that the constant function is included in the set.

where $\phi = \frac{1}{ik} S \operatorname{div} \boldsymbol{j}$. The continuity of $\boldsymbol{j}$ is explicitly imposed by requiring that

$$\underline{(}\psi, \sum_{i=1}^{B} \hat{\boldsymbol{m}}_i \cdot \boldsymbol{k}_i) = 0 \tag{7}$$

for all ψ in the space Y of functions continuous on all γ_{ij}. This leads to the following saddle point formulation: find $(\boldsymbol{j}, \phi)$ in $X \times Y$ such that

$$\begin{cases} t(\boldsymbol{k}, \boldsymbol{j}) + b(\phi, \boldsymbol{k}) & = -\dfrac{1}{\eta} \left\langle \boldsymbol{k}, \boldsymbol{e}^i \right\rangle_{\Gamma}, \\ b(\psi, \boldsymbol{j}) & = 0, \end{cases} \tag{8}$$

for all $(\boldsymbol{k}, \psi)$ in $X \times Y$.

Equation (8) is discretized by constructing a triangular mesh $\mathcal{T}_{i,h}$ for each of the sheets Γ_i. The trial and testing functions $\boldsymbol{j}, \boldsymbol{k}$ are chosen to be in the finite element space of Raviart-Thomas functions on each of the sheets. The normal components are forced to zero on the boundary of Γ, but not on the the junctions γ_j (Fig. 1(a)). The traces of $\mathcal{T}_i$ on γ_{ij} are denoted τ_{ij}. For a given γ_j only the finest trace mesh is retained and is denoted τ_j. The dual of this mesh as realized by its barycentric refinement is denoted τ_j'. The trial and testing functions ϕ, ψ are chosen in the space $Y_{j,h}$ of continuous piecewise linear functions on the dual mesh τ_i. The degrees of freedom are attached to the vertices of the dual mesh (i.e. the segments of the primal mesh), and the value of the functions on the outer segments of the barycentric refinement is chosen in such a way that the constant function is contained is the finite element space (Fig. 1(b)).

As an example, scattering of the electric field

$$\boldsymbol{e}^i(\boldsymbol{r}) = \hat{\boldsymbol{y}} e^{-i\frac{2\pi}{\lambda}x} \tag{9}$$

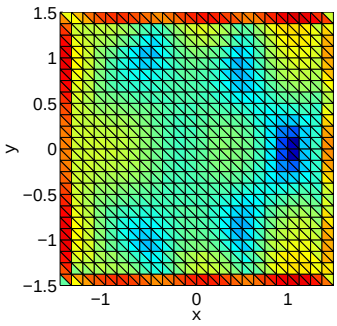

FIGURE 2. Classic EFIE.

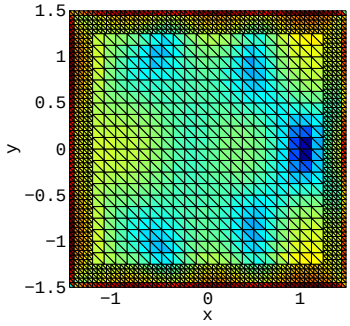

FIGURE 3. Mortar EFIE.

by a metallic square sheet will be considered. This case is of interest because the exact solution for the current density exhibits a singularity at the boundary of Γ. The mortar element methods allows to refine the mesh in the neighbourhood of the boundary without refining the interior of the sheet. In Fig. 2 and Fig. 3 it can be seen that the local refinement has the desired effect: the current distribution on the boundary is refined, while the values in the interior of the sheet remain virtually unchanged.

REFERENCES

[1] F. ANDRIULLI, K. COOLS, H. BAĞCI, F. OLYSLAGER, A. BUFFA, S. CHRISTIANSEN, AND E. MICHIELSSEN, *A multiplicative Calderon preconditioner for the electric field integral equation*, IEEE Transactions on Antennas and Propagation, 56 (2008), pp. 2398–2412.

[2] F. ANDRIULLI, A. TABACCO, AND G. VECCHI, *Solving the EFIE at Low Frequencies With a Conditioning That Grows Only Logarithmically With the Number of Unknowns*, Antennas and Propagation, IEEE Transactions on, 58 (2010), pp. 1614–1624.

[3] E. BLESZYNSKI, M. BLESZYNSKI, AND T. JAROSZEWICZ, *AIM: Adaptive integral method for solving large-scale electromagnetic scatttering and radiation problems*, Radio Science, 31 (1996), pp. 1225–1251.

[4] A. BUFFA AND S. CHRISTIANSEN, *A dual finite element complex on the barycentric refinement*, Mathematics of Computation, 76 (2007), pp. 1743–1769.

[5] S. CHRISTIANSEN AND J.-C. NÉDÉLEC, *A preconditioner for the electric field integral equation based on Calderon formulas*, SIAM J. Numer. Anal., 40 (2002), pp. 1100–1135.

[6] J. FOSTIER AND F. OLYSLAGER, *An asynchronous parallel mlfma for scattering at multiple dielectric objects*, IEEE Transactions on Antennas and Propagation, 56 (2008), pp. 2346–2355.

[7] L. GREENGARD, J. HUANG, V. ROKHLIN, AND S. WANDZURA, *A fast algorithm for particle simulation*, Journal of Computational Physics, 73 (1987), pp. 325–348.

[8] R. F. HARRINGTON, *Field Computation by Moment Methods*, Wiley-IEEE Press, 1993.

[9] M. HEALY AND N. HEUER, *Mortar boundary elements*, SIAM J. Numer. Anal., 48 (2010), pp. 1395–1418.

[10] E. MICHIELSSEN AND A. BOAG, *A multilevel matrix decomposition algorithm for analyzing scattering from large structures*, IEEE Transactions on Antennas and Propagation, 44 (1996), p. 8.

[11] R. Nochetto and B. Stamm, *A posteriori error estimates for the electric field integral equation on polyhedra*, arXiv:1204.3930v1, (2012).
[12] Z. Peng, X.-C. Wang, and J.-F. Lee, *Integral equation based domain decomposition method for solving electromagnetc wave scattering from non-penetrable objects*, IEEE Transactions on Antennas and Propagation, 59 (2011), pp. 3328–3338.
[13] P. Ylä-Oijala, M. Taskinen, and J. Sarvas, *Surface integral equation method for general composite metallic and dielectric structures with junctions*, Progress In Electromagnetics Research, 52 (2005), pp. 81–108.

On the inf-sup constant of the divergence alias LBB constant

Monique Dauge
(joint work with Martin Costabel)

Note: This presentation is mainly based on our paper [9]. It is also related with the survey (in preparation) *"About the inf-sup constant of the divergence"* by C. Bernardi, V. Girault and the authors.

1. The constant of interest and some elementary properties

Here we only consider *bounded connected* domains Ω of $\mathbb{R}^d$, $d \geq 1$. Elements of $\mathbb{R}^d$ are denoted by $\boldsymbol{x} = (x_1, \ldots, x_d)$. For such a domain Ω, the inf-sup constant of the divergence associated with Dirichlet boundary conditions, also called LBB constant after Ladyzhenskaya, Babuška [2] and Brezzi [5], is defined as

$$\beta(\Omega) = \inf_{q \in L^2_\circ(\Omega)} \sup_{\boldsymbol{v} \in H^1_0(\Omega)^d} \frac{\big\langle \operatorname{div} \boldsymbol{v}, q \big\rangle_\Omega}{|\boldsymbol{v}|_{1,\Omega} \, \|q\|_{0,\Omega}} \,. \tag{1}$$

Here $L^2_\circ(\Omega)$ stands for the space of square integrable scalar functions q with zero mean value in Ω endowed with its natural norm $\|\cdot\|_{0,\Omega}$ and natural scalar product $\langle \cdot, \cdot \rangle$, and $H^1_0(\Omega)^d$ is the standard H^1 Sobolev space of vector functions $\boldsymbol{v} = (v_1, \ldots, v_d)$ with square integrable gradients and zero traces on the boundary, endowed with its natural semi-norm $|\boldsymbol{v}|_{1,\Omega}$ defined as $(\sum_{k=1}^d \sum_{j=1}^d \|\partial_{x_j} v_k\|^2_{0,\Omega})^{1/2}$. Since Ω is bounded, by virtue of the Poincaré inequality, the above semi-norm is equivalent to the usual norm in $H^1(\Omega)^d$.

We list some elementary properties of $\beta(\Omega)$:

(a) In any dimension $d \geq 1$, $\beta(\Omega) \geq 0$,
(b) In any dimension $d \geq 1$, $\beta(\Omega) \leq 1$, because of the identity

$$\forall \boldsymbol{v} \in H^1_0(\Omega)^d, \quad |\boldsymbol{v}|^2_{1,\Omega} = \|\operatorname{curl} \boldsymbol{v}\|^2_{0,\Omega} + \|\operatorname{div} \boldsymbol{v}\|^2_{0,\Omega}$$

(c) If $d = 1$, Ω is a finite interval and $\beta(\Omega) = 1$,
(d) In any dimension $d \geq 1$, using a Piola transform it is easy to show that $\beta(\Omega)$ is invariant by translations, dilations, symmetries and rotations. In other words, $\beta(\Omega)$ depends only on the *shape* of Ω.

2. Positiveness of the LBB constant

The constant $\beta(\Omega)$ is positive for Lipschitz domains [20], weakly Lipschitz domains (see [17, §1.2.1] for the distinction between Lipschitz and weakly Lipschitz), and John domains [1] (which include some domains with a fractal boundary). The proof is based on various constructions of a right inverse for the divergence operator, see [4, 15, 1]. In contrast, domains with an external cusp (or thin peak) satisfy $\beta(\Omega) = 0$, see [24].

3. Relation with the Schur complement of the Stokes operator

The Schur complement $\mathcal{S}$ of the Stokes operator is defined as

$$\begin{array}{rccc} \mathcal{S}: & L^2_\circ(\Omega) & \longrightarrow & L^2_\circ(\Omega) \\ & q & \longmapsto & \operatorname{div} \Delta^{-1} \nabla q\,. \end{array}$$

Here Δ^{-1} is the inverse of the Dirichlet vector Laplacian Δ acting from $H^1_0(\Omega)^d$ onto $H^{-1}(\Omega)^d$. The operator $\mathcal{S}$ is bounded self-adjoint, non-negative. But it is not compact, nor its resolvent. It is of order 0. Let $\sigma(\Omega)$ be the bottom of its spectrum. There holds

$$\sigma(\Omega) = \beta(\Omega)^2. \tag{2}$$

The associated eigenvalue problem can be phrased as a spectral Stokes problem—with $\boldsymbol{v} \in H^1_0(\Omega)^d$ and $p \in L^2_\circ(\Omega)$,

$$\left\{ \begin{array}{rcl} -\Delta \boldsymbol{v} + \nabla p & = & 0\,, \\ \operatorname{div} \boldsymbol{v} & = & \sigma p\,. \end{array} \right. \tag{3}$$

Let $\mathfrak{S}(\mathcal{S})$ and $\mathfrak{S}_{\mathsf{ess}}(\mathcal{S})$ be the spectrum and the essential spectrum of $\mathcal{S}$.

4. Relation with the Cosserat spectrum

Let us introduce the family of operators $\sigma \mapsto \mathcal{L}_\sigma$

$$\begin{array}{rccc} \mathcal{L}: & H^1_0(\Omega)^d & \longrightarrow & H^{-1}(\Omega)^d \\ & \boldsymbol{v} & \longmapsto & \sigma \Delta \boldsymbol{v} - \nabla \operatorname{div} \boldsymbol{v} \end{array}$$

The Cosserat spectrum (after Cosserat brothers [7, 8]) $\mathfrak{S}(\mathcal{L})$ [essential spectrum $\mathfrak{S}_{\mathsf{ess}}(\mathcal{L})$] is the set of $\sigma \in \mathbb{R}$ such that $\mathcal{L}_\sigma$ is not invertible [$\mathcal{L}_\sigma$ is not Fredholm]. There holds

$$\mathfrak{S}(\mathcal{L}) = \mathfrak{S}(\mathcal{S}) \cup \{0\} \quad \text{and} \quad \mathfrak{S}_{\mathsf{ess}}(\mathcal{L}) = \mathfrak{S}_{\mathsf{ess}}(\mathcal{S}) \cup \{0\}. \tag{4}$$

The operator $\mathcal{L}$ has non empty essential spectrum: The points 0, $\frac{1}{2}$ and 1 always belong to $\mathfrak{S}_{\mathsf{ess}}(\mathcal{L})$ [19]. If the domain Ω has a smooth boundary, these are the only elements of $\mathfrak{S}_{\mathsf{ess}}(\mathcal{L})$. If Ω is a polygonal domain of $\mathbb{R}^2$, $\mathfrak{S}_{\mathsf{ess}}(\mathcal{L})$ is an interval of the form $[\frac{1}{2} - b, \frac{1}{2} + b]$ with a positive b depending on the corner openings of Ω [10].

A consequence is that for any domain Ω

$$\beta(\Omega)^2 \leq \frac{1}{2}\,.$$

Explicit calculations show that $\beta(\Omega)^2 = \frac{1}{2}$ for the disc $\Omega \subset \mathbb{R}^2$, and more generally $\beta(\Omega)^2 = \frac{1}{d}$ if Ω is a ball in $\mathbb{R}^d$ [10].

5. Relation with the Friedrichs constant (dimension $d = 2$)

Let $\mathfrak{F}(\Omega)$ denote the space of complex valued $L^2(\Omega)$ holomorphic functions and let $\mathfrak{F}_\circ(\Omega)$ be its subspace of functions with mean value 0. After [14] the *Friedrichs constant* $\Gamma(\Omega) \in \mathbb{R} \cup \{\infty\}$ is the smallest constant Γ such that for all $h+ig \in \mathfrak{F}_\circ(\Omega)$

$$\|h\|^2_{L^2(\Omega)} \leq \Gamma \|g\|^2_{L^2(\Omega)} .$$

Theorem 1 ([18], hypotheses fixed in [9])**.** *Let Ω be any bounded connected domain in $\mathbb{R}^2$. The LBB constant $\beta(\Omega)$ is positive if and only if $\Gamma(\Omega)$ is finite and*

$$\Gamma(\Omega) + 1 = \frac{1}{\beta(\Omega)^2} .$$

6. Relation with the Horgan-Payne angle (dimension $d = 2$)

Let Ω be *strictly star-shaped*, which means that there is an open ball $B \subset \Omega$ such that any segment with one end in B and the other in Ω, is contained in Ω. Let O be the center of B and (r, θ) be polar coordinates centered at O. Let $\theta \mapsto r = f(\theta)$ be the polar parametrization of the boundary $\partial\Omega$, defined on $\mathbb{R}/2\pi\mathbb{Z} =: \mathbb{T}$. Since Ω is strictly star-shaped, f belongs to $W^{1,\infty}(\mathbb{T})$. We assume without restriction that $\max_{\theta\in\mathbb{T}} f(\theta) = 1$. After [18], we introduce the function P of $\theta \in \mathbb{T}$ and of a parameter $\alpha \in (0, 1)$ aimed at optimizing an upper bound for $\Gamma(\Omega)$

$$(0,1) \times \mathbb{T} \ni (\alpha, \theta) \longmapsto P(\alpha, \theta) = \frac{1}{\alpha f(\theta)^2} \left(1 + \frac{f'(\theta)^2}{f(\theta)^2 - \alpha f(\theta)^4} \right).$$

We denote by $m(\Omega)$ the original bound of [18]

$$m(\Omega) = \sup_{\theta\in\mathbb{T}} \left\{ \inf_{\alpha \in \left(0, \frac{1}{f(\theta)^2}\right)} P(\alpha, \theta) \right\} \tag{5}$$

and by $M(\Omega)$ our modified Horgan-Payne like bound

$$M(\Omega) = \inf_{\alpha\in(0,1)} \left\{ \sup_{\theta\in\mathbb{T}} P(\alpha, \theta) \right\} \tag{6}$$

The quantity $M(\Omega)$ is always larger than $m(\Omega)$.

Let $\omega(\Omega)$ be the "Horgan-Payne angle" introduced by [23]

$$\omega(\Omega) = \arccos\left(\frac{m(\Omega) - 1}{m(\Omega) + 1} \right).$$

This angle has a simple geometrical interpretation as the minimal angle between radius $[OA]$ and tangent along $\partial\Omega$ at A, for A running in $\partial\Omega$. It is easy to see that $\sin \frac{\omega(\Omega)}{2} = (m(\Omega) + 1)^{-1/2}$. Then, by virtue of Theorem 1, $\Gamma(\Omega) \leq m(\Omega)$ if and only if $\beta(\Omega) \geq \sin \frac{\omega(\Omega)}{2}$.

Theorem 2 ([9]). *Any strictly star-shaped domain Ω satisfies the bounds*

$$\Gamma(\Omega) \leq M(\Omega) \quad \textit{and} \quad \beta(\Omega) \geq \frac{1}{\sqrt{M(\Omega)+1}} \ . \tag{7}$$

If Ω is an ellipse, a triangle, a rectangle or a regular polygon, then $m(\Omega)$ coincides with $M(\Omega)$. Therefore

$$\Gamma(\Omega) \leq m(\Omega) \quad \textit{and} \quad \beta(\Omega) \geq \frac{1}{\sqrt{m(\Omega)+1}} = \sin\frac{\omega(\Omega)}{2} \ . \tag{8}$$

As a matter of fact, there exist strictly star-shaped domains such that $m < M$. And even more:

Theorem 3 ([9]). *There exists a strictly star-shaped domain $\Omega \subset \mathbb{R}^2$ such that*

$$\Gamma(\Omega) > m(\Omega) \quad \textit{i.e.} \quad \beta(\Omega) < \sin\frac{\omega(\Omega)}{2} \ . \tag{9}$$

Counterexamples are provided by symmetric domains with a narrow pass for which we have proved an upper bound for $\beta(\Omega)$ (this can be related to the fact that elongated domains have a small β [6, 21, 11, 12]). This proves that the original result of [18] stating that (8) is valid for any strictly star-shaped domains is erroneous. Nevertheless our positive result of Theorem 2 is still in the spirit of [18] and allows to prove a general simple bound from below for $\beta(\Omega)$ that realizes an improvement of [13] for strictly star-shaped two-dimensional domains.

Though related, discrete inf-sup conditions are a rather different story. Now the choice of distinct discrete spaces for scalar and vector unknowns comes into play, see [16, 3, 22] among many others...

References

[1] G. Acosta, R.G. Durán, M.A. Muschietti, *Solutions of the divergence operator on John domains*, Adv. Math. **206** (2006), 373–401.

[2] I. Babuška, *The finite element method with Lagrange multipliers*, Numer. Math. **20** (1973), 179–192.

[3] C. Bernardi, Y. Maday, *Uniform inf-sup conditions for the spectral discretization of the Stokes problem*, Math. Models Methods Appl. Sci. 9 (1999), no. 3, 395–414.

[4] M.E. Bogovskiĭ, *Solution of the first boundary value problem for the equation of continuity of an incompressible medium*, Soviet Math. Dokl. **20** (1979), 1094–1098.

[5] F. Brezzi, *On the existence, uniqueness and approximation of saddle-point problems arising from Lagrange multipliers*, R.A.I.R.O. Anal. Numér. **8** (1974), 129–151.

[6] E.V. Chizhonkov, M.A. Olshanskii, *On the domain geometry dependence of the LBB condition*, M2AN Math. Model. Numer. Anal. **34** (2000), 935–951.

[7] E. Cosserat, F. Cosserat, *Sur les équations de la théorie de l'élasticité*, Note aux C.R.A.S., Paris **126** (1898), 1089–1091.

[8] E. Cosserat, F. Cosserat, *Sur la déformation infiniment petite d'un ellipsoide élastique*, Note aux C.R.A.S., Paris **127** (1898), 315–318.

[9] M. Costabel, M. Dauge, *On the inequalities of Babuška–Aziz, Friedrichs and Horgan–Payne*, In preparation (2013).

[10] M. Crouzeix, *On an operator related to the convergence of Uzawa's algorithm for the Stokes equation*, in Computational Science for the 21 century, M.-O. Bristeau and al. eds, Wiley (1997), 242–249.

[11] M. Dobrowolski, *On the LBB constant on stretched domains*, Math. Nachr. **254/255** (2003), 64–67.
[12] M. Dobrowolski, *On the LBB condition in the numerical analysis of the Stokes equations*, Appl. Numer. Math. **54** (2005), 314–323.
[13] R.G. Durán, *An elementary proof of the continuity from $L^2_0(\Omega)$ to $H^1_0(\Omega)^n$ of Bogovskii's right inverse of the divergence*, Revista de la Unión Matemática Argentina **53(2)** (2012), 59–78.
[14] K.O. Friedrichs, *On certain inequalities and characteristic value problems for analytic functions and for functions of two variables*, Trans. Amer. Math. Soc. **41** (1937), 321–364.
[15] G.P. Galdi, *An Introduction to the Mathematical Theory of the Navier-Stokes Equations. Vol. I. Linearized Steady Problems*, Springer Tracts in Natural Philosophy **38**. Springer-Verlag (1994).
[16] V. Girault, P.-A. Raviart, *Finite Element Methods for Navier–Stokes Equations, Theory and Algorithms*, Springer–Verlag (1986).
[17] P. Grisvard, *Elliptic Problems in Nonsmooth Domains*, Pitman (1985).
[18] C.O. Horgan, L.E. Payne, *On inequalities of Korn, Friedrichs and Babuška–Aziz*, Arch. Rat. Mech. Anal. **82** (1983), 165–179.
[19] S. G. Mihlin, *The spectrum of the pencil of operators of elasticity theory.* (Russian) Uspehi Mat. Nauk **28** (1973), no. 3(171), 43–82
[20] J. Nečas, *Les méthodes directes en théorie des équations elliptiques*, Masson et Cie (1967).
[21] M.A. Ol'shanskio, E.V. Chizhonkov, *On the best constant in the inf-sup condition for elongated rectangular domains*, Mat. Zametki **67** (2000), 387–396; translation in *Math. Notes* **67** (2000), 325–332.
[22] G. Stoyan, *Towards discrete Velte decompositions and narrow bounds for inf-sup constants*, Comput. Math. Appl. **38** (1999), 243–261.
[23] G. Stoyan, *Iterative Stokes solvers in the harmonic Velte subspace*, Computing **67** (2001), 12–33.
[24] L. Tartar, *An Introduction to Navier-Stokes Equation and Oceanography*, Lecture Notes of the Unione Matematica Italiane **1**, Springer (2006).

DPG Method, an Overview. Global Properties of DPG Test Spaces

Leszek Demkowicz
(joint work with Jesse Chan and Jay Gopalakrishnan)

DPG is a minimum residual method. The presented abstract is an abbreviated version of [3]. Consider any variational problem,

$$\begin{cases} u \in U \\ b(u,v) = l(v) \quad v \in V \end{cases} \quad \Leftrightarrow \quad \begin{array}{l} Bu = l \\ B : U \to V' \quad \langle Bu, v\rangle = b(u,v),\ u \in U, v \in V \end{array}$$

where U, V are two Hilbert spaces, and sesquilinear form $b(u,v)$ and $l \in V'$ satisfy the usual conditions for the problem to be well posed.

The original idea behind the Discontinuous Petrov-Galerkin Method with Optimal Test Functions proposed in [1] was to employ special test functions that realize the supremum in the inf-sup condition:

$$\sup_{v \neq 0} \frac{|b(u,v)|}{\|v\|_V} \geq \gamma \|u\|_U$$

or, equivalently, solve the auxiliary variational problem (inversion of Riesz operator $R_V : V \to V'$),

$$\left\{ \begin{array}{l} v_{\delta u} \in V \\ (v_{\delta u}, \delta v)_V = b(\delta u, \delta v) \quad \delta v \in V \, . \end{array} \right.$$

We named the operator $T : U \to V, \quad \delta u \to v_{\delta u}$, the *trial-to-test operator*, and the Petrov-Galerkin (PG) method with test space $V_h = TU_h$, the *PG method with optimal test functions*. The main point of the idea is that such a method automatically inherits the stability from the continuous level. If form $b(u, v)$ satisfies the continuous inf-sup condition with constant γ on the continuous level $(u \in U, v \in V)$, it satisfies it also on the discrete level for $u \in U_h, v \in V_h$. The method has remarkable properties, it generates a hermitian and positive-definite stiffness matrix and delivers the *best approximation error* in the so-called *energy norm* implied by the form and the test norm $\|v\|_V$,

$$\|u\|_E := \sup_v \frac{|b(u, v)|}{\|v\|_V} = \|Bu\|_{V'} \, .$$

The method needs no a-posteriori error estimation, it comes with an a-posteriori error *evaluation* built-in. The Galerkin error measured in the energy norm equals residual and so it is available for an unknown exact solution u,

$$\|u_h - u\|_E = \|B(u_h - u)\|_{V'} = \|Bu_h - l\|_{V'} = \|R_V^{-1}(Bu_h - l)\|_V \, ,$$

provided we can invert the Riesz operator R_V.

All of these properties become less surprising once we realize that the proposed method is equivalent to the minimum residual method minimizing the residual in the dual test norm, $\|Bu_h - l\|_{V'} \to \min_{u_h \in U_h}$. The perhaps philosophical message of the story is that the minimum residual method *is the most stable version* of a Petrov-Galerkin discretization scheme.

Use of discontinuous test functions makes (an approximate) inversion of the Riesz operator possible. What makes the whole idea practical is the use of broken test spaces. Whereas this is possible within classical functional settings, the idea of *ultraweak variational formulation* is especially attractive. We review now quickly the main algebraic points for two important model problems: convection-dominated diffusion (left) and linear acoustics (right).

Rewrite the problem as a system of first order equations, multiply the individual equations with test functions, integrate over each element K, integrate *both equations* by parts.

$$\left\{ \begin{array}{rll} -\epsilon \Delta u + \mathrm{div}(\beta u) &= f & \text{in } \Omega \\ u &= u_0 & \text{on } \Gamma \end{array} \right. \qquad \left\{ \begin{array}{rll} -\Delta p - \omega^2 p &= 0 & \text{in } \Omega \\ \frac{\partial p}{\partial n} + i\omega p &= i\omega g & \text{on } \Gamma \end{array} \right.$$

$$\left\{ \begin{array}{rll} -\frac{1}{\epsilon}\sigma - \nabla u &= 0 & /\tau, \int_K, \text{by parts} \\ -\mathrm{div}(\sigma - \beta u) &= f & /v, \int_K, \text{by parts} \\ u &= u_0 & \text{on } \Gamma \end{array} \right.$$

$$\left\{ \begin{array}{rll} i\omega p + \mathrm{div} u &= 0 & /q, \int_K, \text{by parts} \\ i\omega u + \nabla p &= 0 & /v, \int_K, \text{by parts} \\ u_n - p &= g & \text{on } \Gamma \end{array} \right.$$

Sum up over all elements in the mesh. As usual, index h next to operators ∇ and div below, is supposed to remind us that the operators are applied *elementwise*. The brackets indicate integrals over the mesh skeleton. The trace and flux variables are declared to be *independent unknowns*, as indicated by placing "hats" over them.

$$\begin{array}{ll} (\sigma, \frac{1}{\epsilon}\tau + \nabla_h v) + (u, \mathrm{div}_h \tau - \beta \nabla_h v) & (p, i\omega q + \mathrm{div}_h v) + (u, i\omega v + \nabla_h q) \\ +\langle \widehat{-u}, \tau_n \rangle + \langle \widehat{-\sigma_n + \beta_n u}, v \rangle & +\langle \widehat{u_n - p}, q \rangle + \langle \hat{p}, v_n + q \rangle \\ = (f, v) & = 0 \end{array}$$

Impose boundary conditions by using extension of boundary data to the whole skeleton and introducing a new unknown w.

$$\begin{array}{ll} u = \widetilde{u_0} + w \quad w = 0 \text{ on } \Gamma & u_n - p = \widetilde{g} + w \quad w = 0 \text{ on } \Gamma \\ (\sigma, \frac{1}{\epsilon}\tau + \nabla_h v) + (u, \mathrm{div}_h \tau - \beta \nabla_h v) & (p, i\omega q + \mathrm{div}_h v) + (u, i\omega v + \nabla_h q) \\ +\langle \widehat{-w}, \tau_n \rangle + \langle \widehat{-\sigma_n + \beta_n u}, v \rangle & +\langle \widehat{w}, q \rangle + \langle \hat{p}, v_n + q \rangle \\ = (f, v) + \langle \widetilde{u_0}, v \rangle & = \langle \tilde{g}, q \rangle \end{array}$$

Both discussed cases can be written in a concise form using the abstract notation:

$$(1) \qquad \underbrace{(u, A_h^* v) + \langle \hat{w}, v \rangle}_{=: b((u,\hat{w}),v)} = \underbrace{(f, v) + \langle \widetilde{u_0}, v \rangle}_{=: l(v)}$$

where u is a group variable, A_h^* is the formal adjoint applied elementwise, and $\hat{w}$ is the group trace/flux unknown satisfying the homogeneous boundary conditions.

Functional setting is as follows. The *field variable* $u \in L^2(\Omega)$. The unknown (abstract) traces come from the trace of graph space for the (global) strong operator A defined by the system of first order PDEs, and are measured with the minimum energy norm extension. Finally, the test functions come from *broken* graph space for the adjoint operator, for both discussed examples equal to $H^1(\Omega_h) \times H(\mathrm{div}, \Omega_h)$. One can prove that the ultraweak variational formulation is well-posed. Moreover, if the original operator is bounded below in the L^2 sense, $\|Au\| \geq \beta \|u\|$, then the inf-sup constant for the sesquilinear form $b((u, \hat{w}), v)$ in (1) is $O(\beta)$. In particular, if β is independent of the perturbation parameter (ϵ or ω), so is the inf-sup constant for the ultraweak formulation. This implies a uniform stability of the DPG method.

Global properties of the optimal broken test spaces. DPG is not a single method but a methodology. For different test norms we obtain different corresponding energy norms (in which the DPG method delivers the best approximation). It is natural to ask the question whether we can construct a test norm to which the corresponding energy norm would coincide with *the norm we want*, say the original norm $\|u\|_U$. The answer is provided by Banach Closed Range Theorem, the optimal norm is given by reversing the order of spaces in the inf-sup condition:

$$\|v\| = \sup_{u \neq 0} \frac{|b(u, v)|}{\|u\|_U} .$$

In context of the ultraweak formulation, the optimal test norm is unfortunately non-localizable (it cannot be represented as a sum of norms over elements) and we

cannot compute with it. However, the proof of well-posedness for the ultraweak formulation establishes an $O(1)$ equivalence with the adjoint operator graph norm. It is for that reason that we initially used the term of the *quasi-optimal test norm* [2]. Thus the test (scaled) graph norm:

$$\|v\|^2_{V,\alpha} := \|A^* v\|^2 + \alpha \|v\|^2 \tag{2}$$

and the corresponding *trial-to-test operator*,

$$(u_p, \hat{w}_p) \to v = T(u_p, \hat{w}_p)$$
$$\begin{cases} v \in V \\ (A_h^* v, A_h^* \delta v) + \alpha (v, \delta v) \quad = (u_p, A_h^* \delta v) + \langle \hat{w}_p, \delta v \rangle \quad \forall \delta v \in V \end{cases}$$

emerge as an optimal choice of the test norm and the resulting optimal test spaces. Above, index p indicates order of trial element spaces $U_p, \hat{W}_p$ for both field variable u and trace $\hat{w}$.

In practice, the inversion of the Riesz operator must be done approximately using an *enriched test space* $V^r \subset V$. This results in an *approximate trial-to-test operator* T^r:

$$(u_p, \hat{w}_p) \to v = T^r(u_p, \hat{w}_p)$$
$$\begin{cases} v \in V^r \subset V \\ (A_h^* v, A_h^* \delta v) + \alpha (v, \delta v) \quad = (u_p, A_h^* \delta v) + \langle \hat{w}_p, \delta v \rangle \quad \forall \delta v \in V^r \end{cases}$$

Unfortunately, for neither of the discussed problems that seems to be satisfactory. For convection-dominated diffusion, the optimal test functions corresponding to the graph norm develop boundary layers and are very difficult to resolve, see [4] for a detailed discussion. For acoustics the situation is different. With a fixed number of elements per wavelength and a moderate r, the resolution of optimal test functions seems to be easy but the theory does not explain the pollution-free behavior of the method.

This motivates a different interpretation of the DPG method. We begin by introducing the *weakly conforming enriched test space* for the ultraweak formulation with *continuous* test functions:

$$V_p^r := \{ v \in V^r \ : \ \langle \hat{w}_p, v \rangle = 0 \quad \forall \hat{w}_p \} \subset V^r$$

and the corresponding *approximate global trial-to-test operator*:

$$u_p \to v = T_p^r u_p$$
$$\begin{cases} v \in V_p^r \\ (A_h^* v, A_h^* \delta v) + \alpha (v, \delta v) \quad = (u_p, A_h^* \delta v) \quad \forall \delta v \in V_p^r \end{cases}$$

One can prove [3, 4] that

$$T_p^r U_p \subset T^r (U_p \times \hat{W}_p) \, .$$

Consequently, both globally (impractical) and locally (practical) computed test functions deliver the same solution u_p.

The punchline is that *DPG can be viewed as a localization technique for computing approximation to globally optimal test functions:*

$$\begin{cases} v \text{ satisfies adjoint BC} \\ (A^*v, A^*\delta v) + \alpha(v, \delta v) = (u_p, A^*\delta v) \quad \forall \delta v \ : \ \delta v \text{ satisfies adjoint BC} \, . \end{cases}$$

In the global setting we can pass with $\alpha \to 0$ in the graph norm (2). The graph norm is equivalent with $\|v\|_{V,0}$ norm with equivalence constants approaching unity as $\alpha \to 0$. Exact optimal test functions corresponding to the $\|v\|_{V,0}$ norm deliver simply L^2-projection. The quasi-conforming approximate optimal test functions realized implicitly by the DPG method *represent a (nonconforming) least-squares approximation* to these pollution-free test spaces. You might say that the least squares are working backstage for the DPG method.

The bottom line for the wave propagation problems is the possibility of a new avenue for trying to explain and possibly improve the performance of the DPG method through the theory of non-conforming Petrov-Galerkin methods (work in progress).

References

[1] L. Demkowicz and J. Gopalakrishnan, *A class of discontinuous Petrov-Galerkin methods. Part II: Optimal test functions*, Num. Meth. Part. D.E., 27 (2011) (proceedings of Mafelap 2009), pp. 70-105.

[2] J. Zitelli, I. Muga, L, Demkowicz, J. Gopalakrishnan, D. Pardo and V. Calo, A class of discontinuous Petrov-Galerkin methods. IV: Wave propagation problems, J.Comp. Phys., 230(2011), pp. 2406-2432.

[3] L. Demkowicz and J. Gopalakrishnan, *An Overview of the DPG Method* , ICES Report, 2 (2013), submitted.

[4] J. Chan, J. Gopalakrishnan, and L. Demkowicz, *Global properties of DPG test spaces for convection-diffusion problems* , ICES Report, 5 (2013).

Aide-mémoire: fast multipole and butterfly algorithms

Laurent Demanet

This note is an overview of the interpolative framework in which both the fast multipole method and the butterfly algorithm can be explained. The question of interest is the fast computation of (a discretization of) integrals of the form $u(x) = \int G(x,y)q(y)dy$, where $G(x,y)$ is a kernel such $1/||x-y||$ (3D Laplace) and $e^{ik||x-y||}/||x-y||$ (3D Helmholtz).

Consider a dyadic tree partitioning of the domain into target boxes A and sources boxes B. This construction is standard, see [14]. Two boxes are said to be well-separated if they are sufficiently far apart in view of their diameter. What "sufficiently far" means is kernel-dependent, and is a linear-algebraic notion rather than a geometrical one: A and B are well-separated when the restriction of $G(x,y)$ to $x \in A$ and $y \in B$ has a low numerical rank. In what follows we do not keep track of the various truncation errors. Throughout, we assume that G is symmetric.

1. Low-frequency interpolative fast multipole method (FMM)

In the Laplace of low-frequency Hemholtz case, two boxes A and B are well-separated when the distance $d(A, B)$ is larger than a small multiple of their side-length. In that case we say that they are in the far-field of one another: $B \in \text{far(A)}$ if and only if $A \in \text{far(B)}$.

For each source box B, we define

$$u^B(x) = \int_B G(x,y)q(y)dy, \qquad x \in \text{far(B)}. \tag{1}$$

For each target box A, we define

$$u^{\text{far(A)}}(x) = \int_{\text{far(A)}} G(x,y)q(y)dy, \qquad x \in A. \tag{2}$$

- An interpolation rule in the x variable,

$$G(x,y) = \sum_n P_n^A(x)G(x_n^A, y), \qquad x \in A, y \in \text{far(A)}, \tag{3}$$

generates a notion of local expansion. Consider check potentials u_n^A at the nodes x_n^A,

$$u_n^A = \int_{\text{far(A)}} G(x_n^A, y)q(y)dy. \tag{4}$$

The interpolation rule in x allows to switch from potentials at x_n^A to potentials everywhere in A: combine (2), (3), (4) to get

$$u^{\text{far(A)}}(x) = \sum_n P_n^A(x)u_n^A, \qquad x \in A. \tag{5}$$

This results in an L2L operation ("translation"), to be used in a downward pass:

$$u_n^A \mathrel{+}= \sum_{n'} P_{n'}^{A_p}(x_n^A)u_{n'}^{A_p}.$$

The symbol += indicates that these check potentials are to be added to those resulting from the M2L operation, see below.

- An interpolation rule in the y variable,

$$G(x,y) = \sum_m G(x, y_m^B)P_m^B(y), \qquad x \in \text{far(B)}, y \in B, \tag{6}$$

generates a notion of multipole (interpolative) expansion. Consider equivalent densities q_m^B at the nodes y_m^B, so that

$$u^B(x) = \sum_m G(x, y_m^B)q_m^B, \qquad x \in \text{far(B)}. \tag{7}$$

The interpolation rule in y allows to switch from densities in B to equivalent densities q_m^B: combine (1), (6), (7) to get

$$q_m^B = \int_B P_m^B(y)q(y)dy. \tag{8}$$

In turns, this implies an M2M operation, to be used in an upward pass:

$$q_m^B = \sum_c \sum_{m'} P_m^B(y_{m'}^{B_c}) q_{m'}^{B_c}.$$

- An M2L conversion rule is

$$u_n^A \mathrel{+}= \sum_m G(x_n^A, y_m^B) q_m^B.$$

The symbol += indicates that these check potentials are to be summed over all B in the interaction list of A (boxes at the same level as A, in its far-field, and which are not descendants of boxes in the far-field of A_p), and added to the check potential resulting from the L2L operation.

Notice how (5) and (8) are transpose equations of one another, provided the interpolation rule is the same in x and in y.

Notice also that (3) and (6) are particular ways of generating separated expansions of blocks of $G(x, y)$, on $A \times \mathrm{far(A)}$ in the former case, and $\mathrm{far(B)} \times B$ in the latter case. The accuracy of these interpolation schemes depend on the separability properties of blocks of G, and how well the collection of P_n^{AB} over n approximates the alive eigenvectors of G.

2. High-frequency interpolative butterfly

The separation condition is much more restrictive in the high-frequency case, prompting the introduction of a different "butterfly" algorithm:

- The check potentials are split into different contributions coming from different sources boxes, and denoted u_n^{AB}; and
- The equivalent densities are split into different contributions generating potentials in different target boxes, and denoted q_m^{AB}.

The interpolation rules are now valid only for $x \in A$ and $y \in B$. The interpolation basis functions depend both on A and on B, and are denoted $P_n^{AB}(x)$.

- An interpolation rule in the x variable,

$$G(x, y) = \sum_n P_n^{AB}(x) G(x_n^A, y), \qquad x \in A, y \in B, \tag{9}$$

generates a notion of local expansion. Consider check potentials u_n^{AB} at the nodes x_n^A,

$$u_n^{AB} = \int_B G(x_n^A, y) q(y) dy. \tag{10}$$

The interpolation rule in x allows to switch from potentials at x_n^A to potentials everywhere in A: combine (1), (9), (10) to get

$$u^B(x) = \sum_n P_n^{AB}(x) u_n^{AB}, \qquad x \in A. \tag{11}$$

- An interpolation rule in the y variable,

$$G(x,y) = \sum_m G(x, y_m^B) P_m^{AB}(y), \qquad x \in A, y \in B, \tag{12}$$

generates a notion of multipole (interpolative) expansion. Consider equivalent densities q_m^{AB} at the nodes y_m^B, so that

$$u^B(x) = \sum_m G(x, y_m^B) q_m^{AB}, \qquad x \in A. \tag{13}$$

The interpolation rule in y allows to switch from densities in B to equivalent densities q_m^B: combine (1), (12), (13) to get

$$q_m^{AB} = \int_B P_m^{AB}(y) q(y) dy. \tag{14}$$

For high-frequency scattering and other oscillatory kernels, we have good separation if

$$\operatorname{diam}(A) \times \operatorname{diam}(B) \lesssim d(A,B) \times \lambda,$$

where $d(A,B)$ is the distance between box centers, and $\lambda = 2\pi/k$ is the wavelength.

The condition on the admissibility of couples of boxes determines the form of an L2L operation:

$$u_n^{AB} \mathrel{+}= \sum_c \sum_{n'} P_{n'}^{A_p B_c}(x_n^A) u_{n'}^{A_p B_c}.$$

An M2M operation is

$$q_m^{AB} = \sum_c \sum_{m'} P_m^{AB}(y_{m'}^{B_c}) q_{m'}^{A_p B_c}.$$

An M2L conversion is

$$u_n^{AB^\uparrow} \mathrel{+}= \sum_m G(x_n^A, y_m^B) q_m^{A^\uparrow B},$$

where B is in the interaction list of A. There is no sum to perform over the interaction list. The notation $A^\uparrow$ refers to some ancestor of A; this precaution arises from the fact that we want A and B on the same level for the M2L translation, but the u_n^{AB} and q_m^{AB} are usually available only for boxes at different levels (B at a higher level than A for u and B at a lower level than A for q).

The choice of interpolation scheme may be dictated by the particular kernel. An all-purpose choice is to use translated copies of the kernel itself:

$$P_n^{AB}(x) = \sum_m G(x, y_m^B) d_{mn}^{AB}.$$

A substitution in (9) reveals that the d coefficients are obtained as the middle factor of a skeleton decomposition of the (A,B) block of G,

$$G(x,y) = \sum_{m,n} G(x, y_m^B) d_{mn}^{AB} G(x_n^A, y).$$

References

[1] C. R. Anderson An implementation of the fast multipole method without multipoles. *SIAM J Sci Statist Comput*, 1992, 13: 923–947

[2] A. Boag, Y. Bresler, and E. Michielssen, A multilevel domain decomposition algorithm for fast $O(N^2 \log N)$ reprojection of tomographic images, *IEEE Trans. Im. Proc.* **9-9** (2000) 1573 – 1582

[3] J. Barnes, P. Hut A hierarchical O(NlogN) force-calculation algorithm. *Nature*, 1986, 324: 446–449

[4] S. Borm, L. Grasedyck, W. Hackbusch *Hierarchical matrices.* Technical Report 21, Max-Planck-Institut fur Mathematikin den Naturwissenschaften, Leipzig, 2003

[5] A. Brandt, Multilevel computations of integral transforms and particle interactions with oscillatory kernels *Comput. Phys. Commun.*, **65** (1991) 24–38

[6] E. Candès, L. Demanet, L. Ying, A Fast Butterfly Algorithm for the Computation of Fourier Integral Operators *SIAM Multiscale Model. Simul.* 7:4 (2009) 1727–1750

[7] B. Engquist and L. Ying. Fast directional multilevel algorithms for oscillatory kernels. *SIAM Journal on Scientific Computing* **29-4** (2007) 1710–1737

[8] L. Greengard, V. Rokhlin, A fast algorithm for particle simulations, *Journal of Computers and Physics* **73** (1987) 325–348.

[9] E. Michielssen and A. Boag, A multilevel matrix decomposition algorithm for analyzing scattering from large structures *IEEE Transactions on Antennas and Propagation* **44** (1996) 1086–1093

[10] S Nilsson, LE Andersson Application of fast backprojection techniques for some inverse problems of synthetic aperture radar *Proc. SPIE* **3370** (1998) 62–72

[11] M. O'Neil and V. Rokhlin, A new class of analysis-based fast transforms *Tech. Rep. 1384, Department of Computer Science, Yale University, August 2007.*

[12] V. Rokhlin Rapid solution of integral equations of scattering theory in two dimensions *J. Comput. Phys.* **86-2** (1990) 414–439

[13] V. Rokhlin Diagonal forms of translation operators for the Helmholtz equation in three dimensions. *Appl Comput Harmon Anal*, 1993, 1: 82–93

[14] L. Ying A pedestrian introduction to fast multipole methods *Sci China Math*, 2012, 55, doi: 10.1007/s11425-012-4392-0

[15] L. Ying, G. Biros, D. Zorin A kernel-independent adaptive fast multipole algorithm in two and three dimensions. *J. Comput Phys*, 2004, 196: 591–626

On the far field of the solutions of Helmholtz equations in periodic waveguide

Sonia Fliss

(joint work with Patrick Joly)

The model problem that we consider in this paper is the propagation of a time harmonic scalar wave in a perfect 2D periodic waveguide. More precisely, we shall assume that the geometry $\Omega \subset \mathbb{R} \times (0,1)$ as well as the material properties of the medium (typically the refractive index) $n_p \in L^\infty(\Omega)$ - with $n_p \geq c > 0$ - are periodic in one direction (without loss of generality, we will suppose the period equal to 1) :

- $\Omega = \bigcup_{p\in\mathbb{Z}} \mathcal{C}_p$ where $\mathcal{C}_p = \mathcal{C} + (p,0)$ and $\mathcal{C} \subset (-1/2, 1/2) \times (0,1)$
- $n_p(x_1+1, x_2) = n_p(x_1, x_2), \quad \forall (x_1, x_2) \in \Omega.$

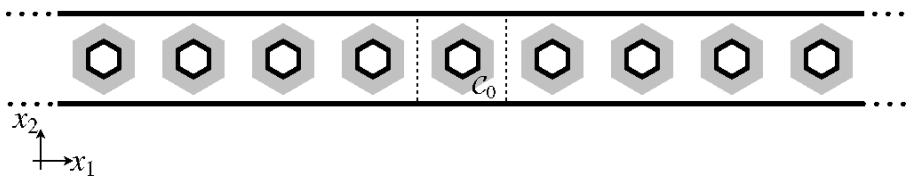

FIGURE 1. Example of waveguide Ω with its periodic geometry (its boundary is drawn with black lines) and level set of the refractive index (typically $n_p = 1$ in the gray regions and $n_p = 2$ in the white regions) .

We consider then the *outgoing* solution of

$$\begin{cases} -\triangle u - \omega^2\, n_p^2\, u = f & \text{in } \Omega \\ \partial_\nu u = 0 & \text{on } \partial\Omega \end{cases} \tag{1}$$

where ν is the exterior normal of Ω and the source term f is supposed to be of compact support in Ω.

In order to define what "outgoing" means in a periodic waveguide, we use the limiting absorption principle and define the solution u as the limit, if it exists and in a sense to be precised, when ε tends to 0^+ of u_ε, unique solution in $H^1(\Omega)$ of

$$\begin{cases} -\triangle u_\varepsilon - (\omega^2 + \imath\varepsilon\omega)\, n_p^2\, u_\varepsilon = f & \text{in } \Omega \\ \partial_\nu u_\varepsilon = 0 & \text{on } \partial\Omega \end{cases} \tag{2}$$

Using the Floquet modes of the periodic medium, we are able to give a semi-analytic expression of u_ε, show in which sense u_ε has a limit when ε tends to 0 and deduce a semi-analytical expression of this limit, which is by definition the "outgoing" solution. We investigate then the asymptotic behavior of the solution, when x_1 tends to $\pm\infty$. This enables us to define a radiation condition and show well-posedness of the Helmholtz equation set in a periodic waveguide.

1. Limiting absorption principle

Using the Floquet Bloch Transform in the x_1-direction and the well posedness in $H^1(\Omega)$ of problem (2), it is easy to show that

$\forall (x_1, x_2) \in \mathcal{C},\ \forall p \in \mathbb{Z},$

$$u_\varepsilon(x_1 + p, x_2) = \frac{1}{2\pi} \sum_{n\in\mathbb{N}} \int_{-\pi}^{\pi} \frac{P_n(f)(x_1, x_2; \xi)}{\lambda_n(\xi) - (\omega^2 + \imath\varepsilon\omega)}\, e^{\imath p\xi}\, d\xi \tag{3}$$

where, for all $\xi \in (-\pi, \pi)$, $\lambda_n(\xi)$ is the n-th eigenvalue and $\varphi_n(\cdot;\xi)$ an associated eigenvector of the self-adjoint and positive operator

$$\left| \begin{array}{l} A(\xi) = -\dfrac{1}{n_p^2}\triangle \\ D(A(\xi)) = \{u \in H^2(\mathcal{C}), \text{ such that } \partial_\nu u|_{\partial\mathcal{C}\cap\partial\Omega} = 0 \\ \qquad u(1/2, x_2) = e^{\imath\xi} u(-1/2, x_2) \text{ and } \partial_{x_1} u(1/2, x_2) = e^{\imath\xi}\partial_{x_1} u(-1/2, x_2)\}. \end{array} \right.$$

We can easily show that for all $n \in \mathbb{N}$ and $\xi \in (-\pi, \pi)$

$$\lambda_n(\xi) = \lambda_n(-\xi). \tag{4}$$

In (3), $P_n(f)$ is a projector defined by

$\forall n \in \mathbb{N},\ \forall \xi \in (-\pi, \pi),\ \forall (x_1, x_2) \in \mathcal{C}$,

$$P_n(f)(x_1, x_2; \xi) = \Big(\hat{f}(\cdot;\xi), \varphi_n(\cdot;\xi)\Big)_{L^2(\mathcal{C})}\ \varphi_n(x_1, x_2; \xi) \tag{5}$$

where $\hat{f}$ is the Floquet-Bloch transform of f.

Let us define the finite sets

$$I(\omega) = \{n \in \mathbb{N},\ \exists\, \xi \in (-\pi, \pi),\ \lambda_n(\xi) = \omega^2\}$$

and for $n \in I(k)$

$$\Xi_n(\omega) = \{\xi \in (-\pi, \pi),\ \lambda_n(\xi) = \omega^2\}.$$

Because of (4), we deduce that if ξ is in $\Xi_n(\omega)$, $-\xi$ is too.

Using the abstract result of [2], or the more explicit result of [1], the limiting absorption principle can be shown except for a countable set of frequencies

$$\sigma_0 = \Big\{\omega \in \mathbb{R}^+,\ \exists\, n \in I(\omega),\ \exists\, \xi \in \Xi_n(\omega),\ \lambda_n'(\xi) = 0\Big\}$$

Theorem 1. *For all $\omega \notin \sigma_0$,*

$$\forall p \in \mathbb{Z}, \quad \lim_{\varepsilon \to 0} \|u - u_\varepsilon\|_{H^1(\mathcal{C}_p)} = 0$$

where u is a solution of (1) *and defined by*
$\forall (x, y) \in \mathcal{C},\ \forall (p, q) \in \mathbb{Z}$,

$$u(x_1 + p, x_2) = \frac{1}{2\pi} \sum_{n \notin I(\omega)} \int_{-\pi}^{\pi} \frac{P_n(f)(x_1, x_2; \xi)}{\lambda_n(\xi) - \omega^2} e^{\imath p\xi} d\xi \tag{6}$$

$$+ \frac{1}{2\pi} \sum_{n \in I(\omega)} \Big[p.v. \int_{-\pi}^{\pi} \frac{P_n(f)(x_1, x_2; \xi)}{\lambda_n(\xi) - \omega^2} e^{\imath p\xi} d\xi + \imath\pi \sum_{\xi \in \Xi_n(\omega)} \frac{P_n(f)(x_1, x_2; \xi)}{|\lambda_n'(\xi)|} e^{\imath p\xi}\Big].$$

2. Asymptotic behaviour of the Green function

In the following $k \notin \sigma_0$. To prove the asymptotic behavior of the Green function, the main property is the C^∞-regularity of the eigenvalues $\xi \mapsto \lambda_n(\xi)$ and of the eigenvectors $\xi \mapsto \varphi_n(\xi)$ with respect to ξ for $n \in I(k)$. Using [3], such property holds except for a countable set of frequencies

$$\tilde{\sigma}_0 = \{\omega \in \mathbb{R}^+,\ \exists n, m \in I(\omega),\ \exists \xi,\ \lambda_n(\xi) = \lambda_m(\xi)\}.$$

Then the proof relies on

- analyticity arguments to deal with the first sum, denoted $\tilde{u}$, in the right hand side of (6). More precisely, one shows that for all $x \in \mathcal{C}$, $p \in \mathbb{Z}$ and $N \in \mathbb{N}$
$$\tilde{u}(x_1 + p, x_2) = \mathcal{O}_{H^1}\left(p^{-N}\right);$$
- non stationary phase theorem to deal with each principal value, denoted $u_{(n)}$, of the second sum in the right hand side of (6). More precisely, one shows that for all $n \in I(k)$, $x \in \mathcal{C}$, $p \in \mathbb{Z}$ and $N \in \mathbb{N}$

$$u_{(n)}(x_1 + p, x_2) = \imath\pi\,\mathrm{sign}(p) \sum_{\xi \in \Xi_n(\omega)} \frac{P_n(f)(x_1, x_2; \xi)}{\lambda_n'(\xi)} e^{\imath p\xi} + \mathcal{O}_{H^1}\left(p^{-N}\right)$$

Theorem 2. *Suppose in the following $\omega \notin \sigma_0 \cup \tilde{\sigma}_0$. For all $x \in \mathcal{C}$ and $N \in \mathbb{N}$*

For $p > 0$

$$u(x_1+p, x_2) = \imath \sum_{n \in I(\omega)} \sum_{\substack{\xi \in \Xi_n(\omega) \\ \lambda_n'(\xi) > 0}} \frac{\left(\hat{f}(\cdot;\xi), \varphi_n(\cdot;\xi)\right)_{L^2(\mathcal{C})}}{|\lambda_n'(\xi)|} \varphi_n(x_1, x_2; \xi) e^{\imath p\xi} + \mathcal{O}_{H^1}\left(p^{-N}\right)$$

For $p < 0$

$$u(x_1+p, x_2) = \imath \sum_{n \in I(\omega)} \sum_{\substack{\xi \in \Xi_n(\omega) \\ \lambda_n'(\xi) < 0}} \frac{\left(\hat{f}(\cdot;\xi), \varphi_n(\cdot;\xi)\right)_{L^2(\mathcal{C})}}{|\lambda_n'(\xi)|} \varphi_n(x_1, x_2; \xi) e^{\imath p\xi} + \mathcal{O}_{H^1}\left(p^{-N}\right)$$

The solution of problem (1) behaves when $x \to +\infty$ (resp. $x \to -\infty$) as a linear combination of the Floquet modes $\varphi_n(\cdot, \xi)$ which propagate to the right (resp. to the left) as $\lambda_n'(\xi) > 0$ (resp. $\lambda_n'(\xi) < 0$). Let us remark that because (4), if ξ is in $\Xi_n(\omega)$, $-\xi$ is too and if $\lambda_n(\xi) > 0$, we have $\lambda_n(-\xi) < 0$. Then for any propagative Floquet mode which is ξ-quasi periodic and propagates to the right, it corresponds a propagative Floquet mode which is $-\xi$-quasi-periodic and propagates to the left.

3. Radiation condition and uniqueness of the solution

We use the last result to define a radiation condition and establish, thanks to arguments used in [4], the well-posedness of the Helmholtz equation set in a periodic waveguide.

Definition 1. *We say that u satisfies the outgoing radiation condition if and only if there exist $(u_n^{\pm})_n$ such that $\forall x \in \mathcal{C}$, $p \in \mathbb{N}$, $N \in \mathbb{N}$*

$$u(x_1 \pm p, x_2) = \sum_{n \in I(\omega)} \sum_{\substack{\xi \in \Xi_n(\omega) \\ \pm \lambda_n'(\xi) > 0}} u_n^{\pm}\, \varphi_n(x;\xi)\, e^{ip\xi} \;+\; \mathcal{O}_{H^1}\left(p^{-N}\right)$$

Theorem 3. *Suppose $\omega \notin \sigma_0 \cup \tilde{\sigma}_0$. Let u be a solution of*

$$\begin{cases} -\triangle u - \omega^2\, n_p^2\, u = 0 & \text{in } \Omega \\ \partial_\nu u = 0 & \text{on } \partial\Omega \end{cases}$$

which satisfies the outgoing radiation condition. Then $u = 0$.

4. Conclusions

This analysis is one of the main tool to solve inverse problems in locally perturbed periodic waveguide when the data are far field measurements of scattering problems.

One challenging perspective of this work is to extend these results to periodic problems in domains which are periodic and infinite in at least 2 directions.

References

[1] S. Fliss, *Etude mathématique et numérique de la propagation des ondes dans des milieux périodiques localement perturbés*, PhD Thesis Ecole Doctorale de Polytechnique,May 2009.

[2] S. Z. Levendorskii, *Acoustic waves in perturbed periodic layer: a limiting absorption principle*, Asymptot. Anal. **16** (1998), no. 1, pp. 15–24.

[3] T. Kato, *Perturbation theory for linear operators*, Springer-Verlag, Classics in Mathematics, Berlin, 1995.

[4] S.A. Nazarov and B.A. Plamenevsky, *Elliptic Problems in Domains with Piecewise Smooth Boundaries*, vol. 13 of de Gruyter Expositions in Mathematics, Berlin, 1994.

Finite Element Heterogeneous Multiscale Method for the Wave Equation: Long Time Effects

Marcus J. Grote

(joint work with Assyr Abdulle, and Christian Stohrer)

1. Introduction

For limited time the propagation of waves in a highly oscillatory medium is well-described by the non-dispersive homogenized wave equation. With increasing time, however, the true solution deviates from the classical homogenization limit, as a large secondary wave train develops unexpectedly. Here, we propose a new finite element heterogeneous multiscale method (FE-HMM), which captures not only the short-time macroscale behavior of the wave field but also those secondary long-time dispersive effects.

2. Long-Time Wave Propagation

Let $\Omega \subset \mathbb{R}^n$ be a domain and $T > 0$. We consider the wave equation

$$\begin{cases} \partial_{tt} u^\varepsilon - \nabla \cdot (a^\varepsilon \nabla u^\varepsilon) = F & \text{in } \Omega \times (0,T), \\ u^\varepsilon(x,0) = f(x) & \text{in } \Omega, \\ \partial_t u^\varepsilon(x,0) = g(x) & \text{in } \Omega, \end{cases} \tag{1}$$

where $a^\varepsilon(x) \in (L^\infty(\Omega))^{d\times d}$ is symmetric, uniformly elliptic, and bounded. Here $\varepsilon > 0$ represents a small scale in the problem, which we cannot afford to fully resolve and thus characterizes the multiscale nature of $a^\varepsilon(x)$. With appropriate Dirichlet or periodic boundary conditions, the solution u^ε is uniquely determined for every $\varepsilon > 0$.

2.1. **Classical homogenization.** According to classical homogenization theory, u^ε converges to the solution u^0 of the "homogenized" wave equation as $\varepsilon \to 0$,

$$\partial_{tt} u^0 - \nabla \cdot (a^0 \nabla u^0) = F,$$

yet the homogenized tensor (or squared velocity field) a^0 can only rarely be computed explicitly. Although u^0 approximates u^ε for short times in the L^2-norm, it becomes increasingly inadequate at later times $T \sim \varepsilon^{-2}$, since it neglects microscopic dispersive effects that accumulate over time, as shown in Figure 1. Here we consider (1) in $\Omega = (-1,1)$ with periodic boundary conditions, let $u(x,0)$ be a Gaussian pulse with zero initial velocity and set

$$a^\varepsilon = \sqrt{2} + \sin\Big(2\pi \frac{x}{\varepsilon}\Big) \text{ with } \varepsilon = \frac{1}{50}. \tag{2}$$

In Figure 1, the reference solution of (1)–(2) corresponds to a direct numerical simulation (DNS), where the micro-scale is fully resolved. After one revolution ($T = 2$), the homogenized and the DNS solution coincide. After fifty revolutions ($T = 100$), however, the DNS displays dispersive effects, which the homogenized solution fails to capture.

2.2. **Effective dispersive equation.** Various formal asymptotic arguments were derived to elucidate that peculiar inherently dispersive long-time behavior of waves propagating through a strongly heterogeneous periodic medium [1]. An effective equation that captures those dispersive effects was recently derived in [2] for the one-dimensional case when a^ε is ε-periodic:

$$\partial_{tt}(u^{\text{eff}} - \varepsilon^2\, b\, \partial_{xx} u^{\text{eff}}) - a^0 \partial_{xx} u^{\text{eff}} = F. \tag{3}$$

Again, a^0 denotes the homogenized effective coefficient from classical homogenization theory whereas $b > 0$ denotes a distinct constant. As shown in Figure 1, u^ε and u^{eff} essentially coincide both at early and later times.

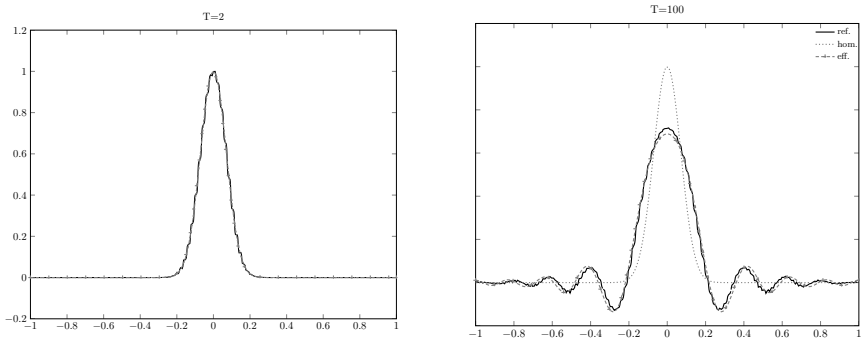

FIGURE 1. Reference (ref.), homogenized (hom.) and effective (eff.) solution: short-time $T = 2$ (left), and long-time $T = 100$ (right).

3. FE Heterogeneous Multiscale Method

In [3], the FE-HMM for elliptic problems [4] was extended to the time dependent wave equation. It was shown to converge to u^0 at finite times, yet it also fails to capture long-time dispersive effects in the true solution. To incorporate those dispersive effects, we not only need an effective bilinear form but also an effective inner product, akin to the weak formulation of (3). Both require the numerical solutions of micro problems on sampling domains K_δ of size δ proportional to ε. An alternative HMM scheme, based on the finite difference approximation of an effective flux, was proposed in [5]. Since it is based on an effective model [2], which is ill-posed, appropriate regularization techniques need to be implemented.

We now give a brief description of our new FE-HMM scheme. First, we generate a macro triangulation $\mathcal{T}_H$ and choose an appropriate macro FE space $S(\Omega, \mathcal{T}_H)$. By macro we mean that $H \gg \varepsilon$ is allowed. Within each macro element $K \in \mathcal{T}_H$ we choose two quadrature formulas $\{x_{K,j}, \omega_{K,j}\}$ and $\{x^L_{K,j}, \omega^L_{K,j}\}$. The HMM solution u_H is given by the following variational problem:

$$\begin{cases} \text{Find } u_H : [0,T] \to S(\Omega, \mathcal{T}_H) \text{ such that} \\ (\partial_{tt} u_H, v_H)_Q + B_H(u_H, v_H) = (F, v_H) \\ \text{for all } v_H \in S(\Omega, \mathcal{T}_H) \text{ and,} \\ \quad u_H(0) = f_H,\ \partial_t u_H(0) = g_H \text{ in } \Omega, \end{cases} \tag{4}$$

where the initial data f_H and g_H are suitable approximations of f and g in $S(\Omega, \mathcal{T}_H)$ whereas the effective bilinear form B_H and the effective inner product $(\cdot,\cdot)_Q$ are defined as follows. The FE-HMM bilinear form is given by

$$B_H(v_H, w_H) = \sum_{K \in \mathcal{T}_H} \sum_{j=1}^{J} \frac{\omega_{K,j}}{|K_\delta|} \int_{K_\delta} a^\varepsilon(x) \nabla v_h(x) \cdot \nabla w_h(x)\, dx,$$

and the FE-HMM inner product by

$$(v_H, w_H)_Q = (v_H, w_H)_H + (v_H, w_H)_M.$$

Here,

$$(v_H, w_H)_H = \sum_{K\in\mathcal{T}_H} \sum_{j=1}^{J_L} \omega_{K,j}^L v_H(x_{K,j}^L) w_H(x_{K,j}^L).$$

Note that $(\cdot,\cdot)_H$ corresponds to a standard approximation of the L^2-inner product by numerical quadrature, whereas the long-time correction is given by

$$(v_H, w_H)_M = \sum_{K\in\mathcal{T}_H} \sum_{j=1}^{J} \frac{\omega_{K,j}}{|K_\delta|} \int_{K_\delta} (v_h(x) - v_{H,\mathrm{lin}}(x))(w_h(x) - v_{H,\mathrm{lin}}(x))\, dx.$$

In the above, the micro solution v_h (resp. w_h) is given by

$$\text{(5)} \qquad \begin{cases} \text{Find } v_h \text{ such that } (v_h - v_{H,\mathrm{lin}}) \in S(K_\delta, \mathcal{T}_h) \text{ and} \\ \displaystyle\int_{K_\delta} a^\varepsilon(x)\nabla v_h(x)\cdot\nabla z_h(x)\, dx = 0, \\ \text{for all } z_h \in S(K_\delta, \mathcal{T}_h). \end{cases}$$

Here $S(K_\delta, \mathcal{T}_h)$ is a micro FE space on the sampling domain K_δ with micro triangulation $\mathcal{T}_h$, and $v_{H,\mathrm{lin}}$ denotes the linearization of v_H at the quadrature point $x_{K,j}$,

$$v_{H,\mathrm{lin}}(x) = v_H(x_{K,j}) + (x - x_{K,j})\cdot\nabla v_H(x_{K,j}).$$

Since B_H is elliptic and bounded and $(\cdot,\cdot)_Q$ is a true inner product, the FE-HMM is well-defined for all $H, h > 0$.

For every quadrature node $x_{K,j}$, we must solve the associated micro problem (5) whose solution is then used both for B_H and $(\cdot,\cdot)_Q$. By choosing two different quadrature formulas for $(\cdot,\cdot)_H$ and $(\cdot,\cdot)_M$, the number of micro problems required, and hence the computational cost, remains the same as for the FE-HMM from[3].

4. Numerical Experiments

We again apply our FE-HMM, defined in (4), to (1)–(2) as in Figure 1. We use cubic FE at the macro- and the micro-scale, with mesh sizes $H = 1/75$ and $h = \varepsilon/20 = 1/1000$. Note that linear or quadratic finite elements could also be used. For time-stepping we use a standard Leap-Frog scheme, with $\Delta t = H/10$. As shown in Figure 2, the new FE-HMM succeeds in capturing, the long-time effects in the true solution. In contrast, the solution of the FE-HMM of [3] is unable to capture those dispersive effects, since this solution was proven to converge to the homogenized solution, u^0, as $\varepsilon \to 0$ on finite time intervals.

References

[1] F. Santosa and W. W. Symes, *A Dispersive Effective Medium for Wave Propagation in Periodic Composites*, SIAM J. Appl. Math., **51**, pp. 984–1005.

[2] A. Lamacz, *Dispersive Effective Models for Waves in Heterogeneous Media*, Math. Models Methods Appl. Sci., **21** (2011), pp. 1871–1899.

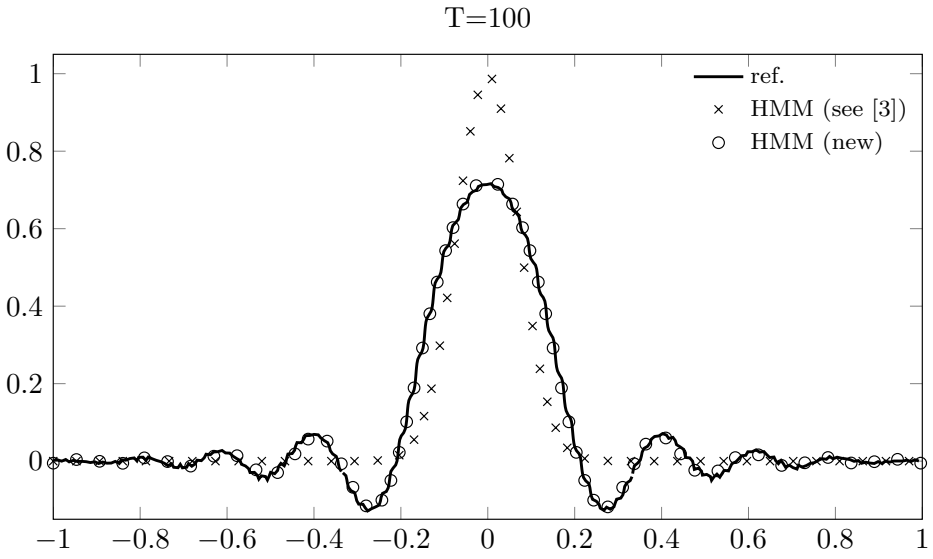

FIGURE 2. Reference solution (ref.), FE-HMM from [3] and new FE-HMM at time $T = 100$.

[3] A. Abdulle and M. J. Grote, *Finite Element Heterogeneous Multiscale Method for the Wave Equation*, Multiscale Model. Simul., **9** (2011), pp. 766–7921.
[4] A. Abdulle, *The Finite Element Heterogeneous Multiscale Method: a computational strategy for multiscale PDEs*, GAKUTO Internat. Seri. Math. Sci. Appl., **31** 2009, pp. 133–182.
[5] B. Engquist, H. Holst and O. Runborg , *Multi-scale methods for wave propagation in heterogeneous media*, Comm. Math. Sci., **9** 2011, pp. 33–56.

Stabilized Galerkin Methods for Magnetic Advection

HOLGER HEUMANN
(joint work with Ralf Hiptmair)

The behavior of electromagnetic fields in the stationary flow field of a conducting fluid can be modelled by the (non-dimensional) advection-diffusion equation [9, Section 5]

$$\underbrace{\mathbf{curl}\,\nu\,\mathbf{curl}\,\mathbf{A}}_{\text{diffusion}} + \underbrace{\alpha\mathbf{A}}_{\text{dissipation}} + \underbrace{\mathbf{curl}\,\mathbf{A}\times\boldsymbol{\beta} + \mathbf{grad}\,(\mathbf{A}\cdot\boldsymbol{\beta})}_{\text{advection}} = \mathbf{f} \quad \text{in } \Omega\,. \tag{1}$$

Here $\Omega \subset \mathbb{R}^3$ is a bounded domain scaled such that $\operatorname{diam}(\Omega) \approx 1$, and the vector field $\mathbf{A} = \mathbf{A}(\boldsymbol{x})$ stands for the magnetic vector potential. The fluid velocity is $\boldsymbol{\beta} = \boldsymbol{\beta}(\boldsymbol{x})$, of which we assume $\boldsymbol{\beta} \in \boldsymbol{W}^{1,\infty}(\Omega)$ and a scaling that achieves $\max_{\boldsymbol{x}} |\boldsymbol{\beta}(\boldsymbol{x})| \approx 1$. The coefficient $\nu = \nu(\boldsymbol{x}) \geq 0$ controls the strength of magnetic diffusion, whereas the conductivity of the fluid enters through the bounded scalar

function $\alpha = \alpha(\boldsymbol{x})$. The model underlying (1) is known as quasi-magneto-static with temporal gauge.

We are keen to obtain methods that are robust with respect to the singular perturbation limit $\nu \to 0$. Necessarily, these methods must remain viable even if $\nu = 0$. Therefore, we confine the presentation to the pure magnetic advection boundary value problem

$$\begin{aligned} \alpha\mathbf{A} + \mathsf{L}_{\boldsymbol{\beta}}\,\mathbf{A} &= \mathbf{f} \quad \text{in } \Omega\,, \\ \mathbf{A}_{|\Gamma_{\text{in}}} &= \mathbf{g} \quad \text{on } \Gamma_{\text{in}}\,, \end{aligned} \tag{2}$$

with *magnetic advection operator* or *Lie-derivative*

$$\mathsf{L}_{\boldsymbol{\beta}}\,\mathbf{u} := \mathbf{grad}(\boldsymbol{\beta}\cdot\mathbf{u}) + \mathbf{curl}\,\mathbf{u}\times\boldsymbol{\beta}\,. \tag{3}$$

We impose Dirichlet boundary conditions on the inflow boundary Γ_{in}, i.e. that part of the domain with $\boldsymbol{\beta}\cdot\mathbf{n} < 0$, with $\mathbf{n}$ the outward normal on $\partial\Omega$.

Our derivation of a stabilized Galerkin methods for the magnetic advection boundary value problem (2) runs parallel to that of the discontinuous Galerkin method for scalar advection [4]. The key tool is the Leibniz rule for the advection operator and the corresponding integration by parts formula

$$(\mathsf{L}_{\boldsymbol{\beta}}\,\mathbf{u},\mathbf{v})_{\Omega} - (\mathbf{u},\mathcal{L}_{\boldsymbol{\beta}}\,\mathbf{v})_{\Omega} = \int_f (\boldsymbol{\beta}\cdot\mathbf{n}_f)(\mathbf{u}\cdot\mathbf{v})\,\mathrm{d}S\,, \tag{4}$$

with the formal adjoint advection operator

$$\mathcal{L}_{\boldsymbol{\beta}}\,\mathbf{u} := \mathbf{curl}(\boldsymbol{\beta}\times\mathbf{u}) - \boldsymbol{\beta}\,\mathrm{div}\,\mathbf{u}\,. \tag{5}$$

Piecewise polynomial trial spaces are used for the Galerkin discretization of the resulting variational problems. As magnetic advection falls into the class of *Friedrichs symmetric operators* [7], e.g.

$$\mathsf{L}_{\boldsymbol{\beta}}\,\mathbf{u} = D\boldsymbol{\beta}^T\mathbf{u} + \sum_{i=1}^{3}\boldsymbol{\beta}_i\partial_i\mathbf{u}$$

we could just appeal to the abstract convergence theory for discontinuous Galerkin approximation from [5, 15, 6].

But, our main interest here is in the use of $\boldsymbol{H}(\mathbf{curl},\Omega)$-conforming piecewise polynomial trial spaces that feature tangential continuity across interelement boundaries. Meanwhile such spaces have become well established and they are known as discrete 1-forms or (higher order) edge elements [18, 19, 11]. There are several reasons for insisting on tangential continuity: Firstly, since $\mathbf{A}$ is a magnetic vector potential we want its $\mathbf{curl}$ to be a well-defined square integrable magnetic flux field. Secondly, $\boldsymbol{H}(\mathbf{curl},\Omega)$-conforming trial and test spaces pave the way for a stable Galerkin discretization of the magnetic diffusion operator $\mathbf{curl}\,\nu\,\mathbf{curl}$. This is important, because we always regard the discretization of the pure advection problem as a mere building block in schemes for the more general advection-diffusion problem (1). Of course, totally continuous $(H^1(\Omega))^3$-conforming trial spaces are an option in principle. However, they usually fail to provide stable Galerkin discretization of the diffusion operator [1, 2].

Our main result [10] reveals that the stabilized Galerkin method with $\boldsymbol{H}(\mathbf{curl}, \Omega)$-conforming approximation spaces enjoys the same rates of convergence as the stabilized Galerkin methods with globally discontinuous approximation spaces [20, 16, 12]. Thus, it suffices to aim stabilization at the discontinuous normal components. In particular, we do not need introduce additional stabilization such as the residual-based techniques [21, Chapter 3.2] [13] [14] for stabilizing Galerkin methods with continuous approximation spaces.

There exists other stabilizing methods based on ad-hoc approaches to upwinding [3, 8, 17], but to the best of our knowledge, hardly any convergence results are available.

References

[1] D. Boffi. Approximation of eigenvalues in mixed form, discrete compactness property, and application to *hp* mixed finite elements. *Computer Methods in Applied Mechanics and Engineering*, 196:3672–3681, 2007.

[2] D. Boffi, F. Brezzi, and L. Gastaldi. On the problem of spurious eigenvalues in the approximation of linear elliptic problems in mixed form. *Math. Comp.*, 69:121–140, 2000.

[3] A. Bossavit. Extrusion, contraction: Their discretization via Whitney forms. *COMPEL*, 22(3):470–480, 2004.

[4] F. Brezzi, L. D. Marini, and E. Süli. Discontinuous Galerkin methods for first-order hyperbolic problems. *Math. Models Methods Appl. Sci.*, 14(12):1893–1903, 2004.

[5] A. Ern and J.-L. Guermond. Discontinuous Galerkin methods for Friedrichs' systems. I. General theory. *SIAM J. Numer. Anal.*, 44(2):753–778, 2006.

[6] R. S. Falk and G. R. Richter. Explicit finite element methods for symmetric hyperbolic equations. *SIAM J. Numer. Anal.*, 36(3):935–952 (electronic), 1999.

[7] K. O. Friedrichs. Symmetric positive linear differential equations. *Comm. Pure Appl. Math.*, 11:333–418, 1958.

[8] F. Henrotte, H. Heumann, E. Lange, and K. Haymeyer. Upwind 3-d vector potential formulation for electromagnetic braking simulations. *IEEE Transactions on Magnetics*, 46(8):2835–2838, 2010.

[9] H. Heumann and R. Hiptmair. Eulerian and semi-Lagrangian methods for convection-diffusion for differential forms. *Discrete Contin. Dyn. Syst.*, 29(4):1471–1495, 2011.

[10] H. Heumann and R. Hiptmair. Stabilized Galerkin Methods For Magnetic Advection. *SAM-report, ETH Zurich, submitted to M2AN*, 2012.

[11] R. Hiptmair. Finite elements in computational electromagnetism. *Acta Numerica*, 11:237–339, 2002.

[12] P. Houston, C. Schwab, and E. Süli. Discontinuous *hp*-finite element methods for advection-diffusion-reaction problems. *SIAM J. Numer. Anal.*, 39(6):2133–2163, 2002.

[13] T. J. R. Hughes and A. Brooks. A multidimensional upwind scheme with no crosswind diffusion. In *Finite Element Methods for Convection Dominated Flows*, volume 34 of *AMD*, pages 19–35. Amer. Soc. Mech. Engrs., New York, 1979.

[14] T. J. R. Hughes, L. P. Franca, and G. M. Hulbert. A new finite element formulation for computational fluid dynamics. VIII. The Galerkin/least-squares method for advective-diffusive equations. *Comput. Methods Appl. Mech. Engrg.*, 73(2):173–189, 1989.

[15] M. Jensen. On the discontinuous Galerkin method for Friedrichs systems in graph spaces. In *Large-scale scientific computing*, volume 3743 of *Lecture Notes in Comput. Sci.*, pages 94–101. Springer, Berlin, 2006.

[16] P. Lasaint and P.-A. Raviart. On a finite element method for solving the neutron transport equation. In *Proc. Sympos., Math. Res. Center, Univ. of Wisconsin-Madison*, number 33, pages 89–123. Academic Press, New York, 1974.

[17] P. Mullen, A. McKenzie, D. Pavlov, L. Durant, Y. Tong, E. Kanso, J. Marsden, and M. Desbrun. Discrete Lie advection of differential forms. *Foundations of Computational Mathematics*, 11(2):131–149, 2011.
[18] J.-C. Nédélec. Mixed finite elements in $\mathbf{R}^3$. *Numer. Math.*, 35(3):315–341, 1980.
[19] J.-C. Nédélec. A new family of mixed finite elements in $\mathbf{R}^3$. *Numer. Math.*, 50(1):57–81, 1986.
[20] W. H. Reed and T. R. Hill. Triangular mesh methods for the neutron transport equation. Tech. Rep. LA-UR-73-479, Los Alamos National Laboratory, Los Alamos, NM, 1973.
[21] H.-G. Roos, M. Stynes, and L. Tobiska. *Robust numerical methods for singularly perturbed differential equations*, volume 24 of *Springer Series in Computational Mathematics*. Springer-Verlag, Berlin, second edition, 2008. Convection-diffusion-reaction and flow problems.

Inverse Problems with Poisson Data

Thorsten Hohage
(joint work with Frank Werner)

Summary. We study inverse problems in the form of ill-posed operator equations in Banach spaces with data described by an inhomogeneous Poisson process. Such problems appear in many applications involving imaging with electromagnetic waves at low energies. Using recent progress in variational regularization methods and concentration inequalities we present convergence rates in expectation.

Introduction. In many imaging problems a time-harmonic electromagnetic wave E interacts with an unknown object of interest $u^\dagger$, and one measures a diffraction pattern $y^\dagger = |E|^2 = F(u^\dagger)$ on a measurement manifold $\mathbb{M}$. The inverse problem consists in finding $u^\dagger$ given $y^\dagger$, i.e. solving

$$F(u^\dagger) = y^\dagger.$$

For small energy densities the *wave-particle duality* of electromagnetic waves becomes important. Here we focus on data consisting of (random) positions of N photons $\{x_1, \dots, x_N\} \subset \mathbb{M}$. The density of these photons is $y^\dagger$.

After binning, practical data typically consist of vectors or arrays of nonnegative integers. Binning induces a deterministic discretization error. For simplicity we neglect it here as it often small compared to the stochatic errors in applications (see [12] for estimates of this error).

Applications include electromagnetic scattering at low energies and/or high frequencies (recall Planck's relation $E_{\text{photon}} = h\nu$), coherent x-ray imaging, scanning fluorescence microscopy (e.g. standard confocal, 4Pi or STED microscopy), Positron Emission Tomography (PET), and astronomical imaging.

The mathematical setup will be as follows: Let $\mathcal{X}$ be a Banach space, $\mathfrak{B} \subset \mathcal{X}$ closed and convex, and $F : \mathfrak{B} \to L^1(\mathbb{M})$ injective with $F(u) \geq 0$ for all $u \in \mathfrak{B}$. $u^\dagger \in \mathfrak{B}$ will denote the exact solution and $y^\dagger := F(u^\dagger)$ the exact data. Measured data are described by a realization $\{x_1, \dots, x_N\}$ of a Poisson process with density $ty^\dagger$. The parameter $t > 0$ can often be interpreted as exposure time. Our aim

is to construct estimators of $u^\dagger$ and study their expected errors in the limit $t = c\mathbb{E}[N] \to \infty$. We refer to [1] for results in the linear case.

Poisson processes. A point process on an open set $\mathbb{M} \subset \mathbb{R}^d$ can either be thought of as a random collection of points $\{x_1, \dots, x_N\} \subset \mathbb{M}$ (we only consider the case that the set is finite a.s.) or as a random counting measure $Y = \sum_{i=1}^N \delta_{x_i}$. A point process Y on $\mathbb{M}$ is called a *Poisson process* with density $y \in L^1(\mathbb{M})$, $y \geq 0$ if

(i) For any disjoint, measurable subsets $A_1, ..., A_n \subset \mathbb{M}$ the random numbers $Y(A_1), ..., Y(A_n)$ are stochastically independent.
(ii) $\mathbb{E}[Y(A)] = \int_A y\, dx$ for any measurable subset $A \subset \mathbb{M}$.

It can be shown that for a Poisson process $Y(A)$ is a Poisson distributed random variable with parameter $\lambda = \int_A y\, dx$ for any measurable $A \subset \mathbb{M}$, i.e. $\mathbb{P}[Y(A) = n] = e^{-\lambda}\frac{\lambda^n}{n!}$. Moreover, if Y is a Poisson process with density y and $\psi : \mathbb{M} \to \mathbb{R}$ is measurable, then

$$\mathbb{E}\Big[\int_{\mathbb{M}} \psi dY\Big] = \int_{\mathbb{M}} \psi y\, dx, \qquad \mathbf{Var}\Big[\int_{\mathbb{M}} \psi dY\Big] = \int_{\mathbb{M}} \psi^2 y\, dx$$

whenever the integrals on the right hand sides exist (see e.g. [14]).

Let $\tilde{Y}_t$, $t > 0$ be a Poisson processes with intensity $ty^\dagger$, and $Y_t := \tilde{Y}_t/t$. t has the role of an exposure time and is proportionalto the expected total number of photons. Then $\mathbb{E}\left[\int_{\mathbb{M}} \psi \,\mathrm{d}Y_t\right] = \int_{\mathbb{M}} \psi y^\dagger \,\mathrm{d}x$ and $\mathbf{Var}[\int_{\mathbb{M}} \psi \,\mathrm{d}Y_t] = \frac{1}{t}\int_{\mathbb{M}} \psi^2 y^\dagger \,\mathrm{d}x$. As the standard deviation for estimating a functional $\langle \psi, y^\dagger \rangle$ of the density is proportional to $\frac{1}{\sqrt{t}}$, this can be interpreted as noise level. However, there is no pointwise noise level or norm bound.

The negative log-likelihood of a Poisson process is given by

$$\mathcal{S}(Y_t; y) = \int_{\mathbb{M}} y\, dx - \int_{\mathbb{M}} \ln(y)\, \mathrm{d}Y_t$$

if $y \geq 0$ and ∞ else. Using the convention $\ln(x) := -\infty$ for $x \leq 0$, its expectation is given by $\mathbb{E}[\mathcal{S}(Y_t; y)] = \int_{\mathbb{M}} \left[y - y^\dagger \ln(y)\right] dx$. The minimum of $y \mapsto \mathbb{E}[\mathcal{S}(Y_t; y)]$ is attained at $y = y^\dagger$. The *Kullback-Leibler divergence* is given by

$$\mathrm{KL}\left(y^\dagger; y\right) = \mathbb{E}[\mathcal{S}(Y_t; y)] - \mathbb{E}\left[\mathcal{S}\left(Y_t; y^\dagger\right)\right] = \int_{\mathbb{M}} \left[y - y^\dagger - y^\dagger \ln\left(\tfrac{y}{y^\dagger}\right)\right] dx\,.$$

Convergence of regularzation methods. Let $\mathcal{X}$ be a Hilbert space, $F : \mathfrak{B} \subset \mathcal{X} \to \mathcal{Y}$ a forward operator mapping to some Banach space $\mathcal{Y}$ and y^{obs} some data which are accessed only via some proper, convex, lower-semicontinuous data misfit functional $\mathcal{S}\left(y^{\mathrm{obs}}; \cdot\right) : \mathcal{Y} \to (-\infty, \infty]$. We first study generalized Tikhonov regularization with some initial guess $u_0 \in \mathcal{X}$:

$$\widehat{u}_\alpha \in \mathrm{argmin}_{u \in \mathfrak{B}} \left[\mathcal{S}\left(y^{\mathrm{obs}}; F(u)\right) + \alpha \|u - u_0\|_{\mathcal{X}}^2\right] \tag{1}$$

Here $\mathcal{X}$ can be replaced by a Banach space and $\|u - u_0\|_{\mathcal{X}}^2$ by more general convex penalty functionals $\mathcal{R}(u)$ such as l^p or L^p norms or entropy functionals. Then one obtains convergence with respect to the Bregman distance of $\mathcal{R}$ (see [3, 6, 4].

The qualitiy of the data is assessed by the following assumption involving an error parameter $\mathrm{err} > 0$ which will tend to 0:

Assumption N: *There exists an ideal data misfit functional* $\mathcal{T} : F(\mathfrak{B}) \times F(\mathfrak{B}) \to [0,\infty]$ *with* $\mathcal{T}\left(y^\dagger; y\right) = 0$ *if and only if* $y^\dagger = y$ *and constants* $C_{\mathrm{err}}, \mathrm{err} > 0$ *such that for all* $u \in \mathfrak{B}$

$$C_{\mathrm{err}}^{-1}\mathcal{T}\left(y^\dagger; F(u)\right) - \mathrm{err} \quad \leq \quad \mathcal{S}\left(y^{\mathrm{obs}}; F(u)\right) - \mathcal{S}\left(y^{\mathrm{obs}}; F(u^\dagger)\right).$$

Note that for the standard deterministic noise model $y^{\mathrm{obs}} \in \mathcal{Y}$, $\|y^{\mathrm{obs}} - y^\dagger\|_{\mathcal{Y}} \leq \delta$ and $\mathcal{S}\left(y_1; y_2\right) = \mathcal{T}\left(y_1; y_2\right) = \|y_1 - y_2\|_{\mathcal{Y}}^p$, Assumption N holds true with $C_{\mathrm{err}} = 2^{p-1}$ and $\mathrm{err} = 2\delta^p$. Based on a concentration inequality in [15] the following can be shown ([16]):

Proposition: *Let* $\mathbb{M} \subset \mathbb{R}^d$ *be a bounded Lipschitz domain,* $s > d/2$*, and assume that* $\sup_{u\in\mathfrak{B}} \|F(u)\|_{H^s} < \infty$*. Choose* $\mathcal{T}\left(y^\dagger; y\right) := \mathrm{KL}\left(y^\dagger + \sigma; y + \sigma\right)$ *with some* $\sigma > 0$ *and* $\mathcal{S}\left(Y_t; y\right) = \int_\Omega (y - \sigma\ln(y+\sigma))\,dx - \int \ln(y+\sigma)\,\mathrm{d}Y_t$*. Then there exists* $C > 0$ *such that Assumption N holds true with* $\mathrm{err} = \frac{\rho}{\sqrt{t}}$ *with probability* $\geq 1 - \exp\left(-\frac{\rho}{C}\right)$ *for all* $t, \rho \geq 1$ *.*

Since [11] it has become popular in regularization theory to express relative smoothness of solutions in terms of variational source conditions:

Assumption SC: *There exists* $\beta \in (0,1]$ *and a concave, increasing function* $\varphi : [0,\infty) \to \mathbb{R}$ *with* $\varphi(0) = 0$ *such that for all* $u \in \mathfrak{B}$

$$\beta\|u - u^\dagger\|^2 \leq \|u - u_0\|^2 - \|u^\dagger - u_0\|^2 + \varphi\left(\mathcal{T}\left(F(u^\dagger); F(u)\right)\right).$$

A classical Hölder source condition $u^\dagger \in \mathrm{ran}((T^*T)^\nu)$ with $\nu \in (0, 1/2]$ for a bounded linear operator T in Hilbert spaces implies a variational source condition with $\varphi(t) = ct^{\frac{2\nu}{2\nu+1}}$. For further relations, see [8]. For linear operators in Hilbert spaces variational source condition turn out to be necessary and sufficient for a given rate of convergence (see [9]). In particular, this shows that variational souce conditions yield sharper results than classical ones where optimality holds only for a supremum over a smoothness class, but not for individual elements. Nevertheless, more work is necessary to interpret such conditions for interesting problems.

The following deterministic error estimate from [16] is interesting in its own right (see [2, 7], and in particular [10] for related results):

Theorem: *Suppose Assumptions N and SC holds true and the Tikhonov functional has a global minimizer.*

(1) *Let* $(-\varphi)^*(s) := \sup_{t\geq 0}[ts + \varphi(t)]$ *denote the Fenchel conjugate. Then*

$$\beta\|\widehat{u}_\alpha - u^\dagger\|^2 \leq \frac{\mathrm{err}}{\alpha} + (-\varphi)^*\left(-\frac{1}{C_{\mathrm{err}}\alpha}\right).$$

(2) *If we choose* $\frac{-1}{C_{\mathrm{err}}\alpha} \in \partial(-\varphi)(C_{\mathrm{err}}\mathrm{err})$*, then*

$$\beta\|\widehat{u}_\alpha - u^\dagger\|^2 \leq C_{\mathrm{err}}\varphi(\mathrm{err}).$$

Note that this theorem in connection with the proposition immediately gives a convergence in probability result. With some more work it is not difficult to show

even convergence in expectation (see [16]):

Corollary: Under the assumptions of the proposition and Assumption SC and with a-priori parameter choice rule $\frac{-1}{\alpha} \in \partial(-\varphi)(t^{-1/2})$ generalized Tikhonov regularization fulfills the error estimate

$$\mathbb{E}\left[\|\widehat{u} - u^\dagger\|^2\right] = \mathcal{O}\left(\varphi\left(t^{-1/2}\right)\right) \qquad t \to \infty.$$

So far we have chosen the regularization parameter α based on φ, but in practice φ is usually unknown. We showed in [16] that Lepskiĭ's balancing principle leads to the same rates (up to a $|\log t|$ factor in the stochastic setting) without knowledge of φ if not only φ, but also $\varphi^{1+\epsilon}$ is concave for some $\epsilon > 0$.

The functional in (1) is non-convex in general, and no general algorithms with guaranteed convergence to a global minimum are known. Therefore, as an alternative we studied Newton-type methods

$$(2) \qquad u_{k+1} \in \operatorname{argmin}_{u \in \mathfrak{B}} \left[\mathcal{S}\left(y^{\text{obs}}; F'[u_k](u - u_k) + F(u_k)\right) + \alpha_k \|u - u_k\|^2\right]$$

with $\alpha_k = \alpha_0 \rho^k$ and $\rho \in (0, 1)$. We used algorithms in [5] with guaranteed convergence to solve the (strongly) convex minimization problems (2).

Under an additional assumption on the local approximation quality of F' (a tangential cone condition) local analogues of the above convergence results for Tikhonov regularization were shown in [12] (see also [13]).

Numerical results. We tested the method (2) for acoustic and electromagnetic inverse obstacle scattering problems without phase and for a phase retrieval problem in x-ray diffraction. Our experiments showed considerable improvements compared to least squares data misfit terms ([12]).

References

[1] A. Antoniadis and J. Bigot. Poisson inverse problems. *Ann. Statist.*, 34(5):2132–2158, 2006.

[2] R. I. Bot and B. Hofmann. An extension of the variational inequality approach for nonlinear ill-posed problems. *Journal of Integral Equations and Applications*, 22(3):369–392, 2010.

[3] L. M. Brègman. A relaxation method of finding a common point of convex sets and its application to the solution of problems in convex programming. *Ž. Vyčisl. Mat. i Mat. Fiz.*, 7:620–631, 1967.

[4] M. Burger and S. Osher. Convergence rates of convex variational regularization. *Inverse Problems*, 20(5):1411–1421, 2004.

[5] A. Chambolle and T. Pock. A first-order primal-dual algorithm for convex problems with applications to imaging. *J. Math. Imaging Vision*, 40(1):120–145, 2011.

[6] P. P. B. Eggermont. Maximum entropy regularization for fredholm integral equations of the first kind. *SIAM J. Math. Anal.*, 24:1557–1576, 1993.

[7] J. Flemming. Theory and examples of variational regularization with non-metric fitting functionals. *J. Inverse Ill-Posed Probl.*, 18(6):677–699, 2010.

[8] J. Flemming. *Generalized Tikhonov regularization and modern convergence rate theory in Banach spaces*. Shaker Verlag, Aachen, 2012.

[9] J. Flemming, B. Hofmann, and P. Mathé. Sharp converse results for the regularization error using distance functions. *Inverse Problems*, 27(2):025006, 18, 2011.

[10] M. Grasmair. Generalized Bregman distances and convergence rates for non-convex regularization methods. *Inverse Problems*, 26:115014 (16pp), 2010.

[11] B. Hofmann, B. Kaltenbacher, C. Pöschl, and O. Scherzer. A convergence rates result for Tikhonov regularization in Banach spaces with non-smooth operators. *Inverse Problems*, 23(3):987–1010, 2007.
[12] T. Hohage and F. Werner. Iteratively regularized Newton-type methods for general data misfit functionals and applications to Poisson data. *Numer. Math.*, 2012. published online.
[13] B. Kaltenbacher and B. Hofmann. Convergence rates for the iteratively regularized Gauss-Newton method in Banach spaces. *Inverse Problems*, 26(3):035007, 21, 2010.
[14] J. F. C. Kingman. *Poisson processes*, volume 3 of *Oxford Studies in Probability*. The Clarendon Press Oxford University Press, New York, 1993. Oxford Science Publications.
[15] P. Reynaud-Bouret. Adaptive estimation of the intensity of inhomogeneous Poisson processes via concentration inequalities. *Probab. Theory Related Fields*, 126(1):103–153, 2003.
[16] F. Werner and T. Hohage. Convergence rates in expectation for tikhonov-type regularization of inverse problems with poisson data. *Inverse Problems*, 28(10):104004, 2012.

Stability Analysis of Time-Domain PML

Manfred Kaltenbacher
(joint work with Barbara Kaltenbacher)

One of the great challenges in computational science is the efficient and stable calculation of waves in unbounded domains. The crucial point for these computations is that the numerical scheme avoids any reflections at the boundaries, even in case the diameter of the computational domain is just a fraction of a wavelength. One of the most used techniques is to surround the computational domain by an additional damping layer and guarantee within the formulation, that no reflections occur at its interface with the computational domain. This so-called perfectly matched layer (PML) technique was first introduced by Berenger [7] using a splitting of the physical variables and considering a system of first order partial differential equations (PDEs) for electromagnetics. Since then, there has been much research work on this technique which subsequently was applied to different PDEs [2, 4, 9, 16, 18, 3, 20, 23, 25]. In the framework of time-harmonic wave propagation, the PML can be interpreted as a complex-valued coordinate stretching [24]. Therewith, a PML formulation for a linear PDE in frequency domain can be considered as a straightforward approach. However, in time domain most PML formulations require a first order hyperbolic system, e.g., [26, 16, 8, 18]. The difficulty arising for the second order wave equation in time domain is, that an inverse Fourier transform of its frequency representation will lead to convolution integrals, see e.g. [21]. A method to avoid convolution integrals is the use of auxiliary variables as demonstrated, e.g., in [23, 3, 17]. E.g., in [17] a PML method for the second-order elastodynamic equations has been formulated. The basic idea of the formulation is to decompose the gradient operator in terms of components perpendicular and parallel to the interface, and then split the mechanical displacement in four variables. However, as noticed in [17] the resulting equations need special treatment for the time stepping and additional memory is needed for the split-field variables. Furthermore, such split-field PML methods suffer from numerical instability, see e.g. [22, 6].

Once a PML formulation has been obtained, the question of stability arises, which is a topic of strong ongoing research. A stability analysis is not trivial and in general it has to be performed for each new formulation. Several works have analyzed the properties of the PML technique, such as [1, 5, 2, 10, 15, 11, 12] among others. E.g., in [10] a time-domain analysis of PML methods for wave equations in 2D by using the Cagniard-de Hoop method has been presented. The main result is to validate the modified fundamental solution extended to the absorbing layers. This method is easily applicable to the wave equation with any time-dependent point souce. However, the evaluation is not easy for general initial value problems of the wave equation, because those in general include not only propagating but also evanescent waves [14].

Our stability analysis investigates the evolution of the energy over time and we are able to show decay of an upper bound on the energy for our formulation, thus achieving long term stability.

The PML formulation, we are investigating, has been first published in [13], and reads as follows (for details see [19])

$$\frac{1}{c^2}\frac{\partial^2 p}{\partial t^2} + \alpha\frac{\partial p}{\partial t} + \beta p + \gamma v - \nabla\cdot\nabla p - \nabla\cdot\vec{u} = 0 \tag{1}$$

$$\frac{\partial \vec{u}}{\partial t} + A\,\vec{u} + B\,\nabla p - C\,\nabla v = 0 \tag{2}$$

$$\frac{\partial v}{\partial t} = p \tag{3}$$

with

$$\alpha = \frac{\sigma_x+\sigma_y+\sigma_z}{c^2}\,;\quad \beta = \frac{\sigma_x\,\sigma_y+\sigma_x\,\sigma_z+\sigma_y\,\sigma_z}{c^2}\,;\quad \gamma = \frac{\sigma_x\sigma_y\sigma_z}{c^2} \tag{4}$$

$$A = \begin{pmatrix} \sigma_x & 0 & 0 \\ 0 & \sigma_y & 0 \\ 0 & 0 & \sigma_z \end{pmatrix};\quad C = \begin{pmatrix} \sigma_y\sigma_z & 0 & 0 \\ 0 & \sigma_x\sigma_z & 0 \\ 0 & 0 & \sigma_x\sigma_y \end{pmatrix} \tag{5}$$

$$B = \begin{pmatrix} \sigma_x-\sigma_y-\sigma_z & 0 & 0 \\ 0 & \sigma_y-\sigma_x-\sigma_z & 0 \\ 0 & 0 & \sigma_z-\sigma_x-\sigma_y \end{pmatrix}. \tag{6}$$

In (1) - (6) σ_x, σ_y, σ_z denote the damping coefficients and $\vec{u}$, v the introduced auxiliary variables. For deriving boundedness of solutions $(p, v, \vec{u})$ of (1)–(3) in an appropriate norm (related to the acoustic energy) we proceed as follows:
(1) Test the system with appropriate multipliers to derive energy estimates; in

detail, these are

$\varphi = \partial p(s)/\partial t$ in (1),

$\varphi = \delta p(s)$ in (1) (with some possibly space dependent factor $0 \le \delta \le c^2\alpha$),

$\vec{\psi} = \nabla p(t)$ in (2),

$\vec{\psi} = F\vec{u}(t)$ in (2) (with some possibly space dependent diagonal matrix $0 \le F$).

(2) Combine these estimates to assess the time evolution of a scalar valued function $\eta(t)$, more precisely, to show that $\eta(t)$ is nonincreasing over time; η can be interpreted as a Lyapunov function for the system (1)–(3).

(3) Prove that by a proper choice of the parameters defining η, the energy can be bounded by a fixed multiple of η.

In the course of this derivation, it turns out that the Lyapunov function for the system is

$$\begin{aligned}\eta(t) \quad := \quad & \frac{1}{2}\Big(\|\frac{1}{c}\frac{\partial p}{\partial t}(t)\|^2 + \|\nabla p(t)\|^2 + \|F^{1/2}\,\vec{u}(t)\|^2 \\ & + \|\sqrt{\beta+\alpha\delta}\,p(t)\|^2 + \|\sqrt{\gamma\delta}\,v(t)\|^2 - \|C^{1/2}\nabla v(t))\|^2 \\ & + 2\langle \gamma v(t), p(t)\rangle + 2\langle \vec{u}(t), \nabla p(t)\rangle + 2\langle \frac{\delta}{c^2}\frac{\partial p}{\partial t}(t), p(t)\rangle \Big)\end{aligned}$$

Here we wish to point out that the sixth term on the right hand side suggests that it is favorable to set $C = 0$ from a stability point of view. Thus we will end up with considering a reduced PML (rPML) where we just set $C \equiv 0$. Furthermore, we want to state that the rPML is a true PML in case of 1D as well as 2D computations. In these cases, we do not need the additional scalar auxiliary variable v and so C is not present. E.g., in 2D we just need the auxiliary vector variable $\vec{u} = (u_x, u_y)^t$ leading to a total number of just three unknowns in the PML region. This can be also seen by analyzing (1)-(3), e.g., assuming waves in the $xy-$plane. Then γ and C get zero ($\sigma_z = 0$) resulting in just three scalar equations for $p\,, u_x, u_y$. So an error just occurs in 3D, when waves propagate towards corners, where all three damping coefficients are active.

There are strong indications that the function η is indeed decreasing for a proper choice of the parameters, see [19] namely

$$\begin{aligned} 0 \le \delta \le c^2\alpha\,; \quad \beta\delta - \gamma \ge 0\,; \quad \delta I + B \ge 0 \\ 4FA(\delta I + B) - (\delta I + A + FB)^2 \ge 0\,. \end{aligned}$$

However, the spatial variation of σ (smooth or piecewise constant) generates a term that cannot be controlled so far, so this remains an open problem. The authors thank Patrick Joly for pointing them to this fact.

References

[1] S. Abarbanel, D. Gottlieb, and J. Hesthaven. Long time behavior of the perfectly matched layer equations in computational electromagnetics. *J. Sci. Comput.*, 17:405–422, 2002.

[2] D. Appelö, T. Hagstrom, and G. Kreiss. Perfectly matched layers for hyperbolic systems: general formulation, well-posedness, and stability. *SIAM J. Appl. Math.*, 67(1):1–23 (electronic), 2006.
[3] D. Appelö and G. Kreiss. Application of a perfectly matched layer to the nonlinear wave equation. *Wave Motion*, 44(7-8):531–548, 2007.
[4] H. Barucq, J. Diaz, and M. Tlemcani. New absorbing layers conditions for short water waves. *J. Comput. Phys.*, 229(1):58–72, 2010.
[5] E. Bécache, S. Fauqueux, and P. Joly. Stability of perfectly matched layers, group velocities and anisotropic waves. *J. Comput. Phys.*, 188(2):399–433, 2003.
[6] E. Bécache and P. Joly. On the Analysis of Berenger's Perfectly Matched Layers for Maxwell's equations. *Math. Mod. Numer. Anal.*, 36:87–119, 2002.
[7] J.-P. Berenger. A perfectly matched layer for the absorption of electromagnetic waves. *J. Comput. Phys.*, 114(2):185–200, 1994.
[8] G. C. Cohen. *Higher-Order Numerical Methods for Transient Wave Equations*. Springer, 2002.
[9] F. Collino and C. Tsogka. Application of the PML absorbing layer model to the linear elastodynamic problem in anisotropic heterogeneous media. *Geophysics*, 88:43–73, 2001.
[10] J. Diaz and P. Joly. A time domain analysis of PML models in acoustics. *Comput. Methods Appl. Mech. Engrg.*, 195(29-32):3820–3853, 2006.
[11] K. Duru and G. Kreiss. A well-posed and discretely stable perfectly matched layer for elastic wave equations in second order formulation. Technical Report 2010-004, Department of Information Technology, Uppsala University, Feb. 2010.
[12] K. Duru and G. Kreiss On the Accuracy and Stability of the Perfectly Matched Layer in Transient Waveguides *J. Sci. Comput.*, 53:642-671, 2012.
[13] M. Grote and I. Sim. Efficient pml for the wave equation. *Proceedings of Waves 2009*, Peau, France, 2009.
[14] T. Hagstrom and T. Warburton. Complete radiation boundary conditions: minimizing the long time error growth of local methods. *SIAM Journal on Numerical Analysis*, 47:3678–3704, 2009.
[15] J. S. Hesthaven. On the analysis and construction of perfectly matched layers for the linearized Euler equations. *J. Comput. Phys.*, 142(1):129–147, 1998.
[16] F. Q. Hu. A stable, perfectly matched layer for linearized Euler equations in unsplit physical variables. *J. Comput. Phys.*, 173(2):455–480, 2001.
[17] D. Komatitsch and J. Tromp. A perfectly matched layer absorbing boundary condition for the second-order seismic wave equation. *Geophys. J. Int.*, 154:146–153, 2003.
[18] T. Lähivaara and T. Huttunen. A non-uniform basis order for the discontinuous Galerkin method of the 3D dissipative wave equation with perfectly matched layer. *J. Comput. Phys.*, 229(13):5144–5160, 2010.
[19] B. Kaltenbacher, M. Kaltenbacher and I. Sim A modied and stable version of a perfectly matched layer technique for the 3-d second order wave equation in time domain with an application to aeroacoustics J. Comput. Phys., 235:407-422, 2013.
[20] F. Nataf. A new approach to perfectly matched layers for the linearized Euler system. *J. Comput. Phys.*, 214(2):757–772, 2006.
[21] T. Rylander and J. Jin. Perfectly matched layer for the time domain finite element method. *J. Comput. Phys.*, page 238–250, 2004.
[22] S.Abarbanel and D. Gottlieb. A Mathematical Analysis of the PML Method. *J. Comput. Phys.*, 134, 1997.
[23] B. Sjögreen and N. A. Petersson. Perfectly matched layers for Maxwell's equations in second order formulation. *J. Comput. Phys.*, 209(1):19–46, 2005.
[24] F. Teixeira and W. Chew. Complex space approach to perfectly matched layers: a review and some developments. *Int. J. Numerical Model*, 13:441–455, 2000.
[25] E. Turkel and A. Yefet. Absorbing PML boundary layers for wave-like equations. *Appl. Numer. Math.*, 27(4):533–557, 1998. Absorbing boundary conditions.

[26] L. Zhao and A. Cangellaris. A general approach for the development of unsplit-field time-domain implementations for perfectly matched layers for FDTD grid truncation. *IEEE Microw. Guided W.*, 6:209–211, 1996.

hp-FEM and *hp*-DGFEM for Helmholtz problems

J. M. Melenk
(joint work with S. Esterhazy, A. Parsania, S. Sauter)

Model problem and regularity. We consider, on a bounded Lipschitz domain $\Omega \subset \mathbb{R}^d$, $d \in \{2,3\}$, the Helmholtz equation

$$-\Delta u - k^2 u = f \quad \text{in } \Omega \subset \mathbb{R}^d, \quad d \in \{2,3\}, \qquad k > 1. \tag{H}$$

Properties of the solution (and the performance of numerical methods) depend on the geometry and the type of boundary conditions. For Robin boundary conditions

$$\partial_n u - \mathbf{i}ku = g, \tag{BC}$$

well-posedness is given with *a priori* bounds of the form $\|u\|_{1,k} := \|\nabla u\|_{L^2(\Omega)} + k\|u\|_{L^2(\Omega)} \le Ck^\theta(\|f\|_{L^2(\Omega)} + \|g\|_{L^2(\partial\Omega)})$ for some $\theta \in [0, 5/2]$, which depends on the geometry of Ω, [5, Thm. 2.4], [13, 3, 10]. For the analysis of numerical methods, the following regularity result is useful (for details see [14] and [6]):

Theorem 1: (regularity by decomposition) *Let $\partial\Omega$ be analytic and $s \ge 0$. Then, for $f \in H^s(\Omega)$ and $g \in H^{s+1/2}(\partial\Omega)$, the solution u can be written as $u = u_{H^{s+2}} + u_{\mathcal{A}}$ where $u_{H^{s+2}} \in H^{s+2}(\Omega)$, $u_{\mathcal{A}}$ is analytic, and for C, γ independent of $k > 1$*

$$\|u_{H^{s+2}}\|_{H^{s+2}(\Omega)} + k^{s+2}\|u_{H^{s+2}}\|_{L^2(\Omega)} \le C\left[\|f\|_{H^s(\Omega)} + \|g\|_{H^{s+1/2}(\partial\Omega)}\right],$$
$$\|\nabla^{n+2} u_{\mathcal{A}}\|_{L^2(\Omega)} \le Ck^{\theta-1}\gamma^n \max\{k,n\}^{n+2}\left[\|f\|_{L^2(\Omega)} + \|g\|_{H^{1/2}(\partial\Omega)}\right] \qquad \forall n \in \mathbb{N}_0.$$

Conforming *hp*-FEM. The performance of high order FEM (*hp*-FEM) based on the (standard) H^1-conforming discretization of (H), (BC) is analyzed in [15, 16, 5] for piecewise smooth geometries. The numerical analysis is based on a Gårding setting and requires a *scale resolution condition*. A typical result is:

Theorem 2: *Let $\partial\Omega$ be analytic and $V_N \subset H^1(\Omega)$ be the space of (mapped) polynomials of degree p on mesh $\mathcal{T}$ (mesh size h; see [16] for precise conditions on the element maps). Let $s \ge 0$, $f \in H^s(\Omega)$, $g \in H^{s+1/2}(\partial\Omega)$. Then there exist constants c_1, $c_2 > 0$ such that under the scale resolution condition*

$$\frac{kh}{p} \le c_1 \quad \text{and} \quad p \ge c_2 \log k \tag{SRC}$$

the hp-FEM approximation u_N exists and, for some C, $\sigma > 0$ indep. of k, h, p,

$$\|u - u_N\|_{1,k} \le C\left[\left(\frac{h}{p}\right)^{s+1} + k^\theta\left(\frac{kh}{\sigma p}\right)^p\right]. \tag{C}$$

The different way in which h and k enter the *a priori* estimate (C) is visible in the following numerical example of the h-FEM for the problem:

$$-u'' - k^2 u = x^\alpha \quad \text{on } (0,1), \qquad u(0) = 0, \quad u'(1) - \mathbf{i}ku(1) = 0.$$

Taking $\alpha = -1/2$ (corresponding to $s = 0$ in (C)), we show $|u - u_N|_{H^1(0,1)}$ versus the number of degrees of freedom for the h-FEM for $p = 1$ (left) and $p = 2$ (right). Since $\theta = 0$ and $s = 0$ in the present 1D example, the k-dependence in (C) should differ markedly for the cases $p = 1$ and $p = 2$, which is indeed visible.

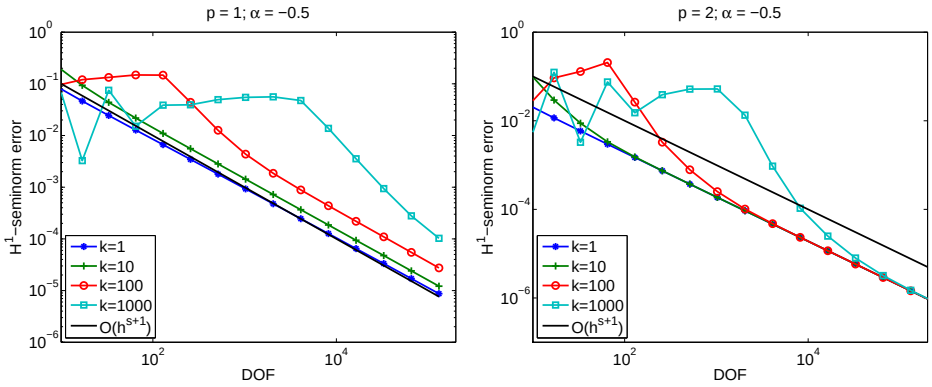

DG-formulation. Stable methods that yield some approximation (and even best approximation) without a scale resolution condition exist: Least Squares Methods (e.g., [17]) and related methods such as the Ultra Weak Variational Formulation, [2, 12], plane wave DG methods ([9, 11]), and the DPG method, [4]. While these methods are stable in some (possibly method-dependent) norm, the performance in standard norms such as $L^2(\Omega)$ is less obvious and often requires a good understanding of regularity properties of the solution or suitable adjoint problems (see, e.g., [17] and also [6] for more details).

A DG-formulation that is closely related to the UWVF is formulated in [1, 9, 11]; further related DG-formulations can be found in [7, 8]. This DG-formulation reads as follows for an arbitrary space $V_N \subset \prod_{K\in\mathcal{T}} H^2(K)$ of piecewise H^2-functions based on a mesh $\mathcal{T}$:

Find $u_N \in V_N$ such that $a_N(u_N, v) = l(v) := \sum_{K\in\mathcal{T}} \int_K f\overline{v}\ \forall v \in V_N$, where

$$\begin{aligned} a_N(u_N, v) \quad &= \quad \sum_{K\in\mathcal{T}} \int_K \nabla u_N \cdot \nabla\overline{v} - k^2 u_N \overline{v} \\ &\quad + \int_{\partial K} (\widehat{u}_N - u_N)\nabla\overline{v}\cdot\mathbf{n} - \mathbf{i}k \int_{\partial K} \widehat{\boldsymbol{\sigma}}_N \cdot \mathbf{n}\overline{v}. \end{aligned}$$

The numerical traces $\widehat{u}_N$ and the numerical fluxes $\widehat{\boldsymbol{\sigma}}_N$ have the following form on the skeleton $\mathfrak{S} = \mathfrak{S}^{\mathcal{I}} \dot\cup \mathfrak{S}^{\mathcal{B}}$, where $\mathfrak{S}^{\mathcal{I}}$ and $\mathfrak{S}^{\mathcal{B}}$ denote the faces in Ω and on the

boundary $\partial\Omega$, respectively:

$$\text{on } \mathfrak{S}^{\mathcal{I}} \text{ (interior faces):} \quad \widehat{\boldsymbol{\sigma}}_N = \frac{1}{\mathbf{i}k}\{\!\{\nabla_{\mathcal{T}} u\}\!\} - \alpha[\![u]\!], \qquad \widehat{u}_N = \{\!\{u\}\!\} - \beta\frac{1}{\mathbf{i}k}[\![\nabla_{\mathcal{T}} u]\!]$$

$$\text{on } \mathfrak{S}^{\mathcal{B}} \text{ (boundary faces):} \quad \widehat{\boldsymbol{\sigma}}_N = \frac{1}{\mathbf{i}k}\nabla_{\mathcal{T}} u - \frac{1-\delta}{\mathbf{i}k}(\nabla_{\mathcal{T}} u_N - \mathbf{i}k u_N \mathbf{n} - g\mathbf{n})$$

$$\widehat{u}_N = u_N - \delta\frac{1}{\mathbf{i}k}\left(\nabla_{\mathcal{T}} u_N \cdot \mathbf{n} - \mathbf{i}k u_N - g\right)$$

Here, the jumps $[\![\cdot]\!]$ and the averages $\{\!\{\cdot\}\!\}$ are defined as follows: for a scalar quantity u on a face $e = \overline{K_1} \cap \overline{K_2}$, we set $[\![u]\!] = u_{K_1}\mathbf{n}_{K_1} + u_{K_2}\mathbf{n}_{K_2}$ and $\{\!\{u\}\!\} = (u_{K_1} + u_{K_2})/2$, where $\mathbf{n}$ is an outer normal vector and the subscript K_i indicates the element on which the trace is taken. For a vectorial quantity $\boldsymbol{\sigma}$ the jump and average is given by $[\![\boldsymbol{\sigma}]\!] = \boldsymbol{\sigma}_{K_1} \cdot \mathbf{n}_{K_1} + \boldsymbol{\sigma}_{K_2}\mathbf{n}_{K_2}$ and $\{\!\{\boldsymbol{\sigma}\}\!\} = (\boldsymbol{\sigma}_{K_1} + \boldsymbol{\sigma}_{K_2})/2$. The functions α, β, δ are positive functions on the skeleton $\mathfrak{S}$ with $\delta \in (0, 1/2)$. This DG-formulation is conveniently analyzed with the aid of the following norms, [9]:

$$\begin{aligned}\|v\|_{DG}^2 :=& \|\nabla_{\mathcal{T}} v\|_{L^2(\Omega)}^2 + k^{-1}\|\beta^{1/2}[\![\nabla_{\mathcal{T}} v]\!]\|_{L^2(\mathfrak{S}^{\mathcal{I}})}^2 + k\|\alpha^{1/2}[\![v]\!]\|_{L^2(\mathfrak{S}^{\mathcal{I}})}^2 \\ &+ k^{-1}\|\delta^{1/2}\nabla_{\mathcal{T}} v \cdot \mathbf{n}\|_{L^2(\mathfrak{S}^{\mathcal{B}})}^2 + k\|(1-\delta)^{1/2} v\|_{L^2(\mathfrak{S}^{\mathcal{B}})}^2 + k^2\|v\|_{L^2(\Omega)}^2,\end{aligned}$$

$$\|v\|_{DG^+}^2 := \|v\|_{DG}^2 + k^{-1}\|\alpha^{-1/2}\{\!\{\nabla_{\mathcal{T}} v\}\!\}\|_{L^2(\mathfrak{S}^{\mathcal{I}})}^2.$$

***hp*-DGFEM on general meshes.** Let $\mathcal{T}$ be a mesh, possibly with hanging nodes; the mesh should be shape regular in the sense that certain polynomial inverse estimates hold true. The coefficient functions α, β, δ on $\mathfrak{S}$ are chosen as

$$\alpha = \mathtt{a}\frac{p^2}{h}, \quad \beta = \mathtt{b}\frac{h}{p}, \quad \delta = \mathtt{d}\frac{h}{p},$$

where $h = h(x)$ denotes the minimal mesh size of the elements sharing the point $x \in \mathfrak{S}$. Let V_N consist of piecewise (mapped) polynomials of degree p. Then we have the following result (see [14] for the precise conditions on the element maps):

Theorem 3: *Let $\partial\Omega$ be analytic. Then there are c_1, $c_2 > 0$ independent of $k \geq 1$ such that for fixed $\mathtt{a}$, $\mathtt{b}$, $\mathtt{d} > 0$ with $\mathtt{a}$ sufficiently large the condition*

$$\text{(SRC-DG)} \qquad \frac{kh}{\sqrt{p}} \leq c_1 \quad \text{and} \quad p \geq c_2 \log k$$

implies existence of the hp-DGFEM solution u_N and

$$\|u - u_N\|_{DG} \leq C \inf_{v \in V_N} \|u - v\|_{DG^+}.$$

***hp*-DGFEM on conforming meshes.** Constrasting (SRC-DG) with (SRC), we note a loss of $p^{1/2}$, which which is typical of p-version DG-methods on rather general meshes. For spaces V_N admitting an $H^1(\Omega)$-conforming subspace that is sufficiently rich, this scale resolution condition can be relaxed to take the form (SRC) familiar from the conforming setting:

Theorem 4: *Let $\partial\Omega$ be analytic and let $\mathcal{T}$ be* regular. *Then there are constants c_1, $c_2 > 0$ independent of $k \geq 1$ such that for*

$$\text{(SRC-DG-II)} \qquad \frac{kh}{p} \leq c_1 \quad \text{and} \quad p \geq c_2 \log k$$

the hp-DGFEM satisfies

$$\|u - u_N\|_{DG} \leq C \inf_{v \in V_N} \|u - v\|_{DG+}.$$

The key ingredient of the proof of Theorem 4 is the construction of an interpolation operator on triangles/tetrahedra that leads to a globally $H^1(\Omega)$-conforming approximation with good approximation properties in the broken H^2-norm. The basic step is:

Lemma 5: *Let $\widehat{K} \subset \mathbb{R}^d$ be the reference triangle or tetrahedron. Let $s > 5/2$ for $d = 2$ and $s > 5$ for $d = 3$. Then, for p sufficiently large, there exists a polynomial approximation operator $I_p : H^s(\widehat{K}) \to \mathcal{P}_p$ such that*

$$\sum_{j=0}^{2} p^{-j} \|u - I_p u\|_{H^j(\widehat{K})} \leq C p^{-s} \|u\|_{H^s(\widehat{K})}$$

with the following boundary behavior: For each vertex V we have $(I_p u)(V) = u(V)$, for each edge e, the restriction $(I_p u)|_e$ depends solely on $u|_e$, and for each face f (for $d = 3$), the restriction $(I_p u)|_f$ depends solely on $u|_f$.

References

[1] A. Buffa and P. Monk. Error estimates for the ultra weak variational formulation of the Helmholtz equation. *M2AN (Math. Model. Numer. Anal.)*, 42(6):925–940, 2008.

[2] O. Cessenat and B. Després. application of the ultra-weak variational formulation to the 2d Helmholtz problem. *SIAM J. Numer. Anal.*, 35:255–299, 1998.

[3] P. Cummings and X. Feng. Sharp regularity coefficient estimates for complex-valued acoustic and elastic Helmholtz equations. *Math. Models Methods Appl. Sci.*, 16(1):139–160, 2006.

[4] L. Demkowicz, J. Gopalakrishnan, I. Muga, and J. Zitelli. Wavenumber explicit analysis of a DPG method for the multidimensional Helmholtz equation. *Comput. Methods Appl. Mech. Engrg.*, 213/216:126–138, 2012.

[5] S. Esterhazy and J.M. Melenk. On stability of discretizations of the Helmholtz equation. In I.G. Graham, T.Y. Hou, O. Lakkis, and R. Scheichl, editors, *Numerical Analysis of Multiscale Problems*, volume 83 of *Lect. Notes Comput. Sci. Eng.*, 285–324. Springer, 2012.

[6] S. Esterhazy and J.M. Melenk. An analysis of discretizations of the Helmholtz equation in L^2 and in negative norms (extended version). Technical Report 31, Inst. for Analysis and Sci. Computing, Vienna Univ. of Technology, 2012. Available at `http://www.asc.tuwien.ac.at`.

[7] X. Feng and H. Wu. *hp*-discontinuous Galerkin methods for the Helmholtz equation with large wave number. *Math. Comp.*, 80:1997–2024, 2011.

[8] X. Feng and Y. Xing. Absolutely stable local discontinuous Galerkin methods for the Helmholtz equation with large wave number. *Math. Comp.*, (in press).

[9] C. Gittelson, R. Hiptmair, and I. Perugia. Plane wave discontinuous Galerkin methods. *M2AN (Mathematical Modelling and Numerical Analysis)*, 43:297–331, 2009.

[10] U. Hetmaniuk. Stability estimates for a class of Helmholtz problems. *Commun. Math. Sci.*, 5(3):665–678, 2007.

[11] R. Hiptmair, A. Moiola, and I. Perugia. Plane wave discontinuous Galerkin methods for the 2d Helmholtz equation: analysis of the p-version. *SIAM J. Numer. Anal.*, 49:264–284, 2011.

[12] T. Huttunen and P. Monk. The use of plane waves to approximate wave propagation in anisotropic media. *J. Computational Mathematics*, 25:350–367, 2007.

[13] J.M. Melenk. *On Generalized Finite Element Methods*. PhD thesis, Univ. of Maryland, 1995.

[14] J.M. Melenk, A. Parsania, and S. Sauter. General DG-Methods for Highly Indefinite Helmholtz Problems. (submitted)

[15] J.M. Melenk and S. Sauter. Convergence analysis for finite element discretizations of the Helmholtz equation with Dirichlet-to-Neumann boundary conditions. *Math. Comp.*, 79:1871–1914, 2010.
[16] J.M. Melenk and S. Sauter. Wavenumber explicit convergence analysis for finite element discretizations of the Helmholtz equation. *SIAM J. Numer. Anal.*, 49:1210–1243, 2011.
[17] P. Monk and D.Q. Wang. A least squares methods for the Helmholtz equation. *Comput. Meth. Appl. Mech. Engrg.*, 175:121–136, 1999.

Interpolation based Directional Fast Multipole Method

Matthias Messner
(joint work with Martin Schanz, Olivier Coulaud and Eric Darve)

Since the invention of the FMM [4] extensive research has been done on algorithms which reduce the cost of matrix-vector products like

$$f_i = \sum_{j=1}^{N} K(x_i, y_j) w_j \quad \text{for all} \quad j = 1, \dots, N, \tag{1}$$

from $\mathcal{O}(N^2)$ to $\mathcal{O}(N)$ or $\mathcal{O}(N \log N)$ depending on the type of the underlying kernel function K. Most FMMs have been developed and optimized for specific kernel functions. However, some have also been formulated so the FMM is independent of the kernel function. We address the optimization of one of these formulations, the so called black-box FMM introduced in [3]. It works for all kernel functions that are asymptotically smooth, such as $1/|x-y|$ and is based on the approximation of the kernel function by means of a Chebyshev interpolation scheme as

$$K(x,y) \sim \sum_{|\alpha| \le \ell} S_\ell(x, \bar{x}_\alpha) \sum_{|\beta| \le \ell} K(\bar{x}_\alpha, \bar{y}_\beta)\, S_\ell(y, \bar{y}_\beta), \tag{2}$$

with the interpolation polynomial S_ℓ of interpolation order ℓ. The multi-indices α and β identify the interpolation points $\bar{x}_\alpha$ and $\bar{y}_\beta$ which are constructed via the tensor-product rule from the roots of the Chebyshev polynomial of first kind T_ℓ. This formulation has been extended to the directional FMM for oscillatory kernels in [9] and is suitable for any kernel function of the type

$$K(x,y) = G(x,y) e^{\imath k |x-y|}.$$

Here, G is an asymptotically smooth function, $\imath^2 = -1$ the imaginary unit and k the wave-number. In [2], the two admissibility criteria

$$\textit{separation} \quad \mathcal{O}(kw^2) \quad \text{and } \textit{cone-aperture} \quad \mathcal{O}(1/kw)$$

have been developed for such kernels in the high-frequency regime. The criteria say that a cluster-pair X and Y, centered at c_X and c_Y and of width w, is admissible (part of the far-field) if their distance $|c|$ with $c = c_X - c_Y$ satisfies the separation criterion and if $|c/|c| - u|$ satisfies the cone-aperture criterion. The authors of [2] proved that if these criteria hold the kernel function K is low-rank. This is not sufficient in our case. We require the interpolation error to decay exponentially

fast with ℓ and and to be independent on k. We proof this by using the idea of directional smoothness (see [1])

$$K^u(x,y) = K(x,y)e^{-\imath ku\cdot(x-y)},$$

where u is a directional unit vector. As long as the two admissibility criteria hold, the directional kernel K^u is bounded in the complex domain, and the proof is completed [6] and [9]. Once w approaches the size of a wavelength (threshold between low- and high-frequency regime) these two criteria descend to the usual criterion of well separateness. We use these criteria to separate near- and far-field. Finally, the near-field is evaluated directly by using Eqn. (1) and in the FMM notation it corresponds to the P2P operation. The far-field is evaluated efficiently by using the following fast summation scheme. We interpolate K^u (see Eqn. (2), plug it into Eqn. 1 and obtain

$$f_i \sim e^{\imath ku\cdot x_i} \sum_{|\alpha|\le\ell} S_\ell(x_i,\bar{x}_\alpha)e^{-\imath ku\cdot\bar{x}_\alpha} \sum_{|\beta|\le\ell} K(\bar{x}_\alpha,\bar{y}_\beta)e^{\imath ku\cdot\bar{y}_\beta} \sum_{j=1}^{N} S_\ell(y_j,\bar{y}_\beta)e^{-\imath ku\cdot y_j}\, w_j.$$

With that, we construct the three-stage fast summation scheme for oscillatory kernels in the high-frequency regime.

(1) Particle to moment (P2M) or moment to moment (M2M) operator: equivalent source values are anterpolated at the interpolation points $\bar{y}_\beta \in Y$ by

$$W^u_\beta = e^{\imath ku\cdot\bar{y}_\beta} \sum_{j=1}^{N} S(y_j,\bar{y}_\beta)\, e^{-\imath ku\cdot y_j}\, w_j \quad \text{for} \quad |\beta| \le \ell.$$

(2) Moment to local operator (M2L): target values are evaluated at the interpolation points $\bar{x}_\alpha \in X$ by

$$F^u_\alpha = \sum_{|\beta|\le\ell} K(\bar{x}_\alpha,\bar{y}_\beta)\, W^u_\beta \quad \text{for} \quad |\alpha| \le \ell.$$

(3) Local to local (L2L) or local to particle (L2P) operator: target values are interpolated at final points $x_i \in X$ by

$$f_i \sim e^{\imath ku\cdot x_i} \sum_{|\alpha|\le\ell} S(x_i,\bar{x}_\alpha)\, e^{-\imath ku\cdot\bar{x}_\alpha}\, F^u_\alpha \quad \text{for} \quad i = 1,\ldots,M.$$

Even though the above scheme is presented as a single-level scheme, it is implemented as a multilevel scheme. In the following, we have a closer look at the directional scheme. Only the P2M, M2M operators from step (1) and the L2L, L2P operators from step (3) are directional, the M2L operator from step (2) is not. Unlike in the low-frequency regime, in the high-frequency regime, the far-field is split into cones by means of the cone-aperture criterion $\mathcal{O}(1/kw)$. The aperture of these cones at the parent level is half their aperture at the child level. Due to a nested cone construction along octree levels, we preserve the accuracy of the Chebyshev interpolation within the multilevel scheme. For a detailed description of all operators we refer to [9]).

The overall complexity of the directional FMM is dominated by the M2L operator. The difference between this (and [2]) and the classical FMM for oscillatory kernels is the following. In the former case, the number of far-field interactions grows but the work per interaction remains constant as we climb up the tree. In the latter case the number of far-field interactions remains constant but the work per interaction increases. Nevertheless, in both cases the product of the number of interactions and the work per interaction grows like $\mathcal{O}(N)$ and with $\mathcal{O}(\log N)$ levels the overall complexity results in the expected $\mathcal{O}(N \log N)$.

In [8] we introduce optimizations of the M2L operator and perform detailed studies. Initially, we investigate the approach presented in [3] and [9]. Its weakness is that many M2L operators end up having suboptimal low-rank approximations. A recompression leads to optimal low-ranks and to the variant with the least computational cost. However, the main bottleneck, the expensive precomputation, is not tackled yet. A new family of optimizations, which exploits symmetries in the arrangement of the M2L operators, does that. Let us sketch the idea. An M2L operator corresponds to a matrix $\mathsf{K}_t \in \mathbb{C}^{\ell^3 \times \ell^3}$ whose entries are computed as $(\mathsf{K}_t)_{ij} = K(\bar{x}_i, \bar{y}_j)$. We associate each M2L operator to a transfer-vector $t = (c_X - c_{Y_t})/w$ which describes the relative position of the far-field interaction Y_t. The full set of transfer-vectors is given by $T \subset \mathbb{Z}^3$. By exploiting axial and

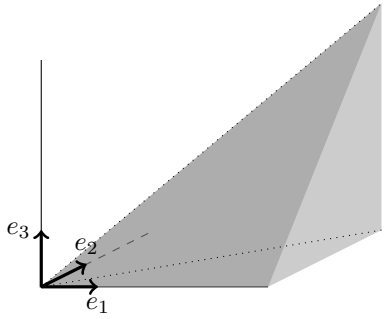

FIGURE 1. The cone $\mathbb{Z}^3_{\text{sym}}$ $(t_1 \geq t_2 \geq t_3 \geq 0)$ is obtained by combining axial and diagonal symmetries.

diagonal symmetries we can reduce T. In Fig. 1 we show the cone $\mathbb{Z}^3_{\text{sym}}$ and with $T_{\text{sym}} = T \cap \mathbb{Z}^3_{\text{sym}}$ we are given the subset of M2L operators to precompute and store. The remaining ones are obtained via permutations thereof. Each reflection $p : T \to T_{\text{sym}}$ of a transfer-vector corresponds to a permutation of the respective M2L operator like

$$\mathsf{K}_t = \mathsf{P}_t \mathsf{K}_{p(t)} \mathsf{P}_t^\top .$$

There are two applications of the FMM as a numerical scheme to perform fast matrix-vector products; 1) quick precomputations for *single* matrix-vector products, and 2) fast operator applications for *multiple* matrix-vector products (iterative solvers). The presented optimizations raise the efficiency for both applications.

On one hand, the exploitation of symmetries cuts down the memory requirement and reduces the precomputation time by a factor larger than 1000. On the other hand, the individual approximation of the M2L operators leads to optimal low-rank approximations and paves the road for blocking schemes. Thus, by means of highly optimized matrix-matrix product implementations, such as Intel's MKL [5] we achieve very high performances due to better cache reuse and data locality. In [8] we present various comparisons of these optimizations.

The directional FMM (dFMM) is implemented in C++ and is freely available via `http://github.com/burgerbua/dfmm` under the BSD 2-Clause license. The scheme has been developed, studied and validated and optimized in [9]and [8] and has been applied in [7] to accelerate the simulation of sound radiation and acoustic scattering problems by means of the boundary element method.

References

[1] A. Brandt, *Multilevel computations of integral transforms and particle interactions with oscillatory kernels*, Computer Physics Communications, 65 (1991), pp. 24–38.

[2] B. Engquist and L. Ying, *Fast directional multilevel algorithms for oscillatory kernels*, SIAM Journal on Scientific Computing, 29 (2007), pp. 1710–1737.

[3] W. Fong and E. Darve, *The black-box fast multipole method*, Journal of Computational Physics, 228 (2009), pp. 8712–8725.

[4] L. Greengard and V. Rokhlin, *A fast algorithm for particle simulations*, Journal of Computational Physics, 73 (1987), pp. 325–348.

[5] Intel, *Intel Math Kernel Library (Intel MKL) 10.3*, 2012. [Online; accessed 28-August-2012].

[6] J. C. Mason and D. C. Handscomb, *Chebyshev Polynomials*, Chapman & Hall/CRC, 2003.

[7] M. Messner, *Fast Boundary Element Methods in Acoustics*, PhD thesis, Graz University of Technology, 2012.

[8] M. Messner, B. Bramas, O. Coulaud, and E. Darve, *Optimized M2L kernels for the Chebyshev interpolation baset fast multipole method*, Journal of Computational Physics, (2012). Submitted (`http://arxiv.org/abs/1210.7292`).

[9] M. Messner, M. Schanz, and E. Darve, *Fast directional multilevel summation for oscillatory kernels based on Chebyshev interpolation*, Journal of Computational Physics, 231 (2012), pp. 1175 – 1196.

On MLMDA/Butterfly Compressibility of Inverse Integral Operators

Eric Michielssen

(joint work with Han Guo, Yang Liu and Jun Hu)

We study the compressibility of inverse integral operators by the MLMDA [1]. Specifically, we apply the MLMDA to blocks of block LU-factorized discretized electric field integral equations (EFIE) for analyzing scattering from both 2D and 3D surfaces. Invariably, we find that the MLMDA realizes compression beyond that provided by low rank (LR) compression schemes. Furthermore, by bypassing all costly LR compression steps, we develop a MLMDA based fast direct solver that exhibits $O(N\mathbf{log}^2 N)$ storage requirements while consuming $O(N^2)$ CPU time. Specifically, our method is designed to solve linear systems of the form

$$\boldsymbol{Z} \cdot \boldsymbol{I} = \boldsymbol{V}, \tag{1}$$

obtained by discretizing the EFIE using Green's functions of the form $H_0^{(2)}$ in 2D and $e^{-jkr}/4\pi r$ in 3D. Both kernels result in the impedance matrix $\boldsymbol{Z}$ in (1) having rank deficit or MLMDA-compressible submatrices. The proposed direct solver involves two steps.

D1: Construction of a hierarchical LR approximation to block-LU decomposition;
This step is similar to the procedure described in [2]. We begin by geometrically decomposing the scatterer into subscatterers. Initially, the scatterer is divided into two level-1 subscatterers of roughly equal size, resulting in two level-1 sets of unknowns. This procedure is repeated $N_l - 1$ times. At level $1 \leq l \leq N_l$, there are 2^l subscatterers, each containing approximately $N/2^l$ unknowns. We assume unknowns in each subscatterer are numbered consecutively. We next identify near- and far-field group pairs: two same-level subscatterers form a far-field pair if the distance between their geometric centers exceeds $2 < \chi < 4$ times the sum of their circumscribing radii (admissibility criterion) and none of their respective ancestors form a far-field pair. Two level-N_l groups form a near-field pair if they do not satisfy the admissibility criterion. We next construct a compressed representation of $\boldsymbol{Z}$ using hierarchical $\mathcal{H}$-matrix techniques [3], i.e. by approximating all interactions between far-field pairs in terms of LR products (or combinations thereof), while storing those between near-field pairs classically. Finally, we invert the $\boldsymbol{Z}$ matrix by hierarchical ($\mathcal{H}$-) block LU decomposition. Consider the block LU decomposition of the level-1 partitioned $\boldsymbol{Z}$ matrix:

$$\boldsymbol{Z} = \begin{bmatrix} \boldsymbol{Z}_{11} & \boldsymbol{Z}_{12} \\ \boldsymbol{Z}_{21} & \boldsymbol{Z}_{22} \end{bmatrix} = \begin{bmatrix} \boldsymbol{L}_{11} & \\ \boldsymbol{L}_{21} & \boldsymbol{L}_{22} \end{bmatrix} \begin{bmatrix} \boldsymbol{U}_{11} & \boldsymbol{U}_{12} \\ & \boldsymbol{U}_{22} \end{bmatrix} \tag{2}$$

In principle, the blocks of $\boldsymbol{Z}$'s LU factors can be computed as follows: (i) $\boldsymbol{L}_{11}$ and $\boldsymbol{U}_{11}$: LU decompose $\boldsymbol{Z}_{11} = \boldsymbol{L}_{11}\boldsymbol{U}_{11}$; (ii) $\boldsymbol{U}_{12}$: solve $\boldsymbol{Z}_{12} = \boldsymbol{L}_{11}\boldsymbol{U}_{12}$; (iii) $\boldsymbol{L}_{21}$: solve $\boldsymbol{Z}_{21} = \boldsymbol{L}_{21}\boldsymbol{U}_{11}$; (iv) $\boldsymbol{L}_{22}$ and $\boldsymbol{U}_{22}$: LU decompose $\boldsymbol{Z}_{22} - \boldsymbol{L}_{21}\boldsymbol{U}_{12} = \boldsymbol{L}_{22}\boldsymbol{U}_{22}$. In practice, procedures (i) and (iv) are executed recursively, optimally leveraging these blocks' hierarchical LR approximation along the way and terminating only when blocks in $\boldsymbol{L}$ and $\boldsymbol{U}$ size-wise match those in the original hierarchical decomposition of $\boldsymbol{Z}$. Procedures (ii) and (iii) (and similar operations in the hierarchical execution of (i) and (iv)) are performed via partitioned forward/backward substitution for hierarchical lower/upper triangular matrices [4]. The resulting hierarchically block LU-decomposed $\boldsymbol{Z}$ comprises a collection of submatrices/blocks $\{\boldsymbol{B}\}$, the majority of which is stored in LR form, and can be used to solve (2) using a process akin to conventional forward/backward substitution. For scatterers that are small or comparable to the wavelength, the CPU/memory requirements of this procedure provably scale almost linear in N. For scatterers spanning many wavelengths, blocks of $\boldsymbol{Z}$ representing interactions between electromagnetically large far-field subscatterers are not LR and the memory requirements of the above procedure have never been shown to scale any better than $O(N^2)$.

D2: Recompression of the LR blocks in LU factors by MLMDA.
Consider a block in $\{\boldsymbol{B}\}$ that maps to a block in $\boldsymbol{Z}$ describing the interactions

between a level-l far-field subscatterer pair. Assuming $\boldsymbol{B}$ is stored in LR form, we attempt to recompress it by a $d(=N_l-l)$-level butterfly. First $\boldsymbol{B}$ is split column-wise into $\sim 2^d$ subblocks matching the unknowns in the corresponding level-N_l subscatterers modeled by $\boldsymbol{B}$'s columns. Each subblock is approximated by a LR product $\boldsymbol{B} = \boldsymbol{P}^{(0)}\boldsymbol{R}^{(0)}$. Next we pair subblocks in $\boldsymbol{P}^{(0)}$, while splitting them row-wise into upper (+) and lower (-) parts. The pairing and splitting operations go along with the unknowns in the level-(N_l-1) and level-$(l+1)$ subscatterers modeled by $\boldsymbol{B}$'s columns and rows, respectively. These newly formed subblocks are once again approximated by LR products $\boldsymbol{P}^{(0)} = \boldsymbol{P}^{(1)}\boldsymbol{R}^{(1)}$. This process is repeated d times, resulting in decompositions $\boldsymbol{P}^{(k-1)} = \boldsymbol{P}^{(k)}\boldsymbol{R}^{(k)},\ k = 1, ..., d$. Generally speaking, $\boldsymbol{P}^{(k-1)}$ contains $2k-1$ column and $2d-k+1$ row blocks that match the unknowns in the level-$(l+k-1)$ and level-(N_l-k+1) subscatterers modeled by $\boldsymbol{B}$'s columns and rows, respectively. Therefore $\boldsymbol{P}^{(k-1)}$ contains $\sim 2^d$ subblocks $\boldsymbol{P}_{i,j}^{(k-1)},\ (i = 1, \ldots, 2^{k-1}; j = 1, \ldots, 2^{d-k+1})$. To construct $\boldsymbol{P}^k$ and $\boldsymbol{R}^k$, each $\boldsymbol{P}_{i,j}^{(k-1)}$ is split into upper (+) and lower (-) blocks as

$$\boldsymbol{P}_{i,j}^{(k-1)} = \begin{pmatrix} \boldsymbol{P}_{i,j}^{(k-1)+} \\ \boldsymbol{P}_{i,j}^{(k-1)-} \end{pmatrix}, \tag{3}$$

and pairs of column-wise blocks for both $\boldsymbol{P}_{i,j}^{(k-1)+}$ and $\boldsymbol{P}_{i,j}^{(k-1)-}$ are approximated by LR products as

$$(\boldsymbol{P}_{i,j^{odd}}^{(k-1)+or-},\ \boldsymbol{P}_{i,j^{odd}+1}^{(k-1)+or-}) = \boldsymbol{P}_{2i-1(+)or2i(-),\lfloor (j^{odd}+1)/2 \rfloor}\boldsymbol{R}_{2i-1(+)or2i(-),\lfloor (j^{odd}+1)/2 \rfloor} \tag{4}$$

Here which $j^{odd} = 2j-1$ and $\lfloor \bullet \rfloor$ rounds downward. After d steps, we obtain

$$\boldsymbol{B} = \boldsymbol{P}^{(d)} \cdot \boldsymbol{R}^{(d)} \cdot \ldots \cdot \boldsymbol{R}^{(1)} \cdot \boldsymbol{R}^{(0)} \tag{5}$$

When this type of butterfly decomposition is applied to blocks $\boldsymbol{B}$ of $\boldsymbol{Z}$, it can be rigorously shown that the (numerical) rank r of all LR products implicit in (5) is of $O(1)$ and approximately constant. In other words, each $\boldsymbol{E}^{(i)},\ 1 \le i \le d$, contains $\sim 2^d$ subblocks of approximate dimension $r \times 2r$, while $\boldsymbol{P}^{(d)}$ and $\boldsymbol{R}^{(0)}$ are composed of 2^d subblocks of approximate dimensions $(m/2^d) \times r$ and $r \times (n/2^d)$ with m and n the number of rows and columns in $\boldsymbol{B}$. The total memory costs for storing all of $\boldsymbol{Z}$ via decompositions (5) scales as $O(N\mathbf{log}^2 N)$. Interestingly, our numerical experiments indicate that blocks $\boldsymbol{B}$ of $\boldsymbol{Z}$'s LU factors behave similarly.

Bypassing the LR compression steps of D2, we obtain a true MLMDA based fast direct solver. Moreover, the high compression ratios observed in 2D persist 3D. Fig. 2(a) shows that for a perfect electriccally conducting sphere, the storage requirements scale as $O(N\mathbf{log}^2 N)$, while the solver's CPU cost asymptotically scales as $O(N^2)$. Fig. 2(b) shows that the bistatic RCS of a sphere modeled using over a million unknowns agrees well with the Mie series. The solver also performs well for more complex scatterers, e.g. the airplane modeled using $438,333$ unknowns shown in fig. 2(c).

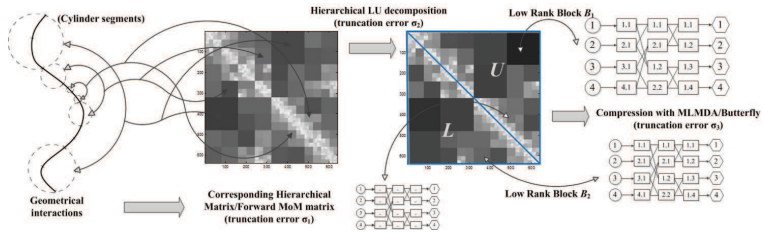

FIGURE 1. D1(left matrix partition) and D2 (right matrix partition)

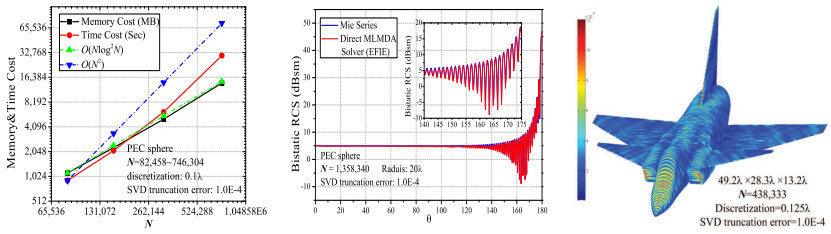

(a) (b) (c)

FIGURE 2. 3D results of the MLMDA-based fast direct solver

REFERENCES

[1] E. MICHIELSSEN AND A. BOAG, *A multilevel matrix decomposition algorithm for analyzing scattering from large structures*, IEEE Trans. Antennas Propag., 44 (1996), pp. 1086-1093.

[2] J. SHAEFFER, *Direct solve of electrically large integral equations for problem sizes to 1 M unknowns*, IEEE Trans. Antennas Propag., 56 (2008), pp. 2306-2313.

[3] S. CHANDLER-WILDE AND S. LANGDON, *Hierarchical Matrices Method and Its Application in Electromagnetic Integral Equations*, International Journal of Antennas and Propagation, 2012 (2012), ID 756259.

[4] M. BEBENDORF, *Hierarchical LU decomposition-based preconditioners for BEM*, Computing, 74 (2005), pp. 225-247.

A sign-definite formulation of the Helmholtz impedance problem

ANDREA MOIOLA
(joint work with Euan A. Spence)

One of the main aims of computational electromagnetic and acoustics is the numerical solution of the Helmholtz equation:

$$-\Delta u - k^2 u = f \qquad \text{in } \Omega \subset \mathbb{R}^d,\ k > 0,\ f \in L^2(\Omega). \tag{1}$$

Despite its wide use in applications and the simplicity of its expression, the numerical solution of this equation at high frequencies ($k \gg 1$) can be extremely costly. This fact is usually ascribed to several reasons: the presence of small oscillations

in the solutions which make the approximation expensive; the "numerical dispersion" which causes the "pollution effect"; the high indefiniteness of the operator. While the first two points are clear, the meaning of the frequently encountered statement "the Helmholtz equation is highly sign-indefinite" is not obvious. We argue that the sign-indefiniteness is a property of most variational reformulations of the Helmholtz equation rather than of the equation itself. In particular, we devise a new sign-definite (continuous and coercive) variational formulation for Helmholtz impedance problems and for sound-soft scattering problems in star-shaped domains. This is obtained by slightly modifying the derivation of the standard formulation with the use of a Morawetz-type multiplier as a test function in the integration by parts. More details and the complete proofs can be found in [7].

Variational problems. A boundary value problems (BVP) is often written as variational formulation (VF):

$$\text{find } u \in \mathcal{V} \text{ such that} \quad a(u,v) = F(v) \quad \forall v \in \mathcal{V}, \tag{2}$$

where $\mathcal{V}$ is a Hilbert space, $a(\cdot,\cdot)$ a bilinear (or sesquilinear) form, $F(\cdot)$ a continuous linear (or antilinear) functional. This allows the formulation of Galerkin discretisations:

$$\text{find } u_N \in \mathcal{V}_N \text{ such that} \quad a(u_N,v_N) = F(v_N) \quad \forall v_N \in \mathcal{V}_N, \tag{3}$$

where $\mathcal{V}_N \subset \mathcal{V}$ is a finite-dimensional space. If $a(\cdot,\cdot)$ is *continuous*, i.e.

$$\exists C_c > 0 \text{ such that} \quad |a(u,v)| \le C_c \|u\|_{\mathcal{V}} \|v\|_{\mathcal{V}} \quad \forall u,v \in \mathcal{V},$$

and *sign-definite* (often called *coercive*) i.e.

$$\exists \alpha > 0 \text{ such that} \quad |a(v,v)| \ge \alpha \|v\|_{\mathcal{V}}^2 \quad \forall v \in \mathcal{V}, \tag{4}$$

then the variational problem (2) enjoys several desirable properties: *(i)* it is well-posed; *(ii)* every Galerkin discretisation (3) is well posed; *(iii)* every Galerkin discretisation satisfies an explicit *quasi-optimality* bound

$$\|u - u_N\|_{\mathcal{V}} \le \frac{C_c}{\alpha} \inf_{v_N \in \mathcal{V}_N} \|u - v_N\|_{\mathcal{V}}, \tag{5}$$

which is independent of the specific Galerkin space $\mathcal{V}_N$ chosen; and *(iv)* its Galerkin matrix inherits similar continuity and positivity properties.

The Helmholtz impedance problem. We consider the Helmholtz equation (1) posed in a bonded domain $\Omega \subset \mathbb{R}^d$ $(d = 2, 3)$ with impedance boundary conditions:

$$\frac{\partial u}{\partial n} - \mathrm{i}ku = g \quad \text{on } \partial\Omega, \quad g \in L^2(\partial\Omega). \tag{6}$$

It is well-known that the Helmholtz impedance BVP (1) and (6) is well-posed, but, for large frequencies $k \gg 1$, the sesquilinear form of its standard VF

(7) find $u \in H^1(\Omega)$ such that

$$\int_\Omega (\nabla u \cdot \nabla \bar{v} - k^2 u \bar{v}) \mathrm{d}\mathbf{x} - \mathrm{i}k \int_{\partial\Omega} u \bar{v} \mathrm{d}s = \int_\Omega f \bar{v} \mathrm{d}\mathbf{x} + \int_{\partial\Omega} g \bar{v} \mathrm{d}s \quad \forall v \in H^1(\Omega),$$

is continuous in $H^1(\Omega)$-norm and *sign-indefinite* (i.e., not sign-definite). The same can be said for most available formulations.

This fact does not give the sign-indefiniteness of the Helmholtz equation (which we did not define), but only the sign-indefiniteness of some VFs. Thus it is natural to ask the question: is it possible to find a sign-definite formulation for this BVP?

In order to answer, we recall that the standard formulation (7) can easily be obtained in four steps:

- *(I)* multiply the Helmholtz operator $\mathcal{L}u := \Delta u + k^2 u$ by a test function v;
- *(II)* use Green's first identity $(\Delta u)\bar{v} = \mathrm{div}[(\nabla u)\bar{v}] - \nabla u \cdot \nabla \bar{v}$;
- *(III)* integrate by parts, transforming the divergence term into a term integrated on $\partial\Omega$;
- *(IV)* impose the data, i.e., substitute the term $\mathcal{L}u$ with $-f$ and $\partial u/\partial n$ with $\mathrm{i}ku + g$, and move the terms containing f and g to the right-hand side.

A novel sign-definite formulation. To obtain the desired formulation we mimic steps *(I–IV)* of the standard derivation above including a *Morawetz-type multiplier*. To this purpose, in step *(I)* we multiply $\mathcal{L}u$ with the special multiplier

$$\mathcal{M}v := \mathbf{x} \cdot \nabla v - ik\beta v + \frac{d-1}{2} v, \tag{8}$$

where $\beta > 0$ is a parameter and d is the space dimension. Due to this choice, we supplement Green's identity in step *(II)* with a *Rellich-type identity*:

$$(\Delta u)(\mathbf{x} \cdot \nabla \bar{v}) = \mathrm{div}\big[(\nabla u)(\mathbf{x} \cdot \nabla \bar{v})\big] - \nabla u \cdot \nabla \bar{v} - \nabla u \cdot \big((\mathbf{x} \cdot \nabla)\nabla \bar{v}\big).$$

After some manipulations we obtain the identity

$$\begin{aligned} -\mathcal{L}u\overline{\mathcal{M}v} =& \nabla u \cdot \nabla \bar{v} + k^2 u \bar{v} + \mathcal{M}u\overline{\mathcal{L}v} \\ & - \mathrm{div}\Big[\nabla u \overline{\mathcal{M}v} + \mathcal{M}u \nabla \bar{v} + \mathbf{x}(k^2 u \bar{v} - \nabla u \cdot \nabla \bar{v})\Big]. \end{aligned}$$

We add the term $\frac{1}{3k^2}\mathcal{L}u\overline{\mathcal{L}v}$ to both sides of this identity and perform steps *(III)* and *(IV)* exactly as above. From this procedure we immediately obtain the sesquilinear form $b(\cdot,\cdot)$ and the antilinear functional $G(\cdot)$:

$$\begin{aligned} b(u,v) :=& \int_\Omega \left(\nabla u \cdot \nabla \bar{v} + k^2 u \bar{v} + \Big(\mathcal{M}u + \frac{1}{3k^2}\mathcal{L}u\Big)\overline{\mathcal{L}v} \right) \mathrm{d}\mathbf{x} - \int_{\partial\Omega} \Big(\mathrm{i}ku\overline{\mathcal{M}v} \\ & + \Big(\mathbf{x} \cdot \nabla_T u - \mathrm{i}k\beta u + \frac{d-1}{2} u\Big)\frac{\partial \bar{v}}{\partial n} + (\mathbf{x} \cdot \mathbf{n})\left(k^2 u \bar{v} - \nabla_T u \cdot \nabla_T \bar{v}\right) \Big) \mathrm{d}s, \\ G(v) :=& \int_\Omega f \left(\overline{\mathcal{M}v} - \frac{1}{3k^2}\overline{\mathcal{L}v} \right) \mathrm{d}\mathbf{x} + \int_{\partial\Omega} g\, \overline{\mathcal{M}v} \mathrm{d}s, \end{aligned}$$

where $\mathbf{n}$ is the outgoing normal. Both $b(\cdot,\cdot)$ and $G(\cdot)$ are continuous in the space

$$V := \big\{ v :\ v \in H^1(\Omega),\ \Delta v \in L^2(\Omega),\ \nabla v \in \big(L^2(\partial\Omega)\big)^d \big\},$$

equipped with the norm

$$\|v\|_V^2 = k^2 \|v\|_{L^2(\Omega)}^2 + \|\nabla v\|_{L^2(\Omega)^d}^2 + k^{-2}\|\Delta v\|_{L^2(\Omega)}^2 + Lk^2 \|v\|_{L^2(\partial\Omega)}^2 + L\|\nabla v\|_{L^2(\partial\Omega)^d}^2,$$

where $L :=\mathrm{diam}(\Omega)$, and they give a new consistent VF, in the sense that

$$(9)\quad u \in V \quad b(u,v) = G(v) \quad \forall v \in V \qquad \Longleftrightarrow \qquad \begin{cases} -\Delta u - k^2 u = f & \text{in } \Omega, \\ \frac{\partial u}{\partial n} - iku = g & \text{on } \partial\Omega. \end{cases}$$

We prove that, if the domain Ω is *star-shaped* with respect to the ball $B_{\gamma L}$, $\gamma > 0$, (i.e. $\mathbf{x}\cdot\mathbf{n}(\mathbf{x}) \geq \gamma L$ for a.e. $\mathbf{x} \in \partial\Omega$) and $\beta \geq 3L/\gamma$, then $b(\cdot,\cdot)$ is sign-definite in V:

$$(10)\qquad \Re\{b(v,v)\} \geq \frac{\gamma}{4}\|v\|_V^2 \qquad \forall v \in V.$$

The explicit continuity and coercivity bounds allow a precise control of the pollution effect in the discretisations of (9). Indeed, *any* conformal Galerkin discretisation is unconditionally well-posed and its quasi-optimality ratio (i.e., the maximal ratio between Galerkin error and best approximation error as in (5), both measured in $\|\cdot\|_V$-norm) grows at most linearly in the wavenumber k.

On the other hand, since $v \in V$ requires $\Delta v \in L^2(\Omega)$, any conformal discretisation that uses piecewise smooth functions (e.g., finite elements) must use $C^1(\Omega)$ functions. This is a severe constraint on the design of numerical schemes for (9).

The formulation in (9) can be generalised to BVPs posed in $\Omega \setminus \overline{D}$, where D is a star-shaped sound-soft scatterer, i.e., Dirichlet boundary conditions are imposed on ∂D; see [7, §4]. Also varying impedance boundary condition, i.e. $\partial u/\partial n - ik\vartheta(\mathbf{x})u = g$, with $0 < \vartheta \in L^\infty(\partial\Omega)$, are allowed.

The Morawetz multiplier $\mathcal{M}v$. The sign-definiteness (10) of the formulation (9) can be proved by using only elementary results, as vector calculus identities and the Cauchy–Schwarz inequality. Moreover, the derivation of (9) is extremely similar to that of the standard formulation (7). Thus the sign-definiteness has to be attributed to the only "exotic" ingredient used: the Morawetz multiplier $\mathcal{M}v$ defined in (8). This multiplier (in several variations) and the corresponding calculus identities have previously been used in a wide variety of contexts.

A simpler multiplier $(\mathbf{x}\cdot\nabla v)$ was used by Rellich in [9] to express Laplace eigenvalues as boundary integrals and later by several authors in the context of spectral analysis. A multiplier more similar to that of (8) has been used by Morawetz to study the energy decay of wave equation solutions and the frequency dependence of Helmholtz solution in the exterior of a scatterer, see e.g. [8]. Numerical analysts used this technique to prove k-explicit stability bounds for interior Helmholtz BVPs, [6, 3, 4], and to investigate the coercivity of classic and new boundary integral operators, [11, 10]. More references are provided in [7].

Are there any other known sign-definite formulations? A few existing variational formulation of the Helmholtz impedance BVP (1) and (6) satisfy (4), but they are all very different from that in (9). In particular, they are either:

- boundary integral equations, see e.g. [11, 10];
- Trefftz formulations, i.e., posed on spaces of piecewise Helmholtz solutions, e.g. the UWVF and the TDG of [1, 5];
- least squares schemes.

A relevant difference between (9) and least squares formulations is that the former can be used to *prove* k-explicit stability bounds on u, while the seconds *requires* these bounds to be well-posed.

We note that, using an appropriate operator $T : \mathcal{V} \to \mathcal{V}$, any well-posed formulation in the form (2) can be translated in a sign-definite one: $a_T(u, v) := a(u, Tv) = F(Tv) =: F_T(v)$. However, the operator T is often not explicit or its approximation by a Galerkin scheme requires some strict assumptions on the discretisation (see [2]).

References

[1] A. Buffa and P. Monk, *Error estimates for the ultra weak variational formulation of the Helmholtz equation*, M2AN, Math. Model. Numer. Anal., 42 (2008), pp. 925–940.

[2] P. Ciarlet Jr., *T-coercivity: Application to the discretization of Helmholtz-like problems*, Comput. Math. Appl., 64 (2012), pp. 22–34.

[3] P. Cummings and X. Feng, *Sharp regularity coefficient estimates for complex-valued acoustic and elastic Helmholtz equations*, Math. Models Methods Appl. Sci., 16 (2006), pp. 139–160.

[4] U. Hetmaniuk, *Stability estimates for a class of Helmholtz problems*, Commun. Math. Sci., 5 (2007), pp. 665–678.

[5] R. Hiptmair, A. Moiola, and I. Perugia, *Plane wave discontinuous Galerkin methods for the 2D Helmholtz equation: analysis of the p-version*, SIAM J. Numer. Anal., 49 (2011), pp. 264–284.

[6] J. M. Melenk, *On Generalized Finite Element Methods*, PhD thesis, University of Maryland, 1995.

[7] A. Moiola and E. A. Spence, *Is the Helmholtz equation really sign indefinite?*, Tech. Report Preprint Series MPS-2012-23, Department of Mathematics and Statistics, University of Reading, 2012. http://www.reading.ac.uk/maths-and-stats/research/maths-preprints.aspx

[8] C. S. Morawetz, *Notes on time decay and scattering for some hyperbolic problems*, Society for Industrial and Applied Mathematics, Philadelphia, Pa., 1975.

[9] F. Rellich, *Darstellung der Eigenwerte von $\Delta u + \lambda u = 0$ durch ein Randintegral*, Math. Z., 46 (1940), pp. 635–636.

[10] E.A. Spence, I.V. Kamotski, and V.P. Smyshlyaev, *Coercivity of combined boundary integral equations in high frequency scattering*. In preparation, 2013.

[11] E. A. Spence, S. N. Chandler-Wilde, I. G. Graham, and V. P. Smyshlyaev, *A new frequency-uniform coercive boundary integral equation for acoustic scattering*, Comm. Pure Appl. Math., 64 (2011), pp. 1384–1415.

Hardy space method for exterior Maxwell problems

Lothar Nannen

(joint work with Thorsten Hohage, Achim Schädle, Joachim Schöberl)

We consider scattering and resonance problems on connected, unbounded domains $\Omega \subset \mathbb{R}^3$, which are complements of compact sets. Scattering or source problems for the time-harmonic Maxwell's equations consist in finding an outgoing electric field $\mathbf{u} \in H_{\mathrm{loc}}(\mathbf{curl}; \Omega)$ satisfying

$$\int_\Omega \mathbf{curl}\,\mathbf{u} \cdot \mathbf{curl}\,\mathbf{v} - \omega^2 \varepsilon\, \mathbf{u} \cdot \mathbf{v}\, dx = l(\mathbf{v}) \qquad \text{for all } \mathbf{v} \in H_{\mathrm{c}}(\mathbf{curl}; \Omega). \tag{1}$$

for a given frequency $\omega > 0$, the local permittivity ε and a linear form $l(\mathbf{v}) = \int_\Omega \mathbf{g}\cdot\mathbf{v}\,dx + \int_{\partial\Omega} \mathbf{g}_{\partial\Omega}\cdot\mathbf{v}\,dx$ with a compactly supported source term $\mathbf{g}$ and boundary data $\mathbf{g}_{\partial\Omega}$. Here $H_c(\mathbf{curl};\Omega)$ denotes the space of all vector fields $\mathbf{v}$ which are compactly supported in $\overline{\Omega}$ and are square integrable together with the curl $\mathbf{curl}\,\mathbf{v}$. $H_{\mathrm{loc}}(\mathbf{curl};\Omega)$ denotes the space of vector fields $\mathbf{v}$, which are square integrable on any compact subset $K \subset \overline{\Omega}$ together with $\mathbf{curl}\,\mathbf{v}$.

The radiation condition defining the term "outgoing" is typically formulated as Silver-Müller radiation condition. Then it is well-known that problem (1) is well-posed (see e.g. [1]). For $\omega > 0$ there exist other radiation conditions, which are equivalent for solutions $\mathbf{u}$ to (1):

(i) A series representation $\mathbf{u}$ in terms of Hankel functions of the first kind (e.g. [1]),
(ii) a boundary integral representation of $\mathbf{u}$ (e.g. [1]),
(iii) the condition that a holomorphic extension of $\mathbf{u}$ with respect to the radial variable (e.g. a complex scaling) is exponentially decreasing (e.g. [2, 3]) and
(iv) the so called pole condition, which characterizes outgoing solutions via the singularities of their Laplace transformed functions ([4] for Helmholtz problems and [5] for Maxwell problems).

Based on these radiation conditions there are several numerical methods to solve (1), e.g. classical infinite element methods [6], non-reflecting boundary conditions [7], boundary integral approaches [8], local high order approximations [9], complex scaling methods (known as perfectly matched layer methods) [10, 11, 12, 3] and Hardy space infinite elements [13, 14, 5].

Except for the two latter these methods depend non-linearly on the frequency ω, since this is the case for the radiation conditions (i) and (ii) on which they are based. This is a severe drawback for resonance problems, where we are looking for eigenpairs $(\mathbf{u},\omega^2)$ consisting of an outgoing resonance function $\mathbf{u} \in H_{\mathrm{loc}}(\mathbf{curl};\Omega)\setminus\{0\}$ and the square of a resonance $\omega \in \mathbb{C}$ such that

$$\int_\Omega \mathbf{curl}\,\mathbf{u}\cdot\mathbf{curl}\,\mathbf{v} = \int_\Omega \omega^2\varepsilon\,\mathbf{u}\cdot\mathbf{v}\,dx \qquad \text{for all } \mathbf{v} \in H_c(\mathbf{curl};\Omega). \tag{2}$$

The radiation conditions (iii) and (iv) are independent of the frequency ω. Therefore methods based on these radiation conditions, namely complex scaling methods and the Hardy space infinite element method, can be constructed such that they lead to a generalized matrix eigenvalue problem of the form

$$S\underline{\mathbf{u}} = \omega^2 M_\varepsilon \underline{\mathbf{u}} \tag{3}$$

with complex symmetric, non-hermitian matrices S and M_ε. This problem can be solved by a standard shift-and-invert Arnoldi method. Although it is possible to solve the non-linear eigenvalue problem resulting e.g. from a boundary element method ([15]), it is desirable to avoid it.

Therefore, currently complex scaling methods based on (iii) are the standard methods for solving resonance problems (see e.g. [16, 17]). Usually, due to the resulting exponential decay of the solution, the unbounded domain is truncated

to a bounded domain consisting of the computational domain and a perfectly matched layer with the artificial, anisotropic damping. The method can be easily implemented in standard finite element codes, since only the bilinear forms have to be changed.

Unfortunately, these methods give rise to spurious resonance modes. It is shown in [17], that the spurious resonance modes arise from a discretization of an essential spectrum. Moreover, several parameter of the complex scaling method like the type of scaling, the thickness of the layer and the underlying finite element method have to be optimized for each specific problem.

The Hardy space infinite element method also leads to spurious resonance modes, but less parameters have to be chosen by hand. Moreover, numerical tests indicate a super-algebraic convergence with respect to the number of degrees of freedom in radial direction. On the other hand, the method is a tensor product method of standard finite element basis functions with special infinite basis functions in the Hardy space of the complex unit disk. Therefore, a non-standard infinite element has to be included in a finite element code.

The numerical tests in [5] for Maxwell problems were made with the open source finite element package Netgen/NGSolve from Joachim Schöberl together with the open source module ngs-waves containing the routines for the infinite elements. Numerical tests comparing a complex scaling method with the Hardy space infinite element method can be found for Helmholtz problems in [14]. They indicate, that the Hardy space infinite element method needs less computational effort than the complex scaling method.

References

[1] D. Colton, R. Kress, *Inverse acoustic and electromagnetic scattering theory*, vol. 93 of Applied Mathematical Sciences, Springer-Verlag, Berlin, second ed., 1998.

[2] P. D. Hislop, I. M. Sigal, *Introduction to spectral theory*, vol. 113 of Applied Mathematical Sciences, Springer-Verlag, Berlin, second ed., 1996.

[3] F. Collino, P. Monk, *The perfectly matched layer in curvilinear coordinates*, SIAM J. Sci. Comput., 19 (1998), pp. 2061–2090.

[4] T. Hohage, F. Schmidt, L. Zschiedrich, *Solving time-harmonic scattering problems based on the pole condition. I. Theory*, SIAM J. Math. Anal., 35 (2003), 183–210.

[5] L. Nannen, T. Hohage, A. Schädle, J. Schöberl *Exact sequences of high order Hardy space infinite elements for exterior Maxwell problems*, accepted for publication in SIAM J. Sci. Comput. (2013).

[6] L. Demkowicz, M. Pal, *An infinite element for Maxwell's equations*, Comput. Methods Appl. Mech. Engrg., 164 (1998), pp. 77–94.

[7] M. J. Grote, J. B. Keller, *Nonreflecting boundary conditions for Maxwell's equation*, J. Comput. Phys., 139 (1998), pp. 327–342.

[8] A. Buffa, M. Costabel,C. Schwab, *Boundary element methods for Maxwell's equations on non-smooth domains*, Numer. Math., 92 (2002), pp. 679–710.

[9] D. Givoli, *High-order local non-reflecting boundary conditions: a review*, Wave Motion, 39 (2004), pp. 319–326.

[10] B. Simon, *The definition of molecular resonance curves by the method of exterior complex scaling*, Phys. Lett. A, 71A (1979).

[11] J.-P. Berenger, *A perfectly matched layer for the absorption of electromagnetic waves*, J. Comput. Phys., 114 (1994), pp. 185–200.

[12] W. C. Chew, W. H. Weedon, *A 3d perfectly matched medium from modified Maxwell's equations with stretched coordinates*, Microwave Optical Tech. Letters, 7 (1994), pp. 590–604.
[13] T. Hohage, L. Nannen, *Hardy space infinite elements for scattering and resonance problems*, SIAM J. Numer. Anal., 47 (2009), 972–996.
[14] L. Nannen, A. Schädle, *Hardy space infinite elements for Helmholtz-type problems with unbounded inhomogeneities*, Wave Motion, 48 (2010), pp. 116–129.
[15] O. Steinbach, G. Unger, *Convergence analysis of a Galerkin boundary element method for the Dirichlet Laplacian eigenvalue problem*, SIAM J. Numer. Anal. 50 (2012), pp. 710–728.
[16] S. Hein, T. Hohage, W. Koch, and J. Schöberl, *m Acoustic resonances in high lift configuration*, J. Fluid Mech., 582 (2007), pp. 179–202.
[17] S. Kim, J. E. Pasciak, *The computation of resonances in open systems using a perfectly matched layer*, Math. Comp., 78 (2009), pp. 1375–1398.

A parallel space-time multigrid method

Martin Neumüller
(joint work with Olaf Steinbach)

As a model problem we consider the heat equation in a bounded domain $\Omega \subset \mathbb{R}^d$, $d = 1, 2, 3$ with boundary $\Gamma := \partial\Omega$ and a simulation interval $[0, T]$,

$$\begin{aligned} \partial_t u(\boldsymbol{x}, t) - \Delta u(\boldsymbol{x}, t) &= f(\boldsymbol{x}, t) && \text{for } (\boldsymbol{x}, t) \in Q := \Omega \times (0, T), \\ u(\boldsymbol{x}, t) &= 0 && \text{for } (\boldsymbol{x}, t) \in \Sigma := \Gamma \times (0, T), \\ u(\boldsymbol{x}, 0) &= u_0(\boldsymbol{x}) && \text{for } (\boldsymbol{x}, t) \in \Sigma_0 := \Omega \times \{0\}. \end{aligned} \tag{1}$$

Subdividing the simulation interval $[0, T]$ in subintervals

$$0 = t_0 < t_1 < \ldots < t_{N-1} < t_N = T, \quad \text{with } t_n = n\,\tau \text{ and } \tau = \frac{T}{N},$$

and using a standard finite element discretization in space and a discontinuous Galerkin approximation in time, this leads to the linear algebraic equations

$$[K_\tau \otimes M_h + M_\tau \otimes K_h]\, \boldsymbol{u}^{n+1} = \boldsymbol{f}^{n+1} + N_\tau \otimes M_h \boldsymbol{u}^n. \tag{2}$$

Here, M_h is the standard mass matrix and K_h is the standard stiffness matrix

$$M_h[i, j] := \int_\Omega \varphi_j(\boldsymbol{x})\varphi_i(\boldsymbol{x}) \mathrm{d}\boldsymbol{x}, \quad K_h[i, j] := \int_\Omega \nabla\varphi_j(\boldsymbol{x}) \cdot \nabla\varphi_i(\boldsymbol{x}) \mathrm{d}\boldsymbol{x}$$

for $i, j = 1, \ldots, N_x$. The matrices with respect to the time discretization, where a discontinuous Galerkin approximation is used, are given by

$$\begin{aligned} K_\tau[k, \ell] &:= -\int_0^\tau \psi_\ell(t)\partial_t\psi_k(t) \mathrm{d}t + \psi_\ell(\tau)\psi_k(\tau), \\ M_\tau[k, \ell] &:= \int_0^\tau \psi_\ell(t)\psi_k(t) \mathrm{d}t, \quad N_\tau[k, \ell] := \psi_\ell(\tau)\psi_k(0) \end{aligned}$$

for $k, \ell = 1, \ldots, N_t$. Moreover, the right hand side is given by

$$\boldsymbol{f}^{n+1}[\ell N_x + j] := \int_{t_n}^{t_{n+1}} \int_\Omega f(\boldsymbol{x}, t)\varphi_j(\boldsymbol{x})\psi_\ell(t) \mathrm{d}\boldsymbol{x}\mathrm{d}t$$

for $j = 1, \ldots, N_x$ and $\ell = 1, \ldots, N_t$. On the time interval $[t_n, t_{n+1}]$ we can therefore define the approximation

$$u_h^{n+1}(\boldsymbol{x}, t) = \sum_{\ell=1}^{N_t} \sum_{j=1}^{N_x} u_{\ell,j}^{n+1}\, \varphi_j(\boldsymbol{x})\, \psi_\ell(t), \quad \text{with } u_{\ell,j}^{n+1} := \boldsymbol{u}^{n+1}[\ell N_x + j],$$

where $\boldsymbol{u}^{n+1}$ is the solution of the linear system (2). Hence we have to solve

$$\begin{pmatrix} A_{\tau,h} & & & & \\ B_{\tau,h} & A_{\tau,h} & & & \\ & B_{\tau,h} & A_{\tau,h} & & \\ & & \ddots & \ddots & \\ & & & B_{\tau,h} & A_{\tau,h} \end{pmatrix} \begin{pmatrix} \boldsymbol{u}_1 \\ \boldsymbol{u}_2 \\ \boldsymbol{u}_3 \\ \vdots \\ \boldsymbol{u}_N \end{pmatrix} = \begin{pmatrix} \boldsymbol{f}_1 \\ \boldsymbol{f}_2 \\ \boldsymbol{f}_3 \\ \vdots \\ \boldsymbol{f}_N \end{pmatrix}, \tag{3}$$

with

$$A_{\tau,h} := K_\tau \otimes M_h + M_\tau \otimes K_h, \qquad B_{\tau,h} := -N_\tau \otimes M_h.$$

The linear system (3) is usually solved by a forward substitution within one time interval, i.e. within one space-time slap. Instead, here we will consider a global multigrid scheme for the solution of (3). For an easier notation we now write the linear system (3) as

$$L_{\tau,h}\, \boldsymbol{x} = \boldsymbol{f}. \tag{4}$$

For a global multigrid scheme we need to define appropriate restriction and prolongation operators and a suitable smoother. Here we use the standard geometric restriction and prolongation operators both in space and time. For the smoother we apply a fixed number of damped block Jacobi iterations

$$\boldsymbol{x}^{k+1} = \boldsymbol{x}^k + \omega_t \widetilde{D}_{\tau,h}^{-1} \left[\boldsymbol{f} - L_{\tau,h} \boldsymbol{x}^k \right]$$

where a block corresponds to one space-time slap. By $\widetilde{D}_{\tau,h}^{-1}$ we denote the approximation of the inverse of the exact block diagonal matrix $D_{\tau,h} := \operatorname{diag}\{A_{\tau,h}\}_{n=1}^{N}$, and for the approximation we use one space multigrid iteration for each space-time slap. For the proposed space-time multigrid approach it is possible to use the exact inverse of the block diagonal matrix $D_{\tau,h}$, but the approximation is much cheaper and it turns out, that we obtain almost the same results.

Next we consider the smoothing behavior of the proposed block Jacobi smoother when we using the exact block diagonal matrix $D_{\tau,h}$. The $(k+1)$-th error of the Jacbi iteration is given by

$$\boldsymbol{x} - \boldsymbol{x}^{k+1} =: \boldsymbol{e}^{k+1} = \left[I - \omega_t D_{\tau,h}^{-1} L_{\tau,h} \right] \boldsymbol{e}^k =: S_{\tau,h} \boldsymbol{e}^k.$$

In what follows we apply the so called local Fourier mode analysis in the one dimensional case, i.e. $d = 1$, for lowest order approximations in space and time. Under the assumption of periodic boundary conditions in space and time we apply

the smoothing operator $S_{\tau,h}$ onto the vector $\boldsymbol{\varphi}(\theta_x, \theta_t)$ with $\varphi_{k,\ell}(\theta_x, \theta_t) = e^{ik\theta_x} e^{i\ell\theta_t}$, $\theta_x, \theta_t \in [-\pi, \pi)$ and we obtain

$$S_{\tau,h}\boldsymbol{\varphi}(\theta_x, \theta_t) = \widetilde{S}_{\tau,h}(\theta_x, \theta_t)\boldsymbol{\varphi}(\theta_x, \theta_t),$$

with

$$\widetilde{S}_{\tau,h}(\theta_x, \theta_t) = 1 - \omega_t - \omega_t \alpha_{\tau,h}(\theta_x) e^{-i\theta_t},$$

and

$$\alpha_{\tau,h}(\theta_x) := \frac{2 + \cos(\theta_x)}{2 + 6\frac{\tau}{h^2} + (1 - 6\frac{\tau}{h^2})\cos(\theta_x)}.$$

Further calculations lead to

$$|\widetilde{S}_{\tau,h}(\theta_x, \theta_t)|^2 = (1 - \omega_t)^2 - 2\omega_t(1 - \omega_t)\alpha_{\tau,h}(\theta_x)\cos(\theta_t) + \omega_t^2 \left(\alpha_{\tau,h}(\theta_x)\right)^2.$$

For an efficient smoother we need to have a fast reduction of the error corresponding to the high frequencies $(\theta_x, \theta_t) \in \Theta^{\text{high}} := [-\pi, \pi)^2 \setminus (-\frac{\pi}{2}, \frac{\pi}{2})^2$. Hence we need to ensure

$$|\widetilde{S}_{\tau,h}(\theta_x, \theta_t)| \leq q < 1, \quad \text{for } (\theta_x, \theta_t) \in \Theta^{\text{high}}.$$

Using standard arguments one can show that

$$\min_{\omega_t \in \mathbb{R}} \max_{\substack{\theta_x \in [0,\pi] \\ \theta_t \in [\frac{\pi}{2}, \pi]}} |\widetilde{S}_{\tau,h}(\theta_x, \theta_t)|^2 = \frac{1}{2}, \tag{5}$$

with the optimal choice for the damping parameter $\omega_t^* = \frac{1}{2}$. Hence a good smoothing behavior for the high frequencies in time is obtained, which is independent of the discretization parameter $\lambda := \frac{\tau}{h^2}$. Moreover, for the optimal choice of the damping parameter $\omega_t = \frac{1}{2}$ one can show that

$$\max_{\substack{\theta_x \in [\frac{\pi}{2}, \pi] \\ \theta_t \in [0, \frac{\pi}{2}]}} |\widetilde{S}_{\tau,h}(\theta_x, \theta_t)|^2 \leq \frac{1}{2}, \qquad \text{if } \lambda \geq \frac{\sqrt{2}}{3}. \tag{6}$$

Hence, if the discretization parameter λ is large enough, a good smoothing behavior for high frequencies in space is obtained. With the two properties (5) and (6) we conclude, that semi coarsening in time is always possible and in addition if the discretization parameter λ is large enough it is possible to apply coarsening in space and time.

One advantage of the presented space-time multigrid approach is that it can be applied parallel in time. To show the parallel performance of this multigrid solver we consider the spatial domain $\Omega = (0, 1)^3$ which is decomposed into 49 152 tetrahedra, and we consider a constant time step size $\tau = 10^{-1}$. For the discretization in space we use piecewise linear continuous ansatz functions whereas for the discretization in time we use piecewise linear discontinuous ansatz functions. On each space-time slap we apply one iteration of a standard geometric multigrid solver to approximate the inverse of the block diagonal matrix $D_{\tau,h}$. Further for the presented space-time smoother we use the damping parameter $\omega_t = \frac{1}{2}$ where we apply

(a) weak scaling results.

cores	time steps	dof	iter	time
1	4	59 768	9	6.8
2	8	119 536	9	8.1
4	16	239 072	9	9.2
8	32	478 144	9	9.2
16	64	956 288	9	9.2
32	128	1 912 576	9	9.3
64	256	3 825 152	9	9.1
128	512	7 650 304	9	9.4
256	1 024	15 300 608	9	9.4
512	2 048	30 601 216	9	9.4
1 024	4 096	61 202 432	9	9.4
2 048	8 192	122 404 864	9	9.5

(b) strong scaling results

cores	time steps	dof	iter	time
1	4 096	61 202 432	9	6 960.7
2	4 096	61 202 432	9	3 964.8
4	4 096	61 202 432	9	2 106.2
8	4 096	61 202 432	9	1 056.0
16	4 096	61 202 432	9	530.4
32	4 096	61 202 432	9	269.5
64	4 096	61 202 432	9	135.2
128	4 096	61 202 432	9	68.2
256	4 096	61 202 432	9	34.7
512	4 096	61 202 432	9	17.9
1 024	4 096	61 202 432	9	9.4
2 048	4 096	61 202 432	9	5.4

TABLE 2. Solving times in [s]

two pre- and post-smoothing steps. For the given setting we apply this space-time multigrid solver until we have reached a relative error reduction of 10^{-8}.

To show the parallel performance we first test the weak scaling behavior. To do so we use a fixed number of time steps per core. In this example we use four time steps for each core. In Table 1(a) the weak scaling results are given. We observe that the number of required multigrid iterations is bounded independent of the number of time steps which are used. Further we observe that the solving times are almost constant, when we increase the number of cores. In Table 1(b) the strong scaling results are presented. For a fixed number of time steps $N = 4096$ one can see that the computational costs can be reduced almost by a factor of $\frac{1}{2}$ when we double the number of cores.

The idea to solve time dependent problems parallel in time is not new. In [2, 4, 8] space-time multigrid approaches are presented where also the parallelization in time is discussed. For example, the performance of a parallel space-time multigrid solver for the unsteady Navier-Stokes equations is presented in [3]. The main difference of this work is the different space-time smoother and the different approximation in time. In [5, 1] the parareal algorithm is introduced and analyzed which also allows to solve parallel in time. The approach in this work is motivated by a general space-time discretization, which was studied in [6, 7].

REFERENCES

[1] M.J. Gander and S. Vandewalle. Analysis of the parareal time-parallel time-integration method. *SIAM J. Sci. Comput.*, 29:556–578, 2007.

[2] W. Hackbusch. Parabolic multigrid methods. *Computing methods in applied sciences and engineering, VI*, page 189–197, 1984.

[3] G. Horton. The time-parallel multigrid method. *Comm. Appl. Numer. Methods*, 8:585–595, 1992.

[4] G. Horton and S. Vandewalle. A space-time multigrid method for parabolic partial differential equations. *SIAM J. Sci. Comput.*, 16:848-864, 1995.

[5] J.-L. Lions, Y. Maday, and G. Turinici. A "parareal" in time discretization of pde's. *C. R. Acad. Sci. Paris Sar. I Math.*, 332:661–668, 2001.
[6] M. Neumüller and O. Steinbach. Refinement of flexible space-time finite element meshes and discontinuous galerkin methods. *Comput. Visual. Sci.Comput. Visual. Sci.*, 14:189–205, 2011.
[7] M. Neumüller and O. Steinbach. A dg space-time domain decomposition. *Domain Decomposition Methods in Science and Engineering XX (R. Bank, M. Holst, O. Widlund, J. Xu eds.). Lecture Notes in Computational Science and Engineering*, 91, 2013.
[8] T. Weinzierl and T. Köppl. A geometric space-time multigrid algorithm for the heat equation. *Numer. Math. Theory Methods Appl.*, 5:110–130, 2012.

A Discontinuous Galerkin Surface Integral Equation Method for Time-harmonic Maxwell's Equations

Zhen Peng
(joint work with Jin-Fa Lee)

We present a discontinuous Galerkin surface integral equation method, herein referred to as IEDG, for time harmonic electromagnetic wave scattering from non-penetrable targets. The proposed IEDG algorithm allows the implementation of the combined field integral equation (CFIE) using square-integrable, $\mathbf{L}^2$, trial and test functions without any considerations of continuity requirements across element boundaries. Due to the local characteristics of $\mathbf{L}^2$ basis functions, it is possible to employ non-conformal surface discretizations of the targets. Furthermore, it enables the possibility to mix different types of elements and employ different order of basis functions within the same discretization. Therefore, the proposed IEDG method is highly flexible to apply adaptation techniques.

Among the previous works addressing the abovementioned topic, we mention recent works [1] and [2]. The former investigates the use of combined current and charge integral equation for non-conforming meshes and a stabilization procedure is proposed for targets with geometrical singularities. The latter proposes a Nitsche-based domain decomposition method for the solution of hypersingular integral equation governing the Laplacian in $\mathbb{R}^3$.

We consider the solution of electromagnetic scattering problem. Denote the time-harmonic electric and magnetic fields by $\mathbf{E}$ and $\mathbf{H}$, respectively. We assume an $e^{-\imath\omega t}$ time dependence, where $\omega = 2\pi f$ is the radial frequency of operation and the imaginary unit is represented by $\imath\left(\equiv\sqrt{-1}\right)$. The free space wave number will be denoted by $k_0 = \omega\sqrt{\mu_0\varepsilon_0}$, where ε_0 and μ_0 are the permittivity and permeability of the free space, respectively. The free space intrinsic impedance is given by $\eta_0 = \sqrt{\mu_0/\varepsilon_0}$. Moreover, we shall introduce two surface trace operators on $\partial\Omega$, the tangential components trace operator $\pi_\tau(\bullet)$ and the twisted tangential trace operator $\gamma_\tau(\bullet)$, which are employed throughout our derivations. They are:

$$\gamma_\tau(\mathbf{u}) := \hat{\mathbf{n}} \times \mathbf{u}|_{\partial\Omega} \tag{1}$$

$$\pi_\tau(\mathbf{u}) := \hat{\mathbf{n}} \times (\mathbf{u} \times \hat{\mathbf{n}})|_{\partial\Omega} = \gamma_\tau(\mathbf{u}) \times \hat{\mathbf{n}} \tag{2}$$

The exterior region Ω_{ext} is homogeneous and assumed to be free space. Surface integral equation method is a natural choice for such an electromagnetic scattering

problem. An auxiliary variable $\mathbf{j}$, which represents the surface electric current, is introduced on $\partial\Omega$, via:

$$\mathbf{j} = \frac{1}{\imath k_0}\gamma_\tau(\nabla \times \mathbf{E}) \in \mathbf{L}^2(\partial\Omega) \tag{3}$$

Specifically, we shall employ discontinuous piecewise polynomial vector functions to approximate the auxiliary variable, $\mathbf{j}$.

Subsequently, the scattered electric field and the scattered magnetic field in Ω_{ext} can be obtained from the Stratton-Chu representation formulas as:

$$\mathbf{E}^s(\mathbf{j};\partial\Omega)(\mathbf{r}) = \mathcal{L}(\mathbf{j};\partial\Omega)(\mathbf{r}) \qquad \mathbf{r} \in \Omega_{\text{ext}} \tag{4}$$

$$\mathbf{H}^s(\mathbf{j};\partial\Omega)(\mathbf{r}) = \frac{1}{\eta_0}\mathcal{K}(\mathbf{j};\partial\Omega)(\mathbf{r}) \qquad \mathbf{r} \in \Omega_{\text{ext}} \tag{5}$$

where $\mathcal{L}$ and $\mathcal{K}$ are, respectively, the electric field integral operator (EFIO) and magnetic field integral operator (MFIO), defined as,

$$\mathcal{L}(\mathbf{f};\partial\Omega)(\mathbf{r}) := \imath k_0 \Psi_{\text{A}}(\mathbf{f};\partial\Omega)(\mathbf{r}) + \frac{1}{-\imath k_0}\nabla\nabla\cdot\Psi_{\text{A}}(\mathbf{f};\partial\Omega)(\mathbf{r}) \tag{6}$$

$$\mathcal{K}(\mathbf{f};\partial\Omega)(\mathbf{r}) := p.v.\,(\nabla \times \Psi_{\text{A}}(\mathbf{f};\partial\Omega)(\mathbf{r})) \tag{7}$$

where *p.v.* stands for *principle value*, and Ψ_{A} is the single-layer vector potential and is defined by

$$\Psi_{\text{A}}(\mathbf{f};\partial\Omega)(\mathbf{r}) = \int_{\partial\Omega} \mathbf{f}(\mathbf{r}')G(\mathbf{r},\mathbf{r}')d\mathbf{r}' \tag{8}$$

and $G(\mathbf{r},\mathbf{r}') := \frac{\exp^{\imath k_0|\mathbf{r}-\mathbf{r}'|}}{4\pi|\mathbf{r}-\mathbf{r}'|}$ is the free-space Green's function. $\mathbf{r}$ and $\mathbf{r}'$ denote the observation point and the source point, respectively.

We proceed to discretize the surface $\partial\Omega$ into N non-overlapping elements $\mathcal{S}_m$ such that $\partial\Omega = \mathcal{S}_1 \cup \mathcal{S}_2 \cdots \cup \mathcal{S}_N$ and the subscript $m \in \mathcal{I} = \{1, ..., N\}$ denotes the restriction of a quantity to $\mathcal{S}_m$. In this work, we uplift the trial function space to be square-integrable functions, $\mathbf{L}^2(\partial\Omega)$, which allows us to construct the trial function space completely independent for each element $\mathcal{S}_m$. The approximation of the current, $\tilde{\mathbf{j}}$, can be written as

$$\tilde{\mathbf{j}}(\mathbf{r}) = \bigoplus_{m=1}^{N} \mathbf{j}_m(\mathbf{r}) \tag{9}$$

where $\mathbf{j}_m(\mathbf{r})$ is the local approximation within each element. Since in the $\mathbf{L}^2(\partial\Omega)$ framework, the trial functions are defined with element-wise compact support, we have the privilege to choose the trial function to best approximate the current locally. Moreover, we denote $\mathcal{C}_{mn}$ and $\mathcal{C}_{nm}$ for the contour boundaries between two adjacent elements $\mathcal{S}_m$ and $\mathcal{S}_n$, with $\mathcal{C}_{mn}$ the contour line on $\mathcal{S}_m$ and $\mathcal{C}_{nm}$ the contour line on $\mathcal{S}_n$. Furthermore, associated with each element contour, $\mathcal{C}_{mn}$, we define a unit normal $\hat{\mathbf{t}}_{mn}$, which points from element $\mathcal{S}_m$ toward element $\mathcal{S}_n$.

The final Galerkin weak statement can be formally stated as:

$$
\begin{aligned}
&\text{Find } \mathbf{j} = \bigoplus_{m\in\mathcal{I}} \mathbf{j}_m, \mathbf{j}_m \in \mathbf{W}_m \text{ such that} \\
&\quad \frac{1}{2} a\left\langle \mathbf{v}, \mathbf{j}\right\rangle + \frac{1}{2} b\left\langle \mathbf{v}, \mathbf{j}\right\rangle \\
&\quad - \frac{1}{2\imath k_0} \sum_{\mathcal{C}_m\in\mathcal{C}} \sum_{n\in\mathcal{I}} \left\langle \hat{\mathbf{t}}_m \cdot \mathbf{v}_m, \Psi_{\mathrm{F}}\left(\nabla'_\tau \cdot \mathbf{j}_n; \mathcal{S}_n\right)\right\rangle_{\mathcal{C}_m} \\
&\quad - \frac{1}{2\imath k_0} \sum_{m\in\mathcal{I}} \sum_{\mathcal{C}_n\in\mathcal{C}} \left\langle \nabla_\tau \cdot \mathbf{v}_m, \Psi_{\mathrm{F}}\left(\hat{\mathbf{t}}_n \cdot \mathbf{j}_n; \mathcal{C}_n\right)\right\rangle_{\mathcal{S}_m} \\
&\quad + \frac{\beta}{\imath k_0} \sum_{\mathcal{C}_m\in\mathcal{C}} \sum_{\mathcal{C}_n\in\mathcal{C}} \left\langle \hat{\mathbf{t}}_m \cdot \mathbf{v}_m, \hat{\mathbf{t}}_n \cdot \mathbf{j}_n\right\rangle_{\mathcal{C}_m} \\
&\quad = \frac{1}{2}\left\langle \mathbf{v}, \mathbf{e}^{\mathrm{inc}}\right\rangle_{\partial\Omega} + \frac{1}{2}\left\langle \mathbf{v}, \bar{\eta}\mathbf{j}^{\mathrm{inc}}\right\rangle_{\partial\Omega} \qquad (10) \\
&\forall \mathbf{v} = \bigoplus_{m\in\mathcal{I}} \mathbf{v}_m, \mathbf{v}_m \in \mathbf{W}_m.
\end{aligned}
$$

where $\mathbf{j}^{\mathrm{inc}} = \eta_0\gamma_\tau\left(\mathbf{H}^{\mathrm{inc}}\right)$ and $\mathbf{e}^{\mathrm{inc}} = \pi_\tau\left(\mathbf{E}^{\mathrm{inc}}\right)$, with $\mathbf{E}^{\mathrm{inc}}$ and $\mathbf{H}^{\mathrm{inc}}$ being the incident electric and magnetic fields on $\partial\Omega$, respectively. In (10), $\mathbf{W}_m$ is taken as the space spanned by the vector basis functions introduced in [3], however, with the degrees of freedom (DOFs) defined independently for each element.

The two sesquilinear forms $a\left\langle \mathbf{v}, \mathbf{j}\right\rangle$ and $b\left\langle \mathbf{v}, \mathbf{j}\right\rangle$ in (10) are derived from the electric field integral equation (EFIE) and magnetic field integral equation (MFIE) surface penalty terms, defined by

(11)

$$
\begin{aligned}
a\left(\mathbf{v}, \mathbf{j}\right) &:= \sum_{m\in\mathcal{I}} \left(\imath k_0 \sum_{n\in\mathcal{I}} \left\langle \mathbf{v}_m, \pi_\tau\left(\Psi_{\mathrm{A}}\left(\mathbf{j}_n; \mathcal{S}_n\right)\right)\right\rangle_{\mathcal{S}_m} + \frac{1}{\imath k_0} \sum_{n\in\mathcal{I}} \left\langle \nabla\cdot\mathbf{v}_m, \Psi_{\mathrm{F}}\left(\nabla'\cdot\mathbf{j}_n; \mathcal{S}_n\right)\right\rangle_{\mathcal{S}_m} \right) \\
b\left(\mathbf{v}, \mathbf{j}\right) &:= \sum_{m\in\mathcal{I}} \left(\frac{1}{2}\left\langle \mathbf{v}_m, \bar{\eta}_m\mathbf{j}_m\right\rangle_{\mathcal{S}_m} + \left\langle \mathbf{v}_m, \bar{\eta}_m \sum_{n\in\mathcal{I}} \gamma_\tau\left(\mathcal{K}\left(\mathbf{j}_n; \mathcal{S}_n\right)\right)\right\rangle_{\mathcal{S}_m} \right)
\end{aligned}
$$

The third and the fourth inner product terms in (10) are closely related to the consistent symmetrization terms in discontinuous Galerkin (DG) literature. The single-layer scalar potential Ψ_{F} is defined as:

$$
\Psi_{\mathrm{F}}\left(f; \mathcal{S}\right)\left(\mathbf{r}\right) = \int_{\mathcal{S}} f(\mathbf{r}')G(\mathbf{r}, \mathbf{r}')dS \qquad (12)
$$

which represents the electric potential generated by a charge distribution on the surface $\mathcal{S}$. Similarly, we have

$$
\Psi_{\mathrm{F}}\left(f; \mathcal{C}\right)\left(\mathbf{r}\right) = \int_{\mathcal{C}} f(\mathbf{r}')G(\mathbf{r}, \mathbf{r}')d\mathbf{r}' \qquad (13)
$$

which corresponds to the electric potential contributed by the charge accumulation on the line contour $\mathcal{C}$.

The fifth inner product term is penalization term. In light of the interior penalty method [4], the interior penalty stabilization function β is taken as $\beta = \alpha h^{-1}$, where h is the mesh size of the discretization and the stabilization parameter α is a positive number independent of h.

References

[1] A. Bendali, F. Collino, M. Fares, and B. Steif, *Extension to nonconforming meshes of the Combined Current and Charge Integral equation*, IEEE Trans. Antennas and Propagation **60** (2012), 4732–4744.

[2] F. Chouly and N. Heuer, *A Nitsche-based domain decomposition method for hypersingular integral equations*, Numerische Mathematik **121** (2012), 705–729.

[3] S. M. Rao, D. R. Wilton, and A. W. Glisson, *Electromagnetic scattering by surfaces of arbitrary shape*, IEEE Trans. Antennas and Propagation **AP-30** (1982), 409–418.

[4] P. Houston, I. Perugia, A. Schneebeli and D. Schötzau, *Interior penalty method for the indefinite time-harmonic Maxwell equations* Numer. Math. **100** (2005), 485–518.

A mathematical toolkit for TDBIE

Francisco-Javier Sayas

Time Domain Boundary Integral Equations are powerful tools for simulation of transient phenomena related to scattering and propagation of acoustic, elastic and electromagnetic waves. This talk attempts to be a review of old and new techniques for analysis, mathematical and numerical, of TDBIE. This means, in particular, that the wide world of their applications will be barely mentioned, leaving relevant important names unmentioned in this note.

The Laplace domain approach: pure Galerkin. Analysis of the equations and of Galerkin-in-space-and-time discretization methods using Laplace domain estimates is the standard —and was, for quite some time, the only— approach to study TDBIE and their discretizations. This is a sort of coercivity analysis: it derives energy inequalities in the resolvent set and integrates back using a Plancherel formula, providing time-domain estimates in norms that are not necessarily physical. Some relevant references are [2, 3, 12, 17]. Much of what was done in these early years (see the survey [16]) was produced by the French school of Numerical Analysis, with a sizeable amount of doctoral theses supervised by Jean-Claude Nédélec and Alain Bachelot. New ideas in the area of Galerkin methods are related to the use of smooth temporal basis functions [28].

The Laplace domain approach: Convolution Quadrature. An alternative to full Galerkin discretization is the use of Galerkin-in-space and Convolution Quadrature. CQ is a technique to discretize causal convolutions, by mixing the Laplace domain with the time domain in a clever way, allowing for the use of the resolvent set in the time-stepping process. The analytical tools to study CQ-BEM were integrally developed in the Laplace domain, with time discretization analyzed using the central theorems of [25]. (Previous work of Christian Lubich on his CQ scheme is related to parabolic problems [23, 24].) Lubich himself detailed the analysis of the discretization with CQ-BEM of the acoustic single layer operator. (The analysis for the Neumann problem based on the indirect representation with a double layer potential can be found in [13].) Analysis of multistep-base CQ can thus be approached with a decided black-box spirit, which shifts the emphasis towards algorithms, solvers and applications [5, 10, 11, 14, 18, 19, 31]. However, it is much more recent that the analysis of Runge-Kutta-based (multistage) CQ methods has

been fully understood. As in the multistep case, the abstract analysis of CQ was first derived for parabolic problems [26]. The corresponding results for RK-based methods are only three years old [7, 8]. This was accompanied by extensive work on implementation and applications [4, 9, 1]. Hyperbolic-CQ has been recently extended to variable time-stepping [21, 22].

Galerkin semidiscretization as an exotic transmission condition. All Laplace domain analysis of TDBIE is carried out in the following way: estimates are given for the discrete or semidiscrete inverse of the integral operator, while any postprocessing of the discrete solution (computing the retarded potential based on the already approximated boundary quantities) is analyzed by throwing the mapping properties of the potentials on top of the error estimates on the boundary. While remaining in the Laplace domain, the analysis in [20] breaks with this trend. The idea is quite simple: the conditions for Galerkin semidiscretization (the unknown has to be in a given discrete space and the equation is tested with the same space) can be read as transmission conditions on a problem set in free space. This is actually what is done to get to any of the coercivity/stability estimates, so the approach just incides in this variational point of view of BIE by extending it to Galerkin semidiscretization-in-space. Apart from giving new insights on more complicated formulations (boundary-field formulations prepared for BEM-FEM discretization, direct BIE, etc), this approach has the advantage that the potential postprocessing is analyzed at the same time as the boundary unknowns and the bounds are much tighter.

Time domain analysis. A paper of Brian Rynne [27] seems to be the first attempt at analysing TDBIE (in this case the time domain EFIE) using techniques developed for hyperbolic equations, without any resort to the Laplace domain. The paper in question uses a straightening of the boundary and results for hyperbolic Cauchy problems (the initial value is set in time and on the flattened boundary of the scatterer), and seems to be only applicable on smooth domains. However, in recent years, we have been developing an approach based on C_0-groups of isometries applied to abstract differential equations of the second order in Hilbert spaces to analyze all this family of operators and their Galerkin semidiscretizations-in-space. As of this moment, this theory has seen three steps in its development:

- Study of the dynamical systems associated to the Galerkin semidiscretization of a wide range of problems [29] with the goal of showing energy conservation and well-posedness of the semidiscrete-in-space equations.
- Direct time domain analysis of the entire Calderón Calculus (all four integral operators, the two potentials, the inverses of the coercive operators of the Calderón projector and the Dirichlet-to-Neumann and Neumann-to-Dirichlet operators) using the same ideas [15].
- Extension of the previous technology to analyze a complete example with semidiscretized TDBIE, including the action of a TDBIE on data, all potential posprocessings and multistep-CQ discretization-in-time [6]. In this case, even the effect of CQ for full discretization is analyzed in the time domain.

What can be learnt from these new approaches is that time-domain techniques provide much tighter (less pessimistic) estimates for operators, their discrete inverses, postprocessing, etc. In particular, all new bounds seem to behave very reasonably for long times, confirming what has been observed in practical applications. While the techniques involved in the analysis are not particularly deep, these early steps have to be taken with great care, making sure that several apparently equivalent problems are effectively so.

In the forthcoming [30], I am trying to develop a streamlined approach to this analysis, so that, when time arrives and we want to apply it to complicated situations, the artillery is ready and the focus can be set on what is new or important in each new situation. These are the basic steps of the time domain analysis at present time.

(1) Identify the problems (the forward operator or potential, a semidiscrete Galerkin inversion of one of the operators, or the complementary of the associated Galerkin projection) as an initial value problem in free space with transmission conditions related to the space semidiscretization. Only some transmission conditions are non-homogeneous.
(2) Cut-off the space sufficiently far from the boundary where potentials and operators are defined. The distance to this artificial boundary has to be taken into account, since the cut-off problem will coincide with the original problem only for a finite time-interval.
(3) Identify the dynamical system associated to the cut-off problem. A checklist of conditions is available, making this part of the analysis an easy game. Transmission conditions have to be lifted in order to fit into traditional settings of non-homogeneous Cauchy problems. Use results from C_0-groups of isometries (bounds related to the associated Duhamel principle and the well-tuned machinery of the Hille-Yosida-Lumer-Philips theory) to prove continuity of the solutions to the cut-off problem for all times.
(4) Show that the strong solutions in the cut-off domain are the same as the weak distributional solutions of the original problem in free space and transfer all results from one to the other.
(5) Finally, take advantage of the convolutional structure (the one that allows to do all the analysis in the Laplace domain), to use shifting theorems to obtain the final version of all bounds.

This work is part of an long term project including several collaborators: Antonio Laliena (University of Zaragoza, Spain), Víctor Domínguez (Public University of Navarre, Spain), Lehel Banjai (Heriot-Watt University, UK), Christian Lubich (University of Tübingen, Germany) and my students at the University of Delaware (Sijiang Lu, Zhixing Fu, Tonatiuh Sánchez-Vizuet, Tianyu Qiu, and Matthew Hassell). This research is partially funded by the NSF (Grant DMS 1216356).

References

[1] J. Ballani, L. Banjai, S. Sauter, and A. Veit. Numerical Solution of Exterior Maxwell Problems by Galerkin BEM and Runge-Kutta Convolution Quadrature. *Numer. Math.* (to appear)

[2] A. Bamberger and T. H. Duong. Formulation variationnelle espace-temps pour le calcul par potentiel retardé de la diffraction d'une onde acoustique. I. *Math. Methods Appl. Sci.*, 8(3):405–435, 1986.

[3] A. Bamberger and T. H. Duong. Formulation variationnelle pour le calcul de la diffraction d'une onde acoustique par une surface rigide. *Math. Methods Appl. Sci.*, 8(4):598–608, 1986.

[4] L. Banjai. Multistep and multistage convolution quadrature for the wave equation: algorithms and experiments. *SIAM J. Sci. Comput.*, 32(5):2964–2994, 2010.

[5] L. Banjai and V. Grühne. Efficient long-time computations of time-domain boundary integrals for 2D and dissipative wave equation. *J. Comput. Appl. Math.*, 235(14):4207–4220, 2011.

[6] L. Banjai, A. Laliena, and F.-J. Sayas. Fully discrete Kirchhoff formulas with CQ-BEM. Submitted.

[7] L. Banja and C. Lubich. An error analysis of Runge-Kutta convolution quadrature. *BIT*, 51(3): 483–496, 2011.

[8] L. Banjai, C. Lubich, and J.M. Melenk. Runge–Kutta convolution quadrature for operators arising in wave propagation. *Numer. Math.*, 119(1): 1–20, 2011.

[9] L. Banjai, M. Messner, M. Schanz. Runge–Kutta convolution quadrature for the boundary element method. *Comput. Methods Appl. Mech. Engrg.*, 245/246, 90–101, 2012.

[10] L. Banjai and S. Sauter. Rapid solution of the wave equation in unbounded domains. *SIAM J. Numer. Anal.* 47(1):227–249, 2008.

[11] L. Banjai and M. Schanz. Wave propagation problems treated with convolution quadrature and BEM. In Langer, M. Schanz, O. Steinbach, and W. Wendland, editors, *Fast Boundary Element Methods in Engineering and Industrial Applications*, pages 145–187, Springer Berlin Heidelberg, 2012,

[12] E. Becache and T. Ha-Duong. A space-time variational formulation for the boundary integral equation in a 2D elastic crack problem. *RAIRO Modél. Math. Anal. Numér.*, 28(2):141–176, 1994.

[13] D.J. Chappell. A convolution quadrature Galerkin boundary element method for the exterior Neumann problem of the wave equation. *Math. Meth. Appl. Sci.*, 32:1585–1608, 2009.

[14] Q. Chen and P. Monk. Discretization of the time domain CFIE for acoustic scattering problems using convolution quadrature. Submitted.

[15] V. Domínguez and F.-J. Sayas. Some properties of layer potentials and boundary integral operators for the wave equation. *J. Int. Equations Appl.* (to appear)

[16] T. Ha-Duong. On retarded potential boundary integral equations and their discretisation. In *Topics in computational wave propagation*, volume 31 of *Lect. Notes Comput. Sci. Eng.*, pages 301–336. Springer, Berlin, 2003.

[17] T. Ha-Duong, B. Ludwig, and I. Terrasse. A Galerkin BEM for transient acoustic scattering by an absorbing obstacle. *Internat. J. Numer. Methods Engrg.*, 57(13):1845–1882, 2003.

[18] W. Hackbusch, W. Kress, and S. A. Sauter. Sparse convolution quadrature for time domain boundary integral formulations of the wave equation by cutoff and panel-clustering. In *Boundary element analysis*, volume 29 of *Lect. Notes Appl. Comput. Mech.*, pages 113–134. Springer, Berlin, 2007.

[19] W. Kress and S. Sauter. Numerical treatment of retarded boundary integral equations by sparse panel clustering. *IMA J. Numer. Anal.*, 28:162–185, 2008.

[20] A. R. Laliena and F.-J. Sayas. Theoretical aspects of the application of convolution quadrature to scattering of acoustic waves. *Numer. Math.*, 112(4):637–678, 2009.

[21] M. López Fernández and S. Sauter. A Generalized Convolution Quadrature with Variable Time Stepping *IMA J. Numer. Anal.* (to appear)

[22] M. López Fernández and S. Sauter. Generalized Convolution Quadrature with Variable Time Stepping. Part II: Algorithm and Numerical Results Preprint 09-2012, University of Zurich
[23] C. Lubich. Convolution quadrature and discretized operational calculus. I. *Numer. Math.*, 52(2):129–145, 1988.
[24] C. Lubich. Convolution quadrature and discretized operational calculus. II. *Numer. Math.*, 52(4):413–425, 1988.
[25] C. Lubich. On the multistep time discretization of linear initial-boundary value problems and their boundary integral equations. *Numer. Math.*, 67(3):365–389, 1994.
[26] C. Lubich and A. Ostermann. Runge-Kutta methods for parabolic equations and convolution quadrature. *Math. Comput.* 60(201), 105–131, 1993.
[27] B.P. Rynne. The well-posedness of the electric field integral equation for transient scattering from a perfectly conducting body. *Math. Methods Appl. Sci.* 22(7), 619-631, 1999.
[28] S. Sauter and A. Veit. A Galerkin Method for Retarded Boundary Integral Equations with Smooth and Compactly Supported Temporal Basis Functions. *Numer. Math.* (to appear)
[29] F.–J. Sayas. Energy estimates for Galerkin semidiscretization of time domain boundary integral equations. *Numer. Math.* (to appear)
[30] F.–J. Sayas. Retarded potentials and time domain boundary integral equations: a road map. Lecture notes (In preparation)
[31] M. Schanz. *Wave Propagation in Viscoelastic and Poroelastic Continua: A Boundary Element Approach (Lecture Notes in Applied and Computational Mechanics)*. Springer, 2001.

Efficient solutions of three dimensional periodic scattering problems

Catalin Turc

(joint work with Oscar Bruno, Stephen Shipman, and Stephanos Venakides)

We consider the problem of scattering of time-harmonic acoustic plane waves from a sound-soft difraction grating. The diffraction grating is given by $\Gamma = \{(x, y, z) : z = f(x, y)\}$ where f is a smooth bi-periodic function of periods d_1 and d_2 respectively, that is $f(x + d_1, y + d_2) = f(x, y)$. Specificaly, we seek to solve the scattering problem

$$\begin{aligned} \Delta u + k^2 u &= 0 \text{ in } \Gamma^+ \\ u &= -u^{inc} \text{ on } \Gamma \end{aligned} \tag{1}$$

where $\Gamma^+ = \{(x, y, z) : z > f(x, y)\}$ and the incidence is taken to be a plane wave given by

$$u^{inc}(\mathbf{x}) = \exp(ik\mathbf{d} \cdot \mathbf{x}) = \exp[i(\alpha x + \beta y - \gamma z)] \tag{2}$$

where $\alpha = k \sin\psi \cos\phi$, $\beta = k \sin\psi \sin\phi$, and $\gamma = k \cos\psi$. In order to ensure well-posedness, we require that the field u be (α, β) quasi-periodic, i.e. $u(\mathbf{x} + d_1\mathbf{e}_1 + d_2\mathbf{e}_2) = e^{i\alpha d_1 + i\beta d_2} u(\mathbf{x})$, and radiative, that is

$$u(\mathbf{x}) = \sum_{r=-\infty}^{\infty} \sum_{s=-\infty}^{\infty} B_{r,s} \exp(i\alpha_r x + i\beta_s y + i\gamma_{r,s} z),\ z > \max f \tag{3}$$

where

$$\alpha_r = \alpha + \frac{2\pi r}{d_1},\ \beta_s = \beta + \frac{2\pi s}{d_2},\ \gamma_{r,s} = (k^2 - \alpha_r^2 - \beta_s^2)^{\frac{1}{2}}. \tag{4}$$

The last square root is chosen so that $\mathrm{Im}(\gamma_{r,s}) \geq 0$; the propagating modes correspond to indices in the set $U = \{(r,s) : \mathrm{Im}(\gamma_{r,s}) = 0\}$. Equations (1) with the radiation conditions (3) have a unique solution [3]. We present next a quasi-periodic integral equation formulation of equations (1) based on quasi-periodic Green's functions. We look for scattered fields u which are solutions of equations (1) in the form of a single layer potential

$$u(\mathbf{x}) = \int_{\Gamma} G_k(|\mathbf{x}-\mathbf{x}'|)\mu(\mathbf{x}')ds(\mathbf{x}') \tag{5}$$

in terms of the unknown surface density μ and the outgoing Green's function $G_k(|\mathbf{z}|) = \frac{e^{ik|\mathbf{z}|}}{4\pi|\mathbf{z}|}$. Using the continuity property of the single layer potentials and the sound soft boundary conditions, the unknown density μ is a solution of the integral equation

$$\int_{\Gamma} G_k(|\mathbf{x}-\mathbf{x}'|)\mu(\mathbf{x}')ds(\mathbf{x}') = -e^{ik\mathbf{d}\cdot\mathbf{x}},\ \mathbf{x} \in \Gamma. \tag{6}$$

Equations (6) can be rewritten in a form that involves (a) a quasi-periodic Green's function $G(\mathbf{x},\mathbf{x}')$ defined for points $\mathbf{x}$ and $\mathbf{x}'$ on $\Gamma^{per} = \{(x,y,z) : 0 \leq x < d_1,\ 0 \leq y < d_2,\ z = f(x,y)\}$ as

$$G(\mathbf{x},\mathbf{x}') = \sum_{m=-\infty}^{\infty}\sum_{n=-\infty}^{\infty} G_k(x-x'+md_1, y-y'+nd_2, z-z')e^{-i\alpha md_1}e^{-i\beta nd_2} \tag{7}$$

and (b) a smooth density μ defined on Γ^{per}; the function $G(\mathbf{x},\mathbf{x}')$ defined in equation (7) is referred to as the (α,β) quasi-periodic Green's function. Specifically, with the notations introduced above, the integral equation formulations for the sound-soft case can be written in the form

$$\int_{\Gamma^{per}} G(\mathbf{x},\mathbf{x}')\mu(\mathbf{x}')ds(\mathbf{x}') = -e^{ik(\alpha x+\beta y+\gamma f(x,y))},\ (x,y),\ (x',y') \in [0,d_1]\times[0,d_2]. \tag{8}$$

The translation invariance of the radiation condition implies that $G(\mathbf{x},\mathbf{x}')$ depends only on $\mathbf{x}-\mathbf{x}'$, which allows one to write $G(\mathbf{x},\mathbf{x}') = G(\mathbf{x}-\mathbf{x}')$. The function $G(\mathbf{x})$ satisfies

$$\begin{aligned} &G(\mathbf{x}+(md_1,nd_2,0)) = G(\mathbf{x})e^{i(\alpha md_1+\beta nd_2)} \quad \text{for all } m,n \in \mathbb{Z}\,, \\ &\nabla^2 G(\mathbf{x}) + k^2\, G(\mathbf{x}) \;=\; -\sum_{m,n}\delta(x-md_1, y-nd_2, z)e^{i(\alpha md_1+\beta nd_2)}\,. \end{aligned}$$

Such a Green function G exists as long as the free-space wavenumber k does not coincide with the wavenumber $\left((\alpha+2\pi j/d_1)^2+(\beta+2\pi\ell/d_2)\right)^{1/2}$, $(j,\ell) \in \mathbb{Z}^2$, of any of the Fourier modes of the lattice. In this case, the pseudo-periodic Green function can be written as the lattice sum

$$G(x,y,z) \;=\; \frac{1}{4\pi}\sum_{m,n\in\mathbb{Z}} \frac{e^{ikr_{mn}}}{r_{mn}}e^{-i(\alpha md_1+\beta nd_2)}\,, \tag{9}$$

in which

$$r_{mn} = ((x + md_1)^2 + (y + nd_2)^2 + z^2)^{\frac{1}{2}} .$$

This sum is only conditionally convergent [2], and its convergence rate of $\sim C/r$ is too slow to be computationally feasible. If the triple (k, α, β) admits a pair of integers (j, ℓ) for which

$$k^2 = \left(\alpha + \frac{2\pi j}{d_1}\right)^2 + \left(\beta + \frac{2\pi \ell}{d_2}\right)^2 , \quad \text{(Wood anomaly condition)} \tag{10}$$

then no pseudo-periodic Green function exists, even if the problem of scattering by a given periodic structure is uniquely solvable.

The very slow conditional convergence of the periodic Green function (7) has been extensively discussed in the literature, and various methods to accelerate its convergence, notably the Ewald's method, have been proposed. We propose a method for fast evaluation of quasi-periodic Green functions consisting of truncating the lattice sum by a smooth cutoff function χ with compact support that is equal to unity in a neighborhood of the origin:

$$G(x, y, z) \approx G^a(x, y, z) := \frac{1}{4\pi} \sum_{m,n\in\mathbb{Z}} \frac{e^{ikr_{mn}}}{r_{mn}} e^{-i(\alpha m d_1 + \beta n d_2)} \chi(\tfrac{d_1 m}{a}, \tfrac{d_2 n}{a}) , \tag{11}$$

in which $r_{mn} = ((x+md_1)^2+(y+nd_2)^2+z^2)^{\frac{1}{2}}$ and a is a large number. Typically, χ will be either a radial function or one that is separable in x and y,

$$\chi(s, t) \,=\, \psi(\sqrt{s^2 + t^2}) \qquad \text{or} \qquad \chi(s, t) \,=\, \psi(s)\psi(t)$$

with $\psi(u)$ being a smooth monotonic function equal to unity for $|u| \le 1$ and equal to nullity for $|u| \ge 2$. Theorem 4 establishes the super-algebraic convergence of the smoothly cut off lattice sum to the periodic Green function.

Theorem 4 (Green function at non-Wood frequencies; super-algebraic convergence)**.** *Let χ be a smooth function of two variables such that*

$$\begin{array}{ll} \chi(s, t) = 1, & \sqrt{s^2 + t^2} \le A, \\ 0 < \chi(s, t) < 1, & A < \sqrt{s^2 + t^2} < B, \\ \chi(s, t) = 0, & B \le \sqrt{s^2 + t^2}, \end{array}$$

for some positive numbers A and B. If $\gamma_{j\ell} \neq 0$ for all $(j, \ell) \in \mathbb{Z}^2$, then the functions

$$G^a(x, y, z) = \frac{1}{4\pi} \sum_{m,n\in\mathbb{Z}} \frac{e^{ik\left((x+md_1)^2+(y+nd_2)^2+z^2\right)^{1/2}}}{\left((x + md_1)^2 + (y + nd_2)^2 + z^2\right)^{1/2}} e^{-i(\alpha m d_1 + \beta n d_2)} \chi(\tfrac{md_1}{a}, \tfrac{nd_2}{a})$$

converge to the radiating quasi-periodic Green function $G(x, y, z)$ super-algebraically as $a \to \infty$. Specifically, for each compact set $K \in \mathbb{R}^3$, there exist constants $C_n = C_n(k)$ such that

$$|G^a(x, y, z) - G(x, y, z)| < \frac{C_n(k)}{a^n}$$

if a is sufficiently large and $(x, y, z) \in K$, $(x, y, z) \notin d_1\mathbb{Z} \times d_2\mathbb{Z} \times \{0\}$.

At and around Wood anomalies we employ a combination of shifts in the z variable of $G_k(\mathbf{x})$, which introduces poles at several perpendicular shifts of the integer lattice $\mathbb{Z}^2$,

$$G_k^p(\mathbf{x}) = \sum_{q=0}^{p} a_{pq} G_k\left(\mathbf{x} + (0,0,qd)\right) .$$

The numbers a_{pq} are chosen to effect a p^{th}-order difference in z, that is

$$a_{pq} = (-1)^q \binom{p}{q}, \qquad 0 \le q \le p\,.$$

The use of the shifted free space Green's functions G_k^p gives rise to quasi-periodic Green's functions G^p that converge even at Wood anomalies. However, for values of the shift d so that $e^{i\gamma_{r,s}d} = 1$ for some indices (r,s), these quasi-periodic Green's functions are not radiative. The remedy is to incorporate in the quasi-periodic Green's function the propagating modes that may have been annihilated by the shifts. Thus, if $d > 0$ the function

$$G^p(\mathbf{x}) = \sum_{m,n\in\mathbb{Z}} G_k^p(r_{mn}) e^{-i(\alpha m d_1 + \beta n d_2)} + \sum_{j,\ell\in U} b_{j\ell}\; e^{i\alpha_j x + i\beta_\ell y + i\gamma_{j\ell} z}, \tag{12}$$

is a quasi-periodic Green's function in the domain $\{z > 0\}$ that converges even at Wood anomalies and is radiative for all but a finite number of values of coefficients $b_{j\ell}$. Furthermore, if we define functions $G^{p,a}$ analogoulsy to the functions G^a in equation (11), then $G^{p,a}$ converge to G^p at an algebraic rate of $a^{1/2-\lceil p/2\rceil}$ throughout the frequency domain. If we look for scattered fields u in terms of single layer potentials with shifted quasi-periodic functions G^p defined in (12) and densities μ^p we obtain the boundary integral equation

$$\int_{\Gamma^{per}} G^p(\mathbf{x},\mathbf{x}')\mu^p(\mathbf{x}')ds(\mathbf{x}') = -e^{ik(\alpha x + \beta y + \gamma f(x,y))},\ (x,y),\ (x',y') \in [0,d_1]\times[0,d_2]. \tag{13}$$

Theorem 5. *For all $d_0 > 0$ integral equations* (13) *are uniquely solvable in $L^2([0,d_1]\times[0,d_2])$ provided that $d \notin D$, where D is a subset of $\mathbb{R}$ such that $D\cap[0,d_0]$ is finite for each d_0.*

We solved integral equations (13) using the high-order Nyström methods introduced in [1] for a bisinusoidal grating whose height to period ratio equals to 1. We present in Table 3 numerical results for the first three Wood anomalies of the periodic configuration at normal incidence, including the number of GMRES iterations needed to reach a residual of 10^{-4}, and errors ϵ_1 in the coefficient $B_{0,0}$ defined in equation (3) and energy balance errors ϵ.

References

[1] Bruno, O., and L. Kunyansky, *Surface scattering in three dimensions: an accelerated high-order solver*, R. Soc. Lon. Proc. Ser. A Math. Phys. Eng. Sci., 2016, 2921–2934 (2001).

[2] Bruno, O. and Reitich, F., *Solution of a boundary-value problem for the Helmholtz equation via variation of the boundary into the complex domain*, Proc. R. Soc. Edinburgh, 122A, 317–340 (1992).

k	Unknowns	a	iter	ϵ_1	ϵ
2π	24×24	20	14	1.9×10^{-2}	3.9×10^{-2}
2π	24×24	30	14	4.2×10^{-3}	4.0×10^{-3}
$2\sqrt{2}\pi$	24×24	30	31	1.6×10^{-2}	4.1×10^{-2}
$2\sqrt{2}\pi$	24×24	40	31	3.4×10^{-3}	6.2×10^{-3}
4π	32×32	30	280	4.6×10^{-2}	4.9×10^{-2}
4π	32×32	40	268	7.4×10^{-3}	6.5×10^{-3}

TABLE 3. Convergence of the solvers using $G^{a,p}$, $p = 3$, shift $d = 2.4$.

[3] CHEN, X. AND FRIEDMAN, A., *Maxwell's Equations in a Periodic Structure*, Trans. Am. Math. Soc., 323(2) 465–507 (1991).
[4] LINTON, C. M., *Lattice Sums for the Helmholtz Equation*, SIAM Rev., 52(4), 630–674 (2010).

Reporter: Ralf Hiptmair

Participants

Prof. Dr. Francesco Andriulli
Telecom Bretagne
Technopole Brest-Iroise
CS 83818
29238 Brest Cedex 3
FRANCE

Prof. Dr. Alex Barnett
Department of Mathematics
Dartmouth College
6188 Kemeny Hall
Hanover, NH 03755-3551
UNITED STATES

Prof. Dr. Mario Bebendorf
Hausdorff Center for Mathematics
Institute for Numerical Simulation
Endenicher Allee 60
53115 Bonn
GERMANY

Dr. Timo Betcke
Department of Mathematics
University College London
Gower Street
London WC1E 6BT
UNITED KINGDOM

Prof. Dr. Anne-Sophie Bonnet-Ben Dhia
ENSTA/UMA
828 Bd des Maréchaux
91762 Palaiseau Cedex
FRANCE

Prof. Dr. Annalisa Buffa
IMATI - "E.Magenes" - CNR
Via Ferrata, 1
27100 Pavia
ITALY

Maxence Cassier
ENSTA ParisTech
828, Boulevard des Marechaux
91762 Palaiseau Cedex
FRANCE

Prof. Dr. Simon N. Chandler-Wilde
Dept. of Mathematics & Statistics
University of Reading
Whiteknights
P.O.Box 220
Reading RG6 6AX
UNITED KINGDOM

Prof. Dr. Zhiming Chen
Institute of Computational Mathematics and Scientific/Engineering Computing
Academy of Mathematics and Systems Sc.
Chinese Academy of Sciences
Beijing 100190
CHINA

Dr. Lucas Chesnel
ENSTA
828, Boulevard des Maréchaux
91762 Palaiseau Cedex
FRANCE

Dr. Patrick Ciarlet
ENSTA/UMA
828, Boulevard des Maréchaux
91762 Palaiseau Cedex
FRANCE

Dr. Xavier Claeys
Institut Superieur de l'Aeronautique et de Espaces
10, avenue Edouard-Belin
31055 Toulouse cedex 4
FRANCE

Prof. Dr. Kristof Cools
George Green Institute for
Electromagnetics Research
The University of Nottingham
University Park
Nottingham NG7 2RD
UNITED KINGDOM

Prof. Dr. Martin Costabel
Département de Mathématiques
Université de Rennes I
Campus de Beaulieu
35042 Rennes Cedex
FRANCE

Prof. Dr. Monique Dauge
I.R.M.A.R.
Université de Rennes I
Campus de Beaulieu
35042 Rennes Cedex
FRANCE

Prof. Dr. Laurent Demanet
Department of Mathematics
Massachusetts Institute of
Technology
77 Massachusetts Avenue
Cambridge, MA 02139-4307
UNITED STATES

Prof. Dr. Leszek F. Demkowicz
Institute for Computational
Engineering and Sciences (ICES)
University of Texas at Austin
1 University Station C
Austin, TX 78712-1085
UNITED STATES

Prof. Dr. Marc Durufle
Mathématiques et Informatique
Université Bordeaux I
351, cours de la Liberation
33405 Talence Cedex
FRANCE

Sonia Fliss
ENSTA/UMA
828, Boulevard des Maréchaux
91762 Palaiseau Cedex
FRANCE

Prof. Dr. Mahadevan Ganesh
Dept. of Applied Mathematics &
Statistics
Colorado School of Mines
Golden CO 80401-1887
UNITED STATES

Prof. Dr. Ivan G. Graham
Dept. of Mathematical Sciences
University of Bath
Claverton Down
Bath BA2 7AY
UNITED KINGDOM

Prof. Dr. Marcus Grote
Mathematisches Institut
Universität Basel
Rheinsprung 21
4051 Basel
SWITZERLAND

Dr. Houssem Haddar
Centre de Mathématiques Appliquées
École Polytechnique
91128 Palaiseau Cedex
FRANCE

Dr. Holger Heumann
Department of Mathematics
Rutgers University
Busch Campus, Hill Center
New Brunswick, NJ 08854-8019
UNITED STATES

Prof. Dr. Ralf Hiptmair
Seminar für Angewandte Mathematik
ETH-Zentrum
Rämistr. 101
8092 Zürich
SWITZERLAND

Prof. Dr. Thorsten Hohage
Institut für Numerische
und Angewandte Mathematik
Universität Göttingen
Lotzestr. 16-18
37083 Göttingen
GERMANY

Prof. Dr. Ronald H. W. Hoppe
Lehrstuhl f. Angewandte Mathematik I
Universität Augsburg
Universitätsstr. 14
86159 Augsburg
GERMANY

Dr. Carlos F. Jerez-Hanckes
Dept. of Electrical Engineering
Pontificia Universidad Catolica de Chile
Av. Vicuna Mackenna 4860, Macul
Santiago de Chile
CHILE

Prof. Dr. Patrick Joly
ENSTA/UMA
828, Boulevard des Maréchaux
91762 Palaiseau Cédex
FRANCE

Prof. Dr. Manfred Kaltenbacher
Institut für Mechanik und Mechatronik
Technische Universität Wien
Wiedner Hauptstr. 8 - 10
1040 Wien
AUSTRIA

Dr. Lars Kielhorn
Seminar for Applied Mathematics
ETH Zürich
Rämistr. 101
8092 Zürich
SWITZERLAND

Prof. Dr. Ulrich Langer
Institut für Numerische Mathematik
Johannes Kepler Universität Linz
Altenbergerstr. 69
4040 Linz
AUSTRIA

Prof. Dr. Armin Lechleiter
Zentrum für Technomathematik
FB 3, Universität Bremen
Postfach 330 440
28334 Bremen
GERMANY

Prof. Dr. Jens Markus Melenk
Institut für Analysis und
Scientific Computing
Technische Universität Wien
Wiedner Hauptstr. 8 - 10
1040 Wien
AUSTRIA

Dr. Matthias Messner
INRIA Bordeaux
200, Avenue de la Vieille Tour
33405 Talence Cedex
FRANCE

Prof. Dr. Eric Michielssen
Electrical Eng. & Comp. Science Dept.
The University of Michigan
Ann Arbor, MI 48109-2122
UNITED STATES

Dr. Andrea Moiola
Department of Mathematics
University of Reading
Whiteknights
Reading RG6 6AX
UNITED KINGDOM

Prof. Dr. Peter Monk
Department of Mathematical Sciences
University of Delaware
501 Ewing Hall
Newark, DE 19716-2553
UNITED STATES

Dr. Lothar Nannen
Institut für Analysis und
Scientific Computing
Technische Universität Wien
Wiedner Hauptstr. 8 - 10
1040 Wien
AUSTRIA

Prof. Dr. Jean-Claude Nedelec
Centre de Mathématiques Appliquées
UMR 7641 - CNRS
École Polytechnique
91128 Palaiseau Cedex
FRANCE

Martin Neumüller
Institut für Numerische Mathematik
Technische Universität Graz
Steyrergasse 30
8010 Graz
AUSTRIA

Dr. Clemens Pechstein
Institut für Numerische Mathematik
Johannes Kepler Universität Linz
Altenbergerstr. 69
4040 Linz
AUSTRIA

Dr. Zhen Peng
ECE Department
The Ohio State University
1320 Kinnear Road
Columbus, OH 43212
UNITED STATES

Prof. Dr. Karim Ramdani
Université de Lorraine
Institut Elie Cartan
Campus de Aiguillettes
Boite Postale 239
54506 Vandoeuvre-les-Nancy Cedex
FRANCE

Dr. Olof Runborg
Department of Mathematics
Kungliga Tekniska Högskolan
10044 Stockholm
SWEDEN

Prof. Dr. Francisco J. Sayas
Department of Mathematical Sciences
University of Delaware
501 Ewing Hall
Newark, DE 19716-2553
UNITED STATES

Dr. Kersten Schmidt
Institut für Mathematik
T.U. Berlin, Sekr. MA 6-4
Straße des 17. Juni 136
10623 Berlin
GERMANY

Prof. Dr. Joachim Schöberl
Institut für Analysis und
Scientific Computing
Technische Universität Wien
Wiedner Hauptstr. 8 - 10
1040 Wien
AUSTRIA

Dr. Euan Spence
Dept. of Mathematical Sciences
University of Bath
Claverton Down
Bath BA2 7AY
UNITED KINGDOM

Prof. Dr. Olaf Steinbach
Institut für Numerische Mathematik
Technische Universität Graz
Steyrergasse 30
8010 Graz
AUSTRIA

Prof. Dr. Sebastien Tordeux
Département de Mathématiques
Université de Pau, Appl. URA 1204
B.P. 290
Avenue de l'Universite
64000 Pau
FRANCE

Prof. Dr. Catalin Turc
Department of Mathematics
New Jersey Institute of Technology
606 Cullimore Hall
323 Martin Luther King Jr. Blvd.
Newark, NJ 07102-1982
UNITED STATES